ENDÜSTRİ MÜHENDİSLİĞİ ALANINDA GÜNCEL KONULAR VE AKADEMİK DEĞERLENDİRMELER

Editör: Doç.Dr. Alper KİRAZ

yaz
yayınları

Endüstri Mühendisliği Alanında
Güncel Konular ve Akademik Değerlendirmeler

Editör

Doç.Dr. Alper KİRAZ

yaz yayınları

2026

yaz
yayınları

Endüstri Mühendisliği Alanında Güncel Konular ve Akademik Değerlendirmeler

Editör: Doç.Dr. Alper KİRAZ

© YAZ Yayınları

Bu kitabın her türlü yayın hakkı Yaz Yayınları'na aittir, tüm hakları saklıdır. Kitabın tamamı ya da bir kısmı 5846 sayılı Kanun'un hükümlerine göre, kitabı yayınlayan firmanın önceden izni alınmaksızın elektronik, mekanik, fotokopi ya da herhangi bir kayıt sistemiyle çoğaltılamaz, yayınlanamaz, depolanamaz.

E_ISBN 978-625-8926-86-6

Ekim 2026 – Afyonkarahisar

Dizgi/Mizanpaj: YAZ Yayınları

Kapak Tasarım: YAZ Yayınları

YAZ Yayınları. Yayıncı Sertifika No: 73086

M.İhtisas OSB Mah. 4A Cad. No:3/3
İscehisar/AFYONKARAHİSAR

www.yazyayinlari.com

yazyayinlari@gmail.com

İÇİNDEKİLER

A Fast Deep Learning Surrogate for Transient Thermal-Hydraulic Behavior in a Two-Stage Metal Hydride Hydrogen Compressor, with a Transparent Evaluation of a Physics-Informed Variant.....1
Ümit YILMAZ

Freight Transport Modes, Modal Integration, and Logistics System Design: Evidence from Türkiye and the World.....41
Danışment VURAL

Business Continuity Management Standards from BS 25999 to ISO 22301: A Compact Fuzzy Standards-Alignment Maturity Assessment Framework for the Operational-Resilience Era.....62
Doğan ŞENGÜL, Cafer Erhan BOZDAĞ

Physical and Organizational Ergonomic Factors in the Classification of Upper-Extremity Musculoskeletal Pain.....90
Seçil KULAÇ

Integrating Fine-Kinney Risk Assessment and Lean Tools to Improve Worker Safety: A Case Study in the Forest Products Industry.....105
Serap AKCAN YETGİN, Ferhat YURDUNKULU, Cemil ÇEVİK, Mustafa AKIN

Yalın Hizmet Yaklaşımı ile Acil Servis Süreçlerinin İyileştirilmesi: Değer Akış Haritalama Uygulaması.....125
Betül TURANOĞLU ŞİRİN

"Bu kitapta yer alan bölümlerde kullanılan kaynakların, görüşlerin, bulguların, sonuçların, tablo, şekil, resim ve her türlü içeriğin sorumluluğu yazar veya yazarlarına ait olup ulusal ve uluslararası telif haklarına konu olabilecek mali ve hukuki sorumluluk da yazarlara aittir."

A FAST DEEP LEARNING SURROGATE FOR TRANSIENT THERMAL-HYDRAULIC BEHAVIOR IN A TWO-STAGE METAL HYDRIDE HYDROGEN COMPRESSOR, WITH A TRANSPARENT EVALUATION OF A PHYSICS-INFORMED VARIANT

Ümit YILMAZ[1]

1. INTRODUCTION

Hydrogen is increasingly regarded as a central energy carrier in the transition toward decarbonized industrial, transport, and power systems. Still, the scalability of a hydrogen economy depends critically on efficient, safe, and low-cost compression, storage, and transportation infrastructure (Omid et al., 2024). Among non-mechanical compression technologies, metal hydride hydrogen compressors (MHHCs) have attracted sustained attention because they are heat-driven rather than electrically driven, contain no moving parts beyond passive valves, and can be powered by low-grade waste heat or renewable thermal sources (Lototskyy et al., 2014; Yartys et al., 2016). An MHHC compresses hydrogen thermally: a metal hydride bed absorbs hydrogen at low temperature and pressure, and desorbs it at higher temperature and pressure, with the achievable pressure ratio governed by the Van't Hoff thermodynamics of the specific alloy, though practically limited by non-ideal behaviors such as hysteresis and plateau sloping (Lototskyy & Linkov, 2022). Multi-stage configurations, in which two or more hydride beds

[1] Instructor Dr., Bursa Technical University, Quality Coordination Office, ORCID: 0000-0003-4268-8598.

with progressively higher-pressure alloys are coupled in a cascade, allow substantially larger overall compression ratios than a single stage can achieve, and have been demonstrated experimentally at pressures ranging from tens to 900 bar (86.5 MPa). These systems typically utilize AB5-type alloys for lower-pressure stages and AB2-type Laves phase alloys for high-pressure stages (Karagiorgis et al., 2017), with recent high-pressure designs focusing almost exclusively on tailored AB2 intermetallics (Galvis E et al., 2020; Ha et al., 2023; Li et al., 2024).

Despite this experimental progress, the engineering design and real-time control of MHHCs remain constrained by the computational cost of the coupled thermal-hydraulic models used to describe them. Depending on the design question being asked, these models range from steady-state, lumped-parameter mass-and-energy-balance formulations suitable for techno-economic screening (Corgnale & Sulic, 2018) to the more detailed, dynamic system- and reactor-level models and commercial simulation environments needed to capture transient charge-discharge behaviour, whose absence hinders optimal system design (Dornheim et al., 2022) and whose computational cost renders them far too slow to embed inside a real-time controller, a fault-detection system, or an iterative design-space search, where thousands of candidate operating points may need to be evaluated. Machine learning techniques, particularly surrogate models trained to reproduce the input-output behavior of a physical simulation or experimental system at a small fraction of the computational cost, are a natural response to this bottleneck and have been applied extensively elsewhere in the hydrogen value chain, including hydrogen production, underground and material-based storage, and safety-critical process monitoring (Mukelabai et al., 2024; Quintanilla et al., 2025; van der Laag et al., 2026).

A parallel and, in recent years, extremely active line of machine learning research has proposed embedding known physical laws directly into the training objective of a neural network, producing so-called physics-informed neural networks (PINNs), which augment a conventional data-fitting loss with a residual term that penalizes violations of a governing equation, boundary condition, or thermodynamic constraint (Karniadakis et al., 2021; Raissi et al., 2019). In principle, this hybridization should improve data efficiency, enforce physical plausibility outside the observed training distribution, and reduce the risk of physically nonsensical predictions, and PINNs have been reported across fluid mechanics (Cai et al., 2021; Sharma et al., 2023), power systems (Huang & Wang, 2023), structural and manufacturing engineering (Xu et al., 2023; Zobeiry & Humfeld, 2021), and reduced-order and surrogate modeling more broadly (Chen et al., 2021; Sun et al., 2020). However, a growing number of studies emphasize that the practical benefit of a physics-informed loss is neither automatic nor uniform across problem settings and that PINN performance claims are frequently based on a single training run, even though multi-seed statistical testing is now standard practice in broader machine learning for establishing that an observed improvement is not simply an artifact of random initialization or mini-batch ordering (Henderson et al., 2018). A closely related, field-general methodological concern is data leakage arising from improper train-test partitioning, which has separately been shown to inflate performance claims across at least seventeen distinct machine-learning-based scientific disciplines (Kapoor & Narayanan, 2023) and which this study addresses directly through the experiment-blocked partitioning protocol. This concern is particularly salient for engineering time-series problems, where a sufficiently expressive recurrent or convolutional architecture, trained on a reasonably diverse operating envelope, may already learn an adequate implicit approximation of the governing

thermodynamics without an explicit physics penalty, such that the practical value of the physics-informed term shows up not in interpolative accuracy but in extrapolative robustness (Farea et al., 2024; Karniadakis et al., 2021), a critical distinction that is rarely tested directly in the applied PINN literature.

This study addresses both gaps in the specific context of a two-stage, exchangeable-vessel MHHC. First, it develops and reports a hybrid LSTM/TCN deep learning surrogate for the transient, multi-point thermal-hydraulic behavior of the compressor, trained on a recently released, openly licensed experimental dataset. Second, it develops a physics-informed variant of the same architecture, in which a Van't Hoff equilibrium constraint derived independently from pressure-composition-isotherm measurements is embedded as a soft penalty on the predicted outlet pressure. Third, rather than reporting a single comparison run, this study subjects the comparison between the two variants to the level of statistical scrutiny recommended in the broader machine learning reproducibility literature: an experiment-blocked, material-stratified data split that prevents information leakage; ten independently seeded training repetitions; a paired non-parametric significance test with an accompanying bootstrap confidence interval; and, distinctly from the great majority of published PINN case studies, a genuine out-of-distribution extrapolation test in which an entire hydride material is withheld from training. Fourth, because point-forecast accuracy is not the only criterion by which a physics-informed model might be judged useful, this study additionally reports a physical-plausibility diagnostic that quantifies how often each model's predictions violate the underlying thermodynamic equilibrium curve, independent of forecast error. The result is twofold: a practical, computationally inexpensive data-driven surrogate for two-stage metal hydride hydrogen compressors in its own right,

and, independent of that surrogate's specific accuracy, a transparent demonstration of how the reported benefit of a physics-informed constraint can shift, or reverse, once it is subjected to the level of statistical and extrapolation scrutiny this study applies, a methodological contribution as central to this work as the specific empirical result.

2. LITERATURE REVIEW

The metal hydride hydrogen compressor has been studied experimentally for several decades as an alternative to mechanical compression, motivated by the absence of moving parts, the possibility of waste-heat or renewable-heat operation, and reduced noise and maintenance requirements (Lototskyy et al., 2014; Yartys et al., 2016). Early single-stage systems using AB5-type alloys such as LaNi5 demonstrated feasibility at moderate pressures. Subsequent work extended the concept to multi-stage cascades in which a lower-pressure AB5 or AB2 alloy in the first stage feeds a higher-pressure AB2 alloy in a second or third stage, substantially increasing the achievable overall compression ratio, as demonstrated effectively in three-stage configurations (Galvis E et al., 2020; Vanhanen et al., 1999). Karagiorgis et al. (2017) reported the design, construction, and operation of a six-stage prototype and documented the practical engineering challenges of heat-and-mass-transfer management within the hydride bed. More recent alloy-development work has pushed achievable delivery pressures substantially higher: Ha et al. (2023) reported a two-stage compressor using Ti-Zr-Cr-Mn-V C14 Laves-phase alloys compressing hydrogen from 1 to 30 MPa across a 20-150 °C temperature swing, while Li et al. (2024) developed Ti-Zr-Mn-based alloys specifically optimized for an 865 bar two-stage system and used a fugacity-corrected Van't Hoff formulation to improve the accuracy of the predicted plateau

pressure at very high pressure. Cao et al. (2021) investigated Ti-Zr-Cr-Fe-V alloys for compressors operating at moderate temperatures. Bellosta von Colbe et al. (2019), in a widely cited review, catalogued the achievements and outstanding engineering challenges across the full range of hydride-based storage and compression concepts, while Jensen et al. (2021) discuss the specific challenges of scaling such systems from laboratory prototypes to real-scale deployment. The underlying thermally driven sorption principle has also been deployed well beyond compression, from solar thermal energy storage (Corgnale et al., 2014) to cryocooler compressors flown on the Planck space telescope (Bowman, 2019). Techno-economic analyses have also examined the cost-competitiveness of metal hydride compression with mechanical alternatives: Corgnale and Sulic (2018) coupled a steady-state mass-and-energy-balance model to an economic model for high-pressure systems, and Stamatakis et al. (2018) reviewed the technology's developmental status and early commercial markets. Most recently, Fleming et al. (2026) proposed a conceptually distinct compressor design in which hydrogen itself, rather than a secondary heat-transfer fluid, is circulated in direct convective contact with the hydride bed, reporting substantially improved specific productivity relative to conventional wall-limited heat-transfer designs. While their analysis relied on system simulations, physical testbeds closely related to this concept from the same research group are the origin of the open dataset used in the present study.

A separate line of work has begun to apply machine learning methods across the hydrogen value chain, motivated in each case by the same underlying bottleneck that motivates this study: physics-based models of hydrogen systems are often too slow, too dependent on tuned constitutive parameters, or too data-hungry in their density functional theory (DFT) or first-principles form to be practical for design iteration, control, or real-time

monitoring. Bhattacharjee et al. (2025) combined unsupervised autoencoder feature learning with a deep multilayer perceptron to predict hydrogen storage capacities in metal hydrides directly from elemental descriptors, reporting close agreement with density-functional-theory benchmarks at a fraction of the computational cost. Broader reviews by van der Laag et al. (2026), Quintanilla et al. (2025), and Mukelabai et al. (2024) map the growing use of predictive modeling and hybrid physics-machine-learning methods across the hydrogen value chain, with van der Laag et al. (2026) explicitly noting limited uptake to date of physics-informed approaches as a specific gap for future work. Ding et al. (2024) and Du et al. (2025) document a parallel expansion of machine learning use in hydrogen production and electrocatalyst design specifically. Within this broader context, however, very few studies apply sequence models such as recurrent neural networks or temporal convolutional networks to the transient, cycle-resolved operational data of a physical hydrogen storage or compression device; the present study's use of a two-stage MHHC's second-by-second sensor record, rather than a static materials-descriptor dataset, is comparatively unusual in this literature and more closely related to time-series surrogate modeling practice in other engineering energy systems, where temporal convolutional network architectures using dilated causal convolutions have been shown to match or exceed the forecasting accuracy of recurrent architectures such as the Long Short-Term Memory network at substantially lower training cost (Hochreiter & Schmidhuber, 1997; Lara-Benítez et al., 2020).

The physics-informed neural network, introduced in its now-standard form by Raissi et al. (2019) and situated within the broader physics-informed machine learning paradigm by Karniadakis et al. (2021) and, more recently, Meng et al. (2025), augments the conventional data-fitting loss of a neural network with an additional term that penalizes violation of a known

governing equation, evaluated either at collocation points or, as in the present study, directly on the network's own output. The approach has been applied extensively in fluid mechanics (Cai et al., 2021; Sharma et al., 2023; Sun et al., 2020), structural and manufacturing engineering (Xu et al., 2023; Zobeiry & Humfeld, 2021), and power systems (Huang & Wang, 2023), and has been extended toward reduced-order modeling (Chen et al., 2021), uncertainty quantification (Yang & Perdikaris, 2019), and alternative representation models that combine physics residuals with more expressive base networks, such as Kolmogorov-Arnold network variants (Toscano et al., 2025).

A recurring theme across recent reviews, however, is that the practical benefit of a physics-informed constraint is highly problem-dependent: Farea et al. (2024) note that PINNs can struggle with stiff or multi-scale systems, so their theoretical generalization advantages still require rigorous validation. Separately, the broader machine learning reproducibility literature has established that comparisons based on a single training run, without repetition across random seeds, are insufficiently powered to distinguish a genuine algorithmic improvement from ordinary training-stochasticity variance (Henderson et al., 2018). Kapoor and Narayanan (2023), in a large-scale audit of machine-learning-based scientific claims across seventeen research fields, identify data leakage and inadequately validated performance claims as pervasive and field-general failure modes, and explicitly recommend the kind of leakage-safe data splitting and rigorous validation protocol that this study adopts. The present study is, to the authors' knowledge, the first to apply this level of statistical scrutiny, including a genuine material-holdout extrapolation test, to a physics-informed neural network for a metal hydride hydrogen compression system, and its findings are discussed in direct

relation to this broader methodological literature rather than in isolation.

3. MATERIALS AND METHODS

3.1. Dataset

The experimental data used in this study describe a laboratory-scale, two-stage, exchangeable-vessel metal hydride hydrogen compressor instrumented with an independent heat-transfer-fluid circuit (Fleming, 2026). The dataset comprises 29 controlled cycling experiments in which one or both compressor stages were charged with one of three hydride materials: MmNiFe (an AB5-type mischmetal-nickel alloy, 12 experiments), TiZrMn (an AB2-type alloy, 11 experiments), and TiCrMn (an AB2-type alloy, 6 experiments). Each experiment record contains second-by-second measurements of feed and stage pressures (five channels, of which one, located near an auxiliary reference tank, is not used in operation and was excluded), two heat-transfer-fluid temperature channels, two heat-transfer-fluid mass-flow channels, three hydrogen mass-flow-controller channels, and twelve spatially distributed bed-temperature sensors, six per stage. A companion hydrogen mass-balance sheet reports, per experiment and per stage, the loaded hydride mass, the theoretical gravimetric capacity, and the total hydrogen mass absorbed and desorbed per cycle, together with the elapsed time boundaries of each absorption and desorption phase. A separate pressure-composition-isotherm (PCI) file reports isothermal absorption and desorption measurements for each of the three materials at multiple temperatures, which this study uses independently of the cycling data to derive the thermodynamic equilibrium relationship.

Two experiments (identified as Experiment 6 and Experiment 7 in the source dataset, both using the TiCrMn

material) were excluded from all analyses because the hydrogen mass-flow-controller channels required for model input were not recorded for these runs; the excluded-experiment identifiers and the specific missing channels are logged programmatically and reported in full in the accompanying analysis code. The final modeling dataset therefore comprises 27 experiments. A data-quality validation step, in which each available flow-sensor channel was numerically integrated over each reported absorption or desorption phase and compared against the hydrogen mass independently reported in the mass-balance sheet, confirmed that the dedicated mass-flow-controller channel (median relative error 6.9% against the reported mass) is the physically meaningful hydrogen-flow signal; the remaining flow channels examined, of which two are evidently associated with the heat-transfer-fluid circuit rather than the hydrogen gas path, showed a median relative error at or above 98% against the reported hydrogen mass and were retained, where applicable, only as heat-transfer-fluid-side model inputs rather than as hydrogen-flow proxies.

3.2. Model Inputs, Targets, and Preprocessing

The model receives eight input channels at each time step: the two feed-side pressures, the two heat-transfer-fluid mass-flow channels, the two dedicated hydrogen mass-flow-controller channels, and the two heat-transfer-fluid temperature channels. The model predicts fourteen target channels: The Stage I and Stage II outlet pressures and the twelve spatially distributed bed-temperature sensors. All inputs and targets were standardized to zero mean and unit variance using scalers fit exclusively on the training partition, to prevent validation or test information from leaking into preprocessing. Sliding windows of sixty consecutive time steps were used as model input, with a prediction horizon of thirty subsequent time steps and a stride of five time steps between consecutive windows; windows were constructed

independently within each experiment and cycle and never span an experiment boundary.

The train, validation, and test partitions were constructed at the level of whole experiments rather than individual time windows, so that no two windows drawn from the same experiment could appear in different partitions; this experiment-blocked design directly prevents the autocorrelation-driven data leakage and sample nonindependence that a naive random or per-window split would introduce, a failure mode consistent with the broader taxonomy of leakage-driven overoptimism documented across the machine-learning-based science literature (Kapoor & Narayanan, 2023). A purely random experiment-level split can nonetheless leave an entire material completely absent from the test partition given the small number of experiments available per material, and an earlier iteration of this partitioning scheme was found to do exactly this. The reported partition therefore additionally stratifies the split by hydride material, allocating approximately 20% of each material's experiments to the test partition and 15% of the remainder to validation, subject to a minimum-representation rule that guarantees a material with only one or two eligible experiments is not left entirely without training or test coverage. Under this scheme, the training partition comprised 18 experiments, the validation partition 4 experiments, and the test partition 5 experiments, with all three hydride materials represented in each partition; a further explicit check confirmed that at least one experiment in which both compressor stages operated simultaneously was retained in the test partition, since the Stage II pressure target carries near-zero variance in single-stage-only experiments.

3.3. Model Architectures

Two neural network architectures were compared, sharing an identical input-output interface and differing only in the

presence of an intermediate temporal convolutional block and, for the physics-informed variant, the training loss. The baseline architecture is a multi-layer Long Short-Term Memory (LSTM) network (Hochreiter & Schmidhuber, 1997) that consumes the input sequence directly, followed by a fully connected head that maps the network's final hidden state, concatenated with a learned material-identity embedding, to the fourteen target channels across the thirty-step prediction horizon. The second architecture augments this baseline with a preceding temporal convolutional block using a dilated causal one-dimensional convolution with a residual connection (Bai et al., 2018). While standalone TCNs have recently been shown to be highly effective for energy-related time-series forecasting (Lara-Benítez et al., 2020), this study employs a hybrid TCN-LSTM architecture. In this design, the TCN block acts as a robust feature extractor that captures complex, multi-scale temporal patterns from the raw input, while the subsequent LSTM layer models the remaining sequential state transitions before mapping to the final prediction; this hybrid architecture is used as the base network for the physics-informed model. Both architectures condition their prediction on the hydride material identity of the active experiment through a small trainable embedding layer, allowing a single model to represent all three materials without being explicitly given the material's physical constants at inference time.

3.4. Physics-Informed Constraint

The physics-informed variant augments the standard mean-squared-error training loss with a soft penalty derived from the Van't Hoff equation, which relates the equilibrium hydrogen pressure of a metal hydride to its temperature through the reaction enthalpy and entropy of hydride formation (Lototskyy et al., 2014; Stamatakis et al., 2018):

$$\ln(P_eq) = -\Delta H/(RT) + \Delta S/R$$

where P_eq is the equilibrium pressure, ΔH and ΔS are the material-specific reaction enthalpy and entropy, R is the universal gas constant, and T is the absolute bed temperature. Material-specific values of ΔH and ΔS were obtained independently of the cycling data used for model training by fitting the Van't Hoff relationship to the pressure-composition-isotherm measurements provided for each material, using the region of minimum local slope in the logarithm of pressure against hydrogen content as the empirical plateau-pressure estimate at each measured isotherm temperature, a standard approach to plateau-pressure identification in metal hydride characterization (Vanhanen et al., 1999). This fitting procedure yielded reaction enthalpies of 21.3 and 26.6 kJ/mol (absorption and desorption, respectively) for TiZrMn, 23.9 and 23.6 kJ/mol for MmNiFe, and 17.4 and 16.1 kJ/mol for TiCrMn, all within the range reported in the broader metal hydride thermodynamics literature for AB2- and AB5-type alloys (Lototskyy et al., 2014; Yartys et al., 2016).

During training, the predicted Stage I outlet pressure at each time step within the prediction horizon is compared against the Van't Hoff equilibrium pressure evaluated at the corresponding predicted (for evaluation purposes, true) Stage I bed temperature and the active experiment's material identity. Because Stage I and Stage II bed temperatures move in near-opposite directions during simultaneous two-stage operation, reflecting the exothermic-endothermic coupling between the two stages, the physics constraint uses only the Stage I temperature sensors when evaluating the Stage I equilibrium relationship, rather than an average across both stages. The operating phase (absorption or desorption) at each time step is inferred from the sign of the local Stage I bed-temperature trend, since absorption is exothermic and desorption is endothermic. The penalty term is a hinge-type loss that penalizes the predicted pressure only when

it falls on the thermodynamically implausible side of the equilibrium curve for the inferred phase (below equilibrium during absorption, or above equilibrium during desorption), scaled to the same standardized units as the primary data-fitting loss so that the two loss components are directly comparable in magnitude; an earlier, unscaled formulation of this penalty was found to differ from the data-fitting loss by roughly three orders of magnitude, which required a correspondingly minuscule loss weight and risked rendering the physics term functionally negligible during optimization. Because the current formulation is scoped to the Stage I pressure target only, no equivalent constraint was applied to the Stage II pressure prediction in this study; extending the constraint to Stage II would require the material identity of each stage individually rather than a single experiment-level material label, and is identified as a direction for future work. The equilibrium pressure itself is treated as a fixed reference evaluated at the current predicted temperature rather than as a differentiable function of it, so that gradients propagate only through the predicted pressure term.

3.5. Hyperparameter Optimization and Training Protocol

Hyperparameters (hidden layer width, number of recurrent layers, temporal convolutional channel width, material-embedding dimension, dropout rate, learning rate, batch size, and, for the physics-informed model, the relative weight of the physics penalty) were tuned using the Tree-structured Parzen Estimator sampler implemented in the Optuna hyperparameter optimization framework (Akiba et al., 2019). The TPE algorithm provides a sequential, model-based refinement over the purely random-search baseline for hyperparameter selection established by Bergstra and Bengio (2012). During the search, a median-based early-pruning rule was applied to terminate unpromising trials, using the validation partition as the optimization objective. All

models were trained with the Adam optimizer, gradient-norm clipping, and a learning-rate reduction schedule triggered by validation-loss plateaus, with early stopping applied after a fixed number of epochs without validation improvement. Model weights, optimizer state, learning-rate-scheduler state, and the complete random-number-generator state (covering the Python, NumPy, and PyTorch CPU and GPU generators) were checkpointed at every improvement in validation loss and at fixed epoch intervals, allowing training to resume deterministically after an interruption; GPU convolution and recurrent-layer algorithms were configured in deterministic mode throughout, since the default GPU-optimized algorithms are not guaranteed to be bit-for-bit reproducible across runs even with an identical random seed, which would otherwise undermine the multi-seed statistical comparison described below.

3.6. Multi-Seed Statistical Validation and Extrapolation Testing

Because a single training run cannot distinguish a genuine difference between two model architectures from ordinary training-stochasticity variance arising from weight initialization and mini-batch ordering (Henderson et al., 2018), the comparison between the physics-informed and purely data-driven architectures was repeated across ten independent training seeds, each retrained from the same tuned hyperparameters. Overall predictive accuracy for each seed was summarized as a normalized root-mean-square error (NRMSE), computed by dividing the root-mean-square error of each of the fourteen target channels by that channel's own standard deviation in the test partition before averaging, which avoids conflating the physically incommensurate units of pressure (bar) and temperature (°C) into a single unscaled aggregate. The paired, per-seed NRMSE values for the two architectures were compared using a two-sided Wilcoxon signed-rank test, a standard non-parametric approach

widely established for algorithm evaluation in machine learning (Demšar, 2006), and a bootstrap (10,000 resamples) 95% confidence interval was constructed for the mean paired difference, providing an effect-size estimate that is not reducible to a binary significance verdict, given the acknowledged low statistical power of a ten-observation paired test.

In addition to this in-distribution comparison, a separate extrapolation test was conducted in which the TiCrMn material was withheld entirely from the training and validation partitions; both architectures were retrained from the same tuned hyperparameters using only the MmNiFe and TiZrMn experiments, and evaluated exclusively on the held-out TiCrMn experiments. This test directly addresses a specific, testable hypothesis: because the physics-informed model's Van't Hoff constraint is derived from independent pressure-composition-isotherm data rather than from the training labels, it applies in principle to a material the network's learned material-embedding representation has never encountered during training, whereas the purely data-driven baseline has no comparable mechanism for representing an unseen material's thermodynamic behavior.

3.7. Physical Plausibility Diagnostic

As a complementary, accuracy-independent evaluation, the predicted Stage I outlet pressure from each trained model was compared against the Van't Hoff equilibrium pressure evaluated at the true (measured) Stage I bed temperature at the corresponding time step, using the same hinge-type violation, now applied diagnostically to already-trained models' test-set predictions rather than as a training loss. This yields, for each model, a distribution of physically-implausible-prediction magnitudes that is independent of the model's point-forecast error and answers a distinct question from the accuracy comparison: whether a model's predictions, right or wrong, tend to remain

closer to or further from what is thermodynamically achievable for the given material and temperature.

4. RESULTS

4.1. Dataset Characterization and Data Quality Validation

Figure 1 shows the distribution of hydride material assignments across the 29 experiments in the source dataset, confirming that all three materials are represented across a range of experimental conditions and that no single material dominates the dataset. Figure 2 presents representative pressure and mean bed-temperature time series for two example experiments, illustrating both the overall cycling behavior of the compressor and the characteristic near-mirror-image relationship between Stage I and Stage II bed temperature that arises during simultaneous two-stage operation. This pattern directly motivated the stage-specific treatment of the physics-informed constraint.

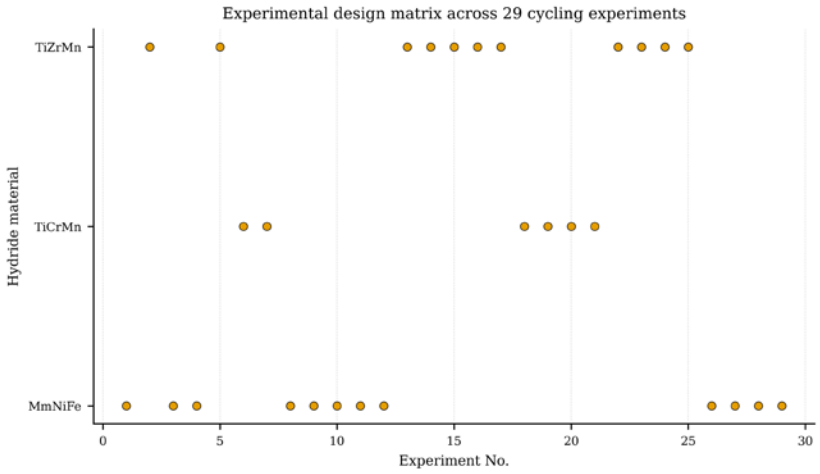

Figure 1. Experimental design matrix showing hydride material assignment across the 29 cycling experiments in the source dataset.

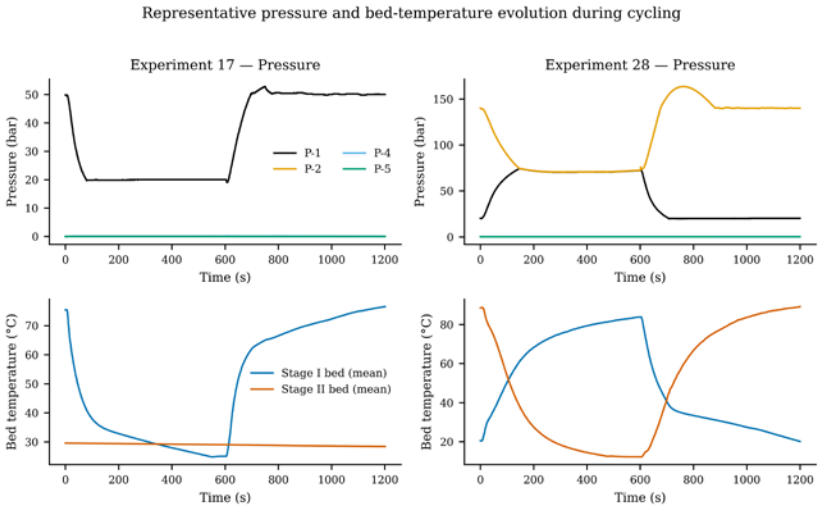

Figure 2. Representative pressure and mean bed-temperature time series for two example experiments, illustrating the near-mirror-image relationship between Stage I and Stage II bed temperature during simultaneous two-stage operation.

Figure 3 shows the progression of the Optuna hyperparameter search across successive trials, illustrating the convergence of the validation loss objective as the Tree-structured Parzen Estimator sampler concentrated its search around increasingly promising regions of the hyperparameter space. Figure 4 shows the training and validation loss curves for both the physics-informed and purely data-driven architectures using the tuned hyperparameters, confirming that both models converged without evidence of divergence or instability during training.

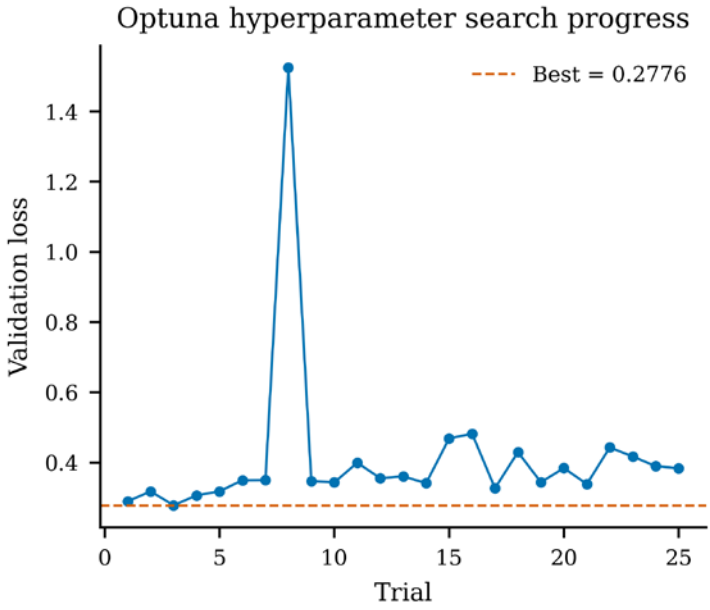

Figure 3. Validation-loss progression across successive Optuna hyperparameter search trials.

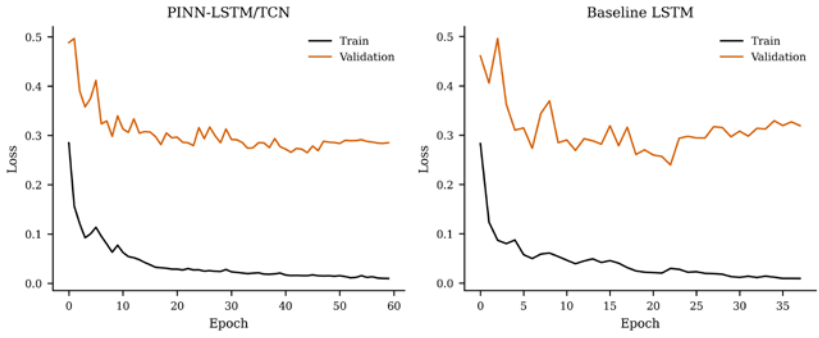

Figure 4. Training and validation loss curves for the PINN-LSTM/TCN and baseline LSTM architectures.

Figure 5 presents the outcome of the hydrogen mass-balance data-quality validation: integrating the dedicated hydrogen mass-flow-controller channel over each reported

absorption or desorption window reproduces the independently reported hydrogen mass with a median relative error of 6.9%, whereas the remaining flow channels examined showed median relative errors at or above 98%, confirming that these auxiliary channels are not suitable proxies for hydrogen mass flow and, where associated with the heat-transfer-fluid circuit, should be interpreted as heat-transfer-fluid-side measurements instead.

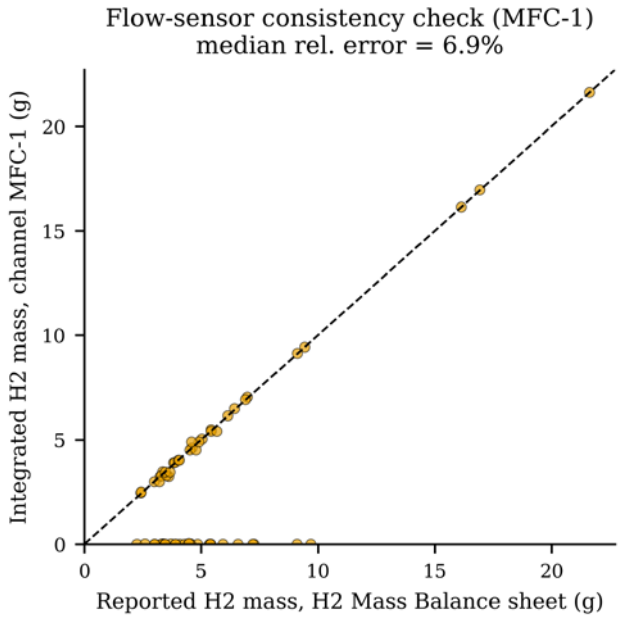

Figure 5. Data-quality validation: integrated hydrogen mass-flow-controller signal compared against independently reported hydrogen mass balance.

4.2. In-Distribution Model Comparison

Table 1 summarizes the overall (mean-across-target) predictive accuracy of the physics-informed LSTM/TCN model, the purely data-driven baseline LSTM model, and a naive persistence baseline that propagates the last observed value of each target forward across the prediction horizon, evaluated on

the held-out test partition using the primary (first-seed) trained model of each architecture.

Table 1. Overall test-set accuracy, primary trained model (normalized root-mean-square error, NRMSE; normalized mean absolute error, NMAE; coefficient of determination, R^2; lower NRMSE/NMAE and higher R^2 indicate better performance).

Model	NRMSE	NMAE	R^2
Naive persistence	0.083	0.035	0.993
PINN-LSTM/TCN	0.347	0.230	0.848
Baseline LSTM	0.367	0.250	0.831

Both trained models achieve a mean R^2 of 0.83-0.85 averaged across all fourteen target channels, though per-channel R^2 varies considerably, from approximately 0.48-0.50 for the Stage I outlet pressure and one bed-temperature sensor to approximately 0.94-0.98 for the best-predicted temperature channels, with the Stage II bed-temperature sensors generally predicted more accurately than the Stage I sensors for both architectures; the naive persistence baseline nonetheless substantially outperforms both trained models on the aggregate metric. This reflects the short (thirty-step) prediction horizon relative to the characteristic timescale of pressure and temperature evolution in the compressor, under which a simple zero-order-hold forecast is already a strong predictor; the practical value of a trained surrogate model in this application is therefore better understood in terms of its ability to anticipate genuine departures from the recent trend, and its substantially lower computational cost relative to a coupled thermal-hydraulic simulation, than in terms of an aggregate accuracy metric computed over a short horizon dominated by slowly evolving state variables. Figure 6 presents parity plots comparing predicted and true values for the Stage I outlet pressure, the Stage II outlet pressure, and the mean bed temperature, for both trained architectures. Figure 7 shows the distribution of Stage I pressure prediction residuals for both architectures.

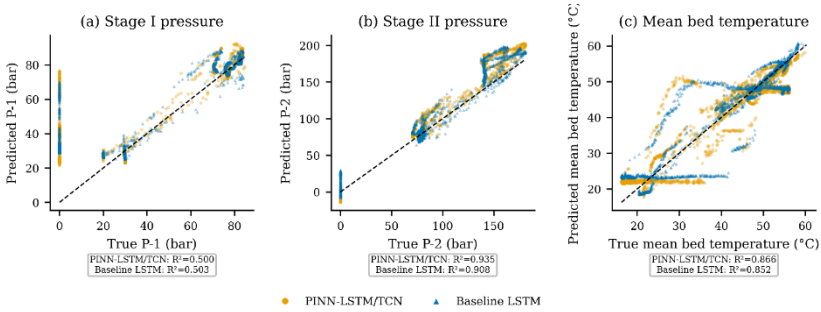

Figure 6. Parity plots of predicted versus true values for Stage I pressure, Stage II pressure, and mean bed temperature, for both trained architectures.

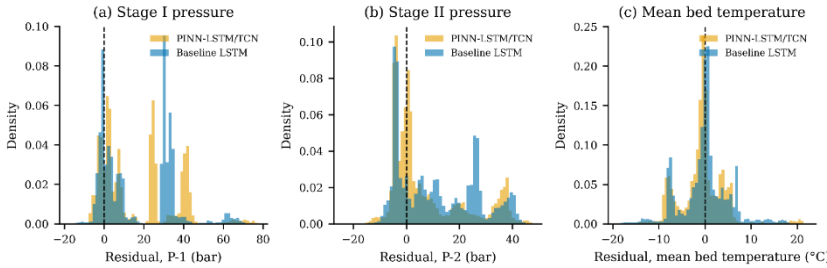

Figure 7. Distribution of Stage I pressure prediction residuals for both trained architectures.

4.3. Multi-Seed Statistical Validation

Table 2 reports the overall NRMSE achieved by each architecture across ten independently seeded training repetitions, using identical tuned hyperparameters and identical experiment-blocked, material-stratified data partitions in every repetition.

Table 2. Overall test-set NRMSE across ten independent training seeds.

Seed	PINN-LSTM/TCN	Baseline LSTM
1	0.347	0.367
2	0.358	0.373
3	0.351	0.328
4	0.322	0.299
5	0.352	0.357
6	0.304	0.341
7	0.350	0.364
8	0.327	0.363
9	0.334	0.332
10	0.330	0.355
Mean ± SD	0.338 ± 0.017	0.348 ± 0.023

The physics-informed model achieved a lower NRMSE than the purely data-driven baseline in seven of the ten seeds, with a mean paired difference of -0.0104 (physics-informed minus baseline; negative values favor the physics-informed model) and a 95% bootstrap confidence interval of [-0.022, 0.003], corresponding to an approximate 3.0% relative reduction in mean NRMSE. A two-sided Wilcoxon signed-rank test on the paired per-seed NRMSE values did not reach conventional statistical significance ($W = 14.0$, $p = 0.193$). The direction and approximate magnitude of this effect were consistent between an earlier five-seed subset of this analysis (four of five seeds favoring the physics-informed model, mean difference -0.0123) and the full ten-seed result reported here, suggesting that the small observed advantage of the physics-informed model, while not statistically confirmed at this sample size, is unlikely to be purely a sampling artifact of any single training repetition; a larger number of training repetitions than was computationally practical for this study would be required to determine conclusively whether this difference reaches statistical significance.

4.4. Out-of-Distribution Extrapolation Test

Table 3 reports the overall test-set accuracy of both architectures when the TiCrMn material is withheld entirely from training and validation, and both models are evaluated exclusively on TiCrMn experiments never seen during training.

Table 3. Overall test-set accuracy under material-holdout extrapolation (TiCrMn withheld from training).

Model	NRMSE	R^2
Baseline LSTM	3.690	-52.6
PINN-LSTM/TCN	4.941	-89.8

Both architectures perform very poorly under this genuine extrapolation condition, with strongly negative R^2 values indicating that neither model's predictions are competitive with simply predicting the mean of the held-out material's target distribution. This reflects the magnitude of the distribution shift involved: at a representative bed temperature of 50 °C, the Van't Hoff equilibrium pressure derived from the pressure-composition-isotherm data is approximately 148 bar for TiCrMn, compared to approximately 33 bar for the two materials seen during training, a more than fourfold difference in the characteristic operating pressure of the withheld material. Extrapolating to an operating regime this far outside the training distribution is a considerably more demanding test than is typically applied to physics-informed models in the applied literature, and the poor absolute performance of both architectures under it should be interpreted as an expected consequence of the severity of this shift rather than as evidence of a training or implementation failure. Within this shared regime of poor absolute performance, however, the physics-informed model performs materially worse than the purely data-driven baseline, with an NRMSE approximately 34% higher. This result does not support the hypothesis that the physics-informed model's independently derived thermodynamic constraint would provide

a meaningful advantage under genuine material extrapolation; a possible explanation is that the encoder layers of both architectures receive input features (feed pressures and mass flows) that are themselves far outside their training range for the held-out material, such that the internal representations available to the physics constraint at the point where it acts on the network's output are already poorly calibrated, limiting the constraint's ability to correct the resulting prediction.

4.5. Physical Plausibility Analysis

Table 4 reports the physical-plausibility diagnostic, applied to the in-distribution test-set predictions of both trained architectures and the naive persistence baseline.

Table 4. Physical plausibility of Stage I pressure predictions relative to the Van't Hoff equilibrium curve (violation magnitude in bar; 0 indicates a physically plausible prediction; percentage of predictions exceeding a 5 bar violation threshold).

Model	Mean violation (bar)	Median violation (bar)	Predictions exceeding 5 bar violation
Naive persistence	16.7	5.5	50.3%
Baseline LSTM	13.2	11.8	58.9%
PINN-LSTM/TCN	11.1	10.5	59.4%

The physics-informed model produces predictions with a lower mean and median deviation from the Van't Hoff equilibrium curve than the purely data-driven baseline, corresponding to an approximate 16% reduction in mean violation magnitude and an approximate 10% reduction in median violation magnitude, even though, its point-forecast accuracy is not significantly better. The proportion of predictions exceeding the 5 bar violation threshold, however, is essentially identical between the two trained models, indicating that the

physics-informed constraint reduces the typical size of a thermodynamically implausible prediction without materially reducing how often such a prediction occurs. Figure 8 shows the full distribution of violation magnitudes for both trained architectures.

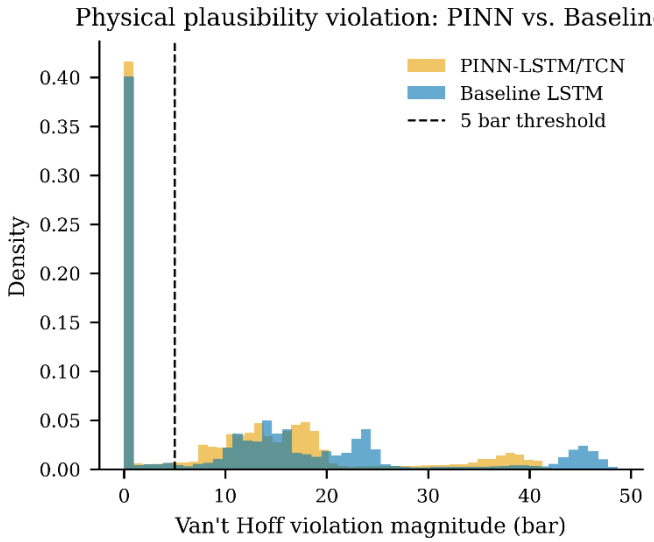

Figure 8. Distribution of Van't Hoff equilibrium violation magnitudes for both trained architectures.

5. DISCUSSION

The central methodological contribution of this study is not the specific numerical result that a physics-informed constraint failed to improve in-distribution accuracy significantly, but the demonstration, through a fully reported multi-seed and extrapolation testing protocol, of how readily such a claim can be either confirmed or overturned depending on the rigor of the evaluation applied to it. Had this study reported only the single-run comparison summarized in Table 1, in which the physics-informed model achieves a numerically lower NRMSE and

higher R^2 than the baseline, it would have been entirely consistent with a substantial fraction of the published physics-informed neural network literature to report this as evidence of the physics constraint's value. The ten-seed repetition shows that this single-run advantage is directionally consistent but statistically inconclusive, and the material-holdout extrapolation test shows that the same constraint that produced a marginal in-distribution advantage produces a clear disadvantage under genuine distribution shift. This pattern is consistent with the broader reproducibility literature: the vulnerability to single-run stochasticity echoes the concerns raised by Henderson et al. (2018) in the context of deep reinforcement learning, while the fragility under genuine distribution shift aligns with the field-general overoptimism documented across machine-learning-based science by Kapoor and Narayanan (2023). It suggests that the routine adoption of multi-seed statistical testing and genuine out-of-distribution evaluation, standard practice in only a minority of applied physics-informed neural network studies to date, would likely change the reported conclusions of at least some published comparisons in this area.

A plausible technical explanation for the absence of a robust in-distribution advantage is that the LSTM/TCN encoder, trained on cycling data spanning three distinct hydride materials and a range of feed pressures and temperatures, already learns an adequate implicit approximation of the pressure-temperature relationship governing hydride equilibrium from the data alone, such that an explicit thermodynamic penalty contributes comparatively little additional information within the training distribution; this would be consistent with the general expectation, noted in the physics-informed machine learning literature (Farea et al., 2024; Karniadakis et al., 2021), that physics constraints are most valuable precisely in data-scarce or out-of-distribution regimes rather than in well-sampled

interpolative settings. The extrapolation result, however, complicates a simple version of this expectation: the physics-informed model's disadvantage under material holdout suggests that a soft, output-level thermodynamic penalty is not, on its own, sufficient to compensate for an encoder whose learned internal representation is itself poorly calibrated to input features (feed pressure and mass flow) that lie far outside the range seen during training for the withheld material. This suggests that a stronger form of physics-informed architecture, in which the physical constraint is embedded earlier in the network, or the input feature normalization is itself made physics-aware, might be necessary to realize an extrapolation benefit, rather than a purely output-level penalty of the kind implemented here.

The physical-plausibility result offers a more encouraging, if narrower, finding: the physics-informed model's predictions deviate less, on average, from the underlying thermodynamic equilibrium curve than the purely data-driven baseline's predictions, even though the two models are statistically indistinguishable on point-forecast accuracy. For applications in which the downstream use of a surrogate model's output includes automated safety or operational-limit checking, a systematic reduction in the typical magnitude of thermodynamically implausible predictions may be of practical value independent of whether it improves a conventional forecast-accuracy metric. However, the present study's finding that the frequency of large violations was not correspondingly reduced indicates that this benefit should not be overstated.

Beyond the physics-informed comparison, the data-driven LSTM/TCN and baseline LSTM surrogate models themselves achieve a mean R^2 of 0.83-0.85 across fourteen physically heterogeneous target channels (individual channels ranging from approximately 0.48 to approximately 0.98), using second-by-second sensor data from an experimental compressor rig rather

than a physics-based simulation. By construction, this inference step executes at a small fraction of the computational cost of the detailed dynamic system-level models typically required to capture such transient behaviour (Dornheim et al., 2022), allowing dynamic operational analysis to be conducted at speeds traditionally reserved for simplified steady-state techno-economic screening (Corgnale & Sulic, 2018). This supports the use of either architecture as a practical surrogate for rapid design-space exploration, control-oriented digital-twin applications, or preliminary fault-anticipation studies in two-stage metal hydride hydrogen compressor systems, independent of the physics-informed comparison that is the primary methodological focus of this study.

6. CONCLUSION

This study developed a deep learning surrogate model for the transient thermal-hydraulic behavior of a two-stage, exchangeable-vessel metal hydride hydrogen compressor, using an openly licensed experimental dataset spanning three hydride materials, and evaluated whether augmenting this surrogate with a physics-informed Van't Hoff equilibrium constraint improves its predictive performance. Using an experiment-blocked, material-stratified data-splitting protocol, ten independently seeded training repetitions, a paired statistical significance test with an accompanying bootstrap confidence interval, and a genuine material-holdout extrapolation test, this study finds that the physics-informed constraint produces a small, directionally consistent but not statistically significant improvement in in-distribution point-forecast accuracy, a materially worse result under genuine out-of-distribution extrapolation to an unseen hydride material, and a modest, statistically uncharacterized improvement in the physical plausibility of its predictions relative

to the underlying thermodynamic equilibrium curve. These mixed and, in the extrapolation case, negative findings are reported transparently alongside the purely data-driven surrogate model's own strong performance, which achieves a mean R^2 of 0.83-0.85 across all fourteen predicted state variables, with individual-channel R^2 ranging from approximately 0.48 to approximately 0.98.

Several limitations of this study should be considered when interpreting these findings. First, the physics-informed constraint implemented here is scoped to the Stage I outlet pressure only, using a single, experiment-level material label; extending an equivalent constraint to the Stage II pressure target would require associating each compressor stage with its own material identity, which the present dataset supports through its hydrogen mass-balance records but which was not implemented in this study. Second, the Van't Hoff plateau-pressure estimates used to parameterize the physics constraint, while derived using a standard minimum-slope plateau-detection method, rely on isotherm data spanning a narrower temperature range and fewer measured isotherms for the TiCrMn material than for the other two materials, which may reduce the reliability of the physics constraint specifically for this material and may be relevant to interpreting the extrapolation result, since TiCrMn is also the material withheld in that test. Third, the phase-labeling heuristic used to determine whether the physics constraint should be evaluated in absorption or desorption mode is derived from the sign of the local bed-temperature trend rather than from the compressor's logged valve or operational state; although this is a thermodynamically well-motivated proxy, it has not been independently validated against the source dataset's operational logs. Fourth, the multi-seed statistical comparison, while a substantial improvement over a single-run comparison, remains based on ten training repetitions; a larger number of repetitions

would provide a more statistically powerful test of whether the observed directional advantage of the physics-informed model reaches conventional significance, at a correspondingly higher computational cost. Fifth, the material-holdout extrapolation test examines a single held-out material under a single random seed for each architecture; a fuller leave-one-material-out cross-validation, repeated across multiple seeds for each held-out material, would provide stronger evidence regarding the generality of the extrapolation finding reported here. Sixth, the mean R^2 reported for the data-driven surrogate models conceals considerable variation across individual target channels: the Stage I outlet pressure and one Stage I bed-temperature sensor are predicted substantially less accurately (R^2 of approximately 0.48-0.50 for both architectures) than the remaining channels, and this weaker performance for exactly the target that the physics-informed constraint is designed to act on may itself be relevant to why the constraint's benefit was limited and inconsistent in this study; identifying and addressing the source of this channel-specific difficulty is a natural priority for future refinement of the surrogate model.

Future work could address these limitations directly, and could additionally examine whether a harder or more expressive physics constraint, or a physics-informed architecture in which thermodynamic information is incorporated earlier in the network rather than only as an output-level penalty, can realize the extrapolation benefit that the present soft, output-level formulation did not. The methodological protocol demonstrated in this study, and in particular its combination of multi-seed statistical testing with genuine extrapolation evaluation, is offered as a template that the applied physics-informed neural network literature could adopt more broadly to distinguish genuine algorithmic improvements from single-run artifacts. The resulting data-driven surrogate model is, independent of the physics-

informed comparison, a practical and computationally inexpensive tool for design-space exploration and control-oriented modeling of two-stage metal hydride hydrogen compression systems.

Data Availability

The dataset is publicly available on Zenodo repository at doi: 10.5281/zenodo.19036733.

Declaration of Competing Interests

The authors declare no known competing financial interests or personal relationships that could have appeared to influence the work reported in this paper.

REFERENCES

Akiba, T., Sano, S., Yanase, T., Ohta, T., & Koyama, M. (2019). *Optuna: A Next-generation Hyperparameter Optimization Framework* Proceedings of the 25th ACM SIGKDD International Conference on Knowledge Discovery & Data Mining, Anchorage, AK, USA. https://doi.org/10.1145/3292500.3330701

Bai, S., Kolter, J. Z., & Koltun, V. (2018). An Empirical Evaluation of Generic Convolutional and Recurrent Networks for Sequence Modeling. *ArXiv, abs/1803.01271*. https://doi.org/10.48550/arXiv.1803.01271

Bellosta von Colbe, J., Ares, J.-R., Barale, J., Baricco, M., Buckley, C., Capurso, G., Gallandat, N., Grant, D. M., Guzik, M. N., Jacob, I., Jensen, E. H., Jensen, T., Jepsen, J., Klassen, T., Lototskyy, M. V., Manickam, K., Montone, A., Puszkiel, J., Sartori, S.,…Dornheim, M. (2019). Application of hydrides in hydrogen storage and compression: Achievements, outlook and perspectives. *International Journal of Hydrogen Energy*, *44*(15), 7780–7808. https://doi.org/10.1016/j.ijhydene.2019.01.104

Bergstra, J., & Bengio, Y. (2012). Random search for hyper-parameter optimization. *J. Mach. Learn. Res.*, *13*(null), 281–305.

Bhattacharjee, S., Das, P., Ram, S., & Lee, S.-C. (2025). A Hybrid Machine Learning Framework for Predicting Hydrogen Storage Capacities in Metal Hydrides: Unsupervised Feature Learning with Deep Neural Networks. *ACS Applied Materials & Interfaces*, *17*(20), 29681–29694. https://doi.org/10.1021/acsami.5c03612

Bowman, R. C. (2019). Metal Hydride Compressors with Gas-Gap Heat Switches: Concept, Development, Testing, and Space Flight Operation for the Planck Sorption Cryocoolers. *Inorganics*, *7*(12), 139. https://doi.org/10.3390/inorganics7120139

Cai, S., Mao, Z., Wang, Z., Yin, M., & Karniadakis, G. E. (2021). Physics-informed neural networks (PINNs) for fluid mechanics: a review. *Acta Mechanica Sinica*, *37*(12), 1727–1738. https://doi.org/10.1007/s10409-021-01148-1

Cao, Z., Zhou, P., Xiao, X., Zhan, L., Li, Z., Wang, S., & Chen, L. (2021). Investigation on Ti–Zr–Cr–Fe–V based alloys for metal hydride hydrogen compressor at moderate working temperatures. *International Journal of Hydrogen Energy*, *46*(41), 21580–21589. https://doi.org/10.1016/j.ijhydene.2021.03.247

Chen, W., Wang, Q., Hesthaven, J. S., & Zhang, C. (2021). Physics-informed machine learning for reduced-order modeling of nonlinear problems. *Journal of Computational Physics*, *446*, 110666. https://doi.org/10.1016/j.jcp.2021.110666

Corgnale, C., Hardy, B., Motyka, T., Zidan, R., Teprovich, J., & Peters, B. (2014). Screening analysis of metal hydride based thermal energy storage systems for concentrating solar power plants. *Renewable and Sustainable Energy Reviews*, *38*, 821–833. https://doi.org/10.1016/j.rser.2014.07.049

Corgnale, C., & Sulic, M. (2018). Techno-Economic Analysis of High-Pressure Metal Hydride Compression Systems. *Metals*, *8*(6), 469. https://doi.org/10.3390/met8060469

Demšar, J. (2006). Statistical Comparisons of Classifiers over Multiple Data Sets. *J. Mach. Learn. Res.*, *7*, 1–30.

Ding, R., Chen, J., Chen, Y., Liu, J., Bando, Y., & Wang, X. (2024). Unlocking the potential: machine learning applications in electrocatalyst design for electrochemical hydrogen energy transformation. *Chem Soc Rev*, *53*(23), 11390–11461. https://doi.org/10.1039/d4cs00844h

Dornheim, M., Baetcke, L., Akiba, E., Ares, J.-R., Autrey, T., Barale, J., Baricco, M., Brooks, K., Chalkiadakis, N., Charbonnier, V., Christensen, S., Bellosta von Colbe, J., Costamagna, M., Dematteis, E., Fernández, J.-F., Gennett, T., Grant, D., Heo, T. W., Hirscher, M.,…Zoulias, E. (2022). Research and development of hydrogen carrier based solutions for hydrogen compression and storage. *Progress in Energy*, *4*(4), 042005. https://doi.org/10.1088/2516-1083/ac7cb7

Du, X., Gao, S., & Yang, G. (2025). Machine Learning Applications in Gray, Blue, and Green Hydrogen Production: A Comprehensive Review. *Gases*, *5*(2), 9. https://doi.org/10.3390/gases5020009

Farea, A., Yli-Harja, O., & Emmert-Streib, F. (2024). Understanding Physics-Informed Neural Networks: Techniques, Applications, Trends, and Challenges. *AI*, *5*(3), 1534–1557. https://doi.org/10.3390/ai5030074

Fleming, L. (2026). *Experimental Dataset for a Two-Stage Metal Hydride Hydrogen Compressor* (Version v1.2) Zenodo. https://doi.org/10.5281/zenodo.19036733

Fleming, L., Passing, M., Puszkiel, J., Klassen, T., & Jepsen, J. (2026). A Metal Hydride Compressor Concept using Hydrogen as a Heat Transfer Fluid. *Communications Engineering*, *5*(1), 49. https://doi.org/10.1038/s44172-026-00615-6

Galvis E, A. R., Leardini, F., Ares, J. R., Cuevas, F., & Fernandez, J. F. (2020). Experimental behaviour of a three-stage metal hydride hydrogen compressor. *Journal of Physics: Energy*, *2*(3), 034006. https://doi.org/10.1088/2515-7655/ab869e

Ha, T., Shukla, V., Na, T., Cho, Y. W., Suh, J.-Y., Shim, J.-H., & Lee, Y.-S. (2023). Development and optimization of a two-stage metal hydride hydrogen compressor with AB2-type alloys. *International Journal of Hydrogen Energy*, *48*(100), 39954–39966. https://doi.org/10.1016/j.ijhydene.2023.08.180

Henderson, P., Islam, R., Bachman, P., Pineau, J., Precup, D., & Meger, D. (2018). *Deep reinforcement learning that matters* Proceedings of the Thirty-Second AAAI Conference on Artificial Intelligence and Thirtieth Innovative Applications of Artificial Intelligence Conference and Eighth AAAI Symposium on Educational Advances in Artificial Intelligence, New Orleans, Louisiana, USA.

Hochreiter, S., & Schmidhuber, J. (1997). Long Short-Term Memory. *Neural Computation*, *9*(8), 1735–1780. https://doi.org/10.1162/neco.1997.9.8.1735

Huang, B., & Wang, J. (2023). Applications of Physics-Informed Neural Networks in Power Systems - A Review. *IEEE Transactions on Power Systems*, *38*(1), 572–588. https://doi.org/10.1109/TPWRS.2022.3162473

Jensen, E. H., Dornheim, M., & Sartori, S. (2021). Scaling up Metal Hydrides for Real-Scale Applications: Achievements, Challenges and Outlook. *Inorganics*, *9*(5), 37. https://doi.org/10.3390/inorganics9050037

Kapoor, S., & Narayanan, A. (2023). Leakage and the reproducibility crisis in machine-learning-based science. *Patterns*, *4*(9), 100804. https://doi.org/10.1016/j.patter.2023.100804

Karagiorgis, G., Christodoulou, C. N., von Storch, H., Tzamalis, G., Deligiannis, K., Hadjipetrou, D., Odysseos, M., Roeb, M., & Sattler, C. (2017). Design, development, construction and operation of a novel metal hydride compressor. *International Journal of Hydrogen Energy*, *42*(17), 12364–12374. https://doi.org/10.1016/j.ijhydene.2017.03.195

Karniadakis, G. E., Kevrekidis, I. G., Lu, L., Perdikaris, P., Wang, S., & Yang, L. (2021). Physics-informed machine learning. *Nature Reviews Physics*, *3*(6), 422–440. https://doi.org/10.1038/s42254-021-00314-5

Lara-Benítez, P., Carranza-García, M., Luna-Romera, J. M., & Riquelme, J. C. (2020). Temporal Convolutional Networks Applied to Energy-Related Time Series Forecasting. *Applied Sciences*, *10*(7), 2322. https://doi.org/10.3390/app10072322

Li, R., Penmathsa, A., Sun, T., Gallandat, N., Li, J., Park, J., Kim, H.-J., Kim, P., Yoon, N., Jang, J.-H., & Züttel, A. (2024). Development of Ti-Zr-Mn based AB2 type metal hydrides alloys for an 865 bar two-stage hydrogen compressor. *International Journal of Hydrogen Energy*, *72*, 687–693. https://doi.org/10.1016/j.ijhydene.2024.05.336

Lototskyy, M., & Linkov, V. (2022). Thermally driven hydrogen compression using metal hydrides. *International Journal of Energy Research*, *46*(15), 22049–22069. https://doi.org/10.1002/er.8189

Lototskyy, M. V., Yartys, V. A., Pollet, B. G., & Bowman, R. C. (2014). Metal hydride hydrogen compressors: A review. *International Journal of Hydrogen Energy*, *39*(11), 5818–5851. https://doi.org/10.1016/j.ijhydene.2014.01.158

Meng, C., Griesemer, S., Cao, D., Seo, S., & Liu, Y. (2025). When physics meets machine learning: a survey of physics-informed machine learning. *Machine Learning for Computational Science and Engineering*, *1*(1), 20. https://doi.org/10.1007/s44379-025-00016-0

Mukelabai, M. D., Barbour, E. R., & Blanchard, R. E. (2024). Modeling and optimization of renewable hydrogen systems: A systematic methodological review and machine learning integration. *Energy and AI*, *18*, 100455. https://doi.org/10.1016/j.egyai.2024.100455

Omid, M. A., Şahin, M. E., & Cora, Ö. N. (2024). Challenges and Future Perspectives on Production, Storage Technologies, and Transportation of Hydrogen: A Review. *Energy Technology*, *12*(4), 2300997. https://doi.org/10.1002/ente.202300997

Quintanilla, P., Elhalwagy, A., Duan, L., Masoudi Soltani, S., Lai, C. S., Foroudi, P., Huda, M. N., & Nandy, M. (2025). Artificial intelligence and robotics in the hydrogen lifecycle: A systematic review. *International Journal of Hydrogen Energy*, *113*, 801–817. https://doi.org/10.1016/j.ijhydene.2025.03.016

Raissi, M., Perdikaris, P., & Karniadakis, G. E. (2019). Physics-informed neural networks: A deep learning framework for solving forward and inverse problems involving nonlinear partial differential equations. *Journal of Computational Physics*, *378*, 686–707. https://doi.org/10.1016/j.jcp.2018.10.045

Sharma, P., Chung, W. T., Akoush, B., & Ihme, M. (2023). A Review of Physics-Informed Machine Learning in Fluid Mechanics. *Energies*, *16*(5), 2343. https://doi.org/10.3390/en16052343

Stamatakis, E., Zoulias, E., Tzamalis, G., Massina, Z., Analytis, V., Christodoulou, C., & Stubos, A. (2018). Metal hydride hydrogen compressors: Current developments & early markets. *Renewable Energy*, *127*, 850–862. https://doi.org/10.1016/j.renene.2018.04.073

Sun, L., Gao, H., Pan, S., & Wang, J.-X. (2020). Surrogate modeling for fluid flows based on physics-constrained deep learning without simulation data. *Computer Methods in Applied Mechanics and Engineering*, *361*, 112732. https://doi.org/10.1016/j.cma.2019.112732

Toscano, J. D., Oommen, V., Varghese, A. J., Zou, Z., Ahmadi Daryakenari, N., Wu, C., & Karniadakis, G. E. (2025). From PINNs to PIKANs: recent advances in physics-informed machine learning. *Machine Learning for Computational Science and Engineering*, *1*(1), 15. https://doi.org/10.1007/s44379-025-00015-1

van der Laag, R., Rizzato, A., Bäck, T., & Fan, Y. (2026). Machine learning for hydrogen technologies: A comprehensive review of challenges, opportunities, and emerging trends. *International Journal of Hydrogen Energy*, *197*, 152556. https://doi.org/10.1016/j.ijhydene.2025.152556

Vanhanen, J. P., Hagström, M. T., & Lund, P. D. (1999). Combined hydrogen compressing and heat transforming through metal hydrides. *International Journal of Hydrogen Energy*, *24*(5), 441–448. https://doi.org/10.1016/S0360-3199(98)00095-0

Xu, C., Cao, B. T., Yuan, Y., & Meschke, G. (2023). Transfer learning based physics-informed neural networks for solving inverse problems in engineering structures under different loading scenarios. *Computer Methods in Applied Mechanics and Engineering*, *405*, 115852. https://doi.org/10.1016/j.cma.2022.115852

Yang, Y., & Perdikaris, P. (2019). Adversarial uncertainty quantification in physics-informed neural networks. *Journal of Computational Physics*, *394*, 136–152. https://doi.org/10.1016/j.jcp.2019.05.027

Yartys, V. A., Lototskyy, M., Linkov, V., Grant, D., Stuart, A., Eriksen, J., Denys, R., & Bowman, R. C. (2016). Metal hydride hydrogen compression: recent advances and future prospects. *Applied Physics A*, *122*(4), 415. https://doi.org/10.1007/s00339-016-9863-7

Zobeiry, N., & Humfeld, K. D. (2021). A physics-informed machine learning approach for solving heat transfer equation in advanced manufacturing and engineering applications. *Engineering Applications of Artificial Intelligence*, *101*, 104232. https://doi.org/10.1016/j.engappai.2021.104232

FREIGHT TRANSPORT MODES, MODAL INTEGRATION, AND LOGISTICS SYSTEM DESIGN: EVIDENCE FROM TÜRKİYE AND THE WORLD[1]

Danışment VURAL[2]

1. INTRODUCTION

Freight transport is the physical link that converts geographically dispersed production, storage, and consumption activities into an operational supply chain. It affects delivered cost, lead time, inventory exposure, service reliability, market reach, and the environmental burden of economic activity. For this reason, transport mode choice is not merely the selection of a vehicle. It is a system-design decision involving infrastructure, terminals, shipment characteristics, schedules, handling requirements, contractual responsibility, and the risk profile of the entire movement. A mode that appears inexpensive when only line-haul charges are considered may become unattractive once access, transfer, waiting, inventory, damage, and delay costs are included.

The principal freight modes, which include road, rail, maritime, air, pipeline, and inland waterway transport, have markedly different technical and economic characteristics. Road transport offers dense network access and door-to-door flexibility; rail and waterways provide economies of scale;

---

1 This chapter is derived from the author's doctoral dissertation.

2 Asst. Prof. Dr., Atılım University, Faculty of Engineering, Department of Industrial Engineering, Ankara, Türkiye. ORCID: 0000-0003-4028-3810.

maritime transport enables high-capacity international trade; air transport serves high-value and time-critical flows; and pipelines provide continuous movement for a limited range of commodities. None is universally superior. Their suitability depends on shipment size, distance, value density, perishability, frequency, network availability, and the shipper's tolerance for variation in transit time.

The growing importance of containers and other standardized loading units has also shifted attention from isolated modes to integrated transport chains. Multimodal, intermodal, and combined transport are frequently used as if they were synonyms, although each term highlights a different feature of the transport operation. Conceptual ambiguity is not trivial: it affects statistical reporting, contract design, policy targets, terminal planning, and the interpretation of research results. Vural (2014) addresses these distinctions while developing a multimodal and combined transport model. The present chapter retains that conceptual foundation but rebuilds it with current terminology and recent evidence.

The purpose of this chapter is threefold. First, it clarifies the definitions and boundaries of the major freight transport concepts. Second, it compares the principal modes through a common decision framework. Third, it interprets recent evidence from the European Union and Türkiye while explicitly distinguishing incompatible measurement units and statistical scopes. This last point is important because tonnes, tonne-kilometres, twenty-foot equivalent units (TEU), cargo tonne-kilometres, and port-handling volumes answer different questions and cannot be combined without qualification. The chapter concludes by discussing the implications of modal integration for industrial engineering and logistics system design.

2. CONCEPTUAL FRAMEWORK

2.1. Freight Transport Mode

A freight transport mode can be defined as a technologically and institutionally distinct system for moving goods. It combines a guideway or operating environment, a vehicle or vessel, terminals or access points, operating rules, labour and control processes, and a characteristic cost–service structure. A truck on a road, a train on a railway, a vessel on a navigable waterway, an aircraft operating through airports, and a product flowing through a pipeline therefore represent different modes not simply because the vehicles differ, but because the supporting networks and operating logics differ.

This system perspective prevents an overly narrow comparison. Rail, for example, should not be evaluated only by the speed of a train between two terminals. Its complete service also includes collection, terminal handling, line haul, and final delivery. Maritime transport likewise depends on port access and on how efficiently cargo moves through the port to the hinterland. For a shipper, the relevant unit of analysis is the complete end-to-end logistics chain, not the isolated line-haul segment.

2.2. Multimodal, Intermodal, and Combined Transport

The 2026 Glossary for Transport Statistics treats multimodal transport as the broad category and intermodal transport as a particular form of multimodal movement (Eurostat, ITF & UNECE, 2026). In practical terms, multimodal transport means that goods are carried by two or more modes in one origin–destination movement. The term does not by itself require the goods to remain in the same loading unit, nor does it necessarily define the number of contracts or responsible parties. In legal usage, however, “multimodal transport” is often associated with

a single contract and a multimodal transport operator responsible for the whole movement.

Intermodal transport is more specific. The goods move in the same intermodal transport unit (for example, a container, swap body, or semi-trailer) or in the same road vehicle, and the goods themselves are not handled when the mode changes. The loading unit is transferred, but its contents remain undisturbed. This property reduces repeated handling, supports standardization, and makes rail–road, sea–road, and rail–sea chains operationally feasible. It also shifts the analytical focus from individual vehicles to terminals, transfer technology, loading-unit compatibility, and coordinated services.

Combined transport is generally understood in the European context as an intermodal operation in which the major part of the journey is performed by rail, inland waterway, or sea, while the initial and final road legs are kept as short as practicable. It is therefore a policy-relevant subset of intermodal transport, designed to preserve the accessibility of road transport while shifting the long-haul portion to modes with greater scale or lower external cost. Exact regulatory thresholds can vary by jurisdiction and programme.

Table 1. Core distinctions among integrated freight transport concepts

Concept	Minimum modal condition	Treatment of goods at transfer	Defining emphasis
Multimodal transport	Two or more modes	May or may not involve handling of the goods	The complete movement uses multiple modes; contractual structure should be stated separately.
Intermodal transport	Two or more successive modes	Goods remain in the same loading unit or road vehicle	Continuity of the loading unit and transfer between modes.
Combined transport	Intermodal operation	Goods remain in the same loading unit or road vehicle	Major leg by rail, inland waterway, or sea; road used mainly for short first/last legs.
Synchromodal transport	Multiple available modes	Usually unitized and dynamically assigned	Real-time, flexible mode and route selection within an integrated service network.

Sources: Vural (2014); Eurostat, ITF, and UNECE (2026). Note. Synchromodal transport is an emerging operational extension rather than a universally standardized legal category.

2.3. Measurement and Comparability of Freight Statistics

Freight statistics are frequently misinterpreted because different indicators measure different dimensions. Tonnes measure the mass loaded or handled, but do not reflect distance. Tonne-kilometres measure transport performance by multiplying mass by distance, and are therefore better suited to modal shares within a defined territory. TEU measures container capacity, not cargo mass; a rise in TEU can coincide with a fall in cargo tonnes if average container weight declines or empty-container movements increase. Cargo tonne-kilometres in aviation measure revenue cargo mass over distance, whereas airport “load traffic” may include cargo, mail, and passenger baggage.

Geographical scope is equally important. Port-handling statistics may count international, transit, and cabotage cargo and may record a shipment at more than one terminal. Domestic modal-split tables may include only movements on a specified road network, rail operators, cabotage shipping, or domestic aviation. A figure stating that maritime transport carries most world trade by volume cannot be directly compared with a national inland modal split. In this chapter, each table therefore specifies its unit and scope, and indicators are interpreted rather than mechanically added.

3. CHARACTERISTICS OF THE PRINCIPAL FREIGHT MODES

3.1. Road Freight Transport

Road freight transport provides the highest spatial accessibility among the major modes. Trucks can collect and deliver directly at factories, warehouses, retail facilities, construction sites, and dispersed customer locations. Services can

be scheduled at short notice, shipment sizes can range from parcels to full truckloads, and routes can be changed without constructing dedicated terminals. These characteristics make road transport particularly effective for short and medium distances, small and heterogeneous shipments, time-sensitive replenishment, and first- and last-mile operations.

Its main disadvantages arise from limited vehicle capacity and high dependence on traffic, driver availability, road conditions, and regulatory restrictions. Unit cost is often competitive for short hauls but does not benefit from scale to the same extent as rail or waterborne transport. Congestion, accidents, local air pollution, greenhouse-gas emissions, and road infrastructure wear are significant external costs. For long-haul flows with stable volumes, road-only service may remain operationally convenient yet systemically inefficient if a suitable rail or waterborne alternative exists.

3.2. Rail Freight Transport

Rail freight combines relatively high capacity with lower rolling resistance and strong economies of density. It is well suited to bulk commodities, heavy industrial products, automobiles, containers, and repeated flows over medium to long distances. Block trains, in which wagons move between origin and destination with limited intermediate shunting, can improve transit time and reliability. Electrified rail also offers substantial decarbonization potential where electricity generation is comparatively low-carbon.

Rail is less flexible at the access stage. Unless the shipper and receiver have sidings, road collection and delivery are required. Terminals introduce handling, queueing, schedule coordination, and minimum-volume requirements. Service quality may also be affected by network capacity, border procedures, interoperability, and the priority given to passenger

trains. Distance alone does not determine rail competitiveness. Shipment volume, terminal proximity, service frequency, loading-unit compatibility, and door-to-door reliability can be equally important.

3.3. Maritime Freight Transport

Maritime transport provides the greatest carrying capacity and the lowest line-haul cost per tonne for many long-distance movements. It is the backbone of intercontinental trade in containers, dry bulk, liquid bulk, vehicles, and project cargo. Specialized vessel types and global liner networks allow very large volumes to move between regions that could not be economically connected by land modes. UNCTAD reported that global seaborne trade grew by 2.2% in 2024, illustrating the scale and continuing importance of the sector (UNCTAD, 2025).

The trade-off is speed and dependence on ports and hinterland connections. Congestion, equipment availability, weather, canal disruptions, geopolitical risks, and schedule changes can propagate through supply chains. Maritime service can be highly efficient for large, non-urgent flows. Its end-to-end performance, however, still depends on port operations, customs, storage, and inland transport. Containerization reduces handling of the goods themselves, yet it does not eliminate terminal and coordination costs.

3.4. Air Freight Transport

Air freight offers the shortest transit time over long distances and is used when the value of speed is high. Typical cargo includes pharmaceuticals, electronics, urgent spare parts, perishables, fashion products, high-value components, and emergency shipments. IATA reports that airlines carry more than 62 million tonnes of cargo annually, representing more than one-third of global trade by value but less than one percent by volume (IATA, 2026). This contrast demonstrates that air freight is

selected according to value density and time sensitivity rather than mass.

The mode has high transport charges, strict security and dangerous-goods requirements, capacity constraints, and substantial energy use. Airport access, terminal cut-off times, screening, customs, and flight schedules mean that airport-to-airport speed does not always translate into proportionate door-to-door savings. Air freight is therefore justified when reduced lead time lowers inventory, prevents production stoppage or spoilage, protects market value, or satisfies a critical service requirement.

3.5. Pipeline Transport

Pipelines provide continuous, high-volume movement of liquids, gases, and in some cases slurries. Once installed, they can operate with low labour requirements and relatively stable flow rates, without congestion or vehicle repositioning. They are important for crude oil, petroleum products, natural gas, and industrial feedstocks. Their enclosed infrastructure can offer high operational reliability when appropriately maintained and monitored.

The limitations are severe specialization and low flexibility. Pipeline construction requires high capital expenditure, long approval periods, fixed origin–destination corridors, and long-term demand. Product changes, route changes, and emergency capacity expansion are difficult. Pipelines are best treated as dedicated infrastructure, not as a general-purpose freight service. Strategic assessment must also account for geopolitical exposure, environmental risk, network security, and the consequences of disruption.

3.6. Inland Waterway Transport

Inland waterway transport uses rivers, canals, and lakes to move bulk commodities, containers, heavy units, and project cargo. Barges can carry large quantities with low energy consumption per tonne-kilometre, making the mode attractive where navigable waterways and suitable terminals exist. Its performance is strongest in geographically favourable networks such as the Rhine–Danube system and in corridors where industrial production is located near waterways.

The mode is slow and geographically constrained. Water depth, drought, flooding, lock capacity, seasonal conditions, and terminal access affect reliability. Türkiye does not possess an extensive navigable inland-waterway freight network comparable to those of several European countries; consequently, the mode has limited domestic significance. This is an example of why mode comparisons cannot be separated from geography and infrastructure availability.

4. COMPARATIVE ASSESSMENT AND MODE CHOICE

4.1. A Common Decision Framework

A rational mode decision should minimize generalized logistics cost subject to service, capacity, and risk requirements. Generalized cost includes the freight rate; collection and delivery; terminal handling; documentation; inventory held during transit; safety stock created by uncertain lead time; expected loss, damage, and disruption; and, where relevant, environmental or regulatory costs. The lowest quoted line-haul price is therefore not necessarily the lowest total cost.

The most influential shipment variables are distance, mass and volume, value density, perishability, urgency, shipment

frequency, and the possibility of consolidation. Network variables include origin and destination accessibility, terminal distance, service frequency, schedule reliability, available capacity, border crossings, and compatibility of loading units. Organizational variables include contract structure, visibility, the ability to coordinate several carriers, and the allocation of liability. ITF (2022) emphasizes that mode choice reflects the interaction of infrastructure, service characteristics, shipper requirements, and policy rather than a single cost parameter.

The decision is often discontinuous. A rail or maritime alternative may be unattractive below a minimum volume because terminal and fixed service costs cannot be spread over sufficient cargo. Once volume and distance exceed a threshold, the scale advantage can dominate. Conversely, a disruption, missed sailing, or unreliable transfer may erase the nominal saving. Industrial engineering analysis should therefore test alternative demand levels, service frequencies, and reliability scenarios instead of relying on a static ranking.

Table 2. Relative characteristics of the principal freight modes

Mode	Typical unit cost	Speed	Capacity/economies of scale	Door-to-door access	Typical best fit
Road	Medium; rises on long haul	High for short and medium hauls	Medium	Very high	Dispersed origins/destinations, small to medium lots, first/last mile
Rail	Low to medium at sufficient volume	Medium	High	Low without sidings	Heavy, bulk, automotive, and container flows over medium/long distance
Maritime	Low for large long-haul flows	Low	Very high	Low; port and hinterland links required	International bulk, containers, vehicles, and project cargo
Air	Very high	Very high	Low to medium by mass	Low; airport access required	High-value, urgent, perishable, and critical shipments
Pipeline	Low operating cost after investment	Continuous	Very high for dedicated product	Very low	Stable high-volume liquid and gas flows
Inland waterway	Low	Low	High	Low; waterway/ terminal access required	Bulk, containers, and heavy cargo on navigable corridors

Note. Ratings are relative and context-dependent.

4.2. Reliability, Resilience, and Environmental Performance

Reliability is often more important than average speed. A predictable five-day service may allow lower safety stock than a nominally three-day service with frequent delays. Intermodal chains can diversify exposure across modes, but they also create interfaces at which failures may occur. Terminal congestion, missing documentation, incompatible schedules, or unavailable loading units can cause a delay greater than the line-haul time saved. Resilience depends on alternative routes, reserve capacity, information visibility, and clearly defined recovery procedures.

Environmental comparisons require the same end-to-end discipline. Rail and waterborne modes generally provide lower energy use and emissions per tonne-kilometre when load factors are high, but first/last-mile trucking, empty repositioning, terminal energy, detours, and electricity or fuel mix affect the result. Air freight has a high climate impact per unit transported, but its small mass share and specialized economic role should be acknowledged. Effective decarbonization combines modal shift where feasible with vehicle efficiency, clean energy, consolidation, network redesign, and demand-management measures (McKinnon, 2018).

5. CURRENT GLOBAL AND EUROPEAN EVIDENCE

5.1. Global Freight Indicators

No single global table provides a fully comparable modal split for all freight transport. Maritime statistics are commonly expressed in tonnes and ton-miles of international seaborne trade; road and rail data are often national or territorial tonne-kilometres; pipeline coverage varies; and air cargo is reported in

tonnes or cargo tonne-kilometres. These differences make a single global total misleading. Global evidence is more useful for showing the scale and role of each mode within its own statistical scope.

Maritime transport remains the dominant physical carrier of international merchandise. UNCTAD reported that global seaborne trade grew by 2.2% in 2024 and forecast growth of only 0.5% for 2025 amid weak demand, rerouting, and geopolitical uncertainty (UNCTAD, 2025). Air freight occupies the opposite end of the spectrum: its mass share is small, while its share of trade value is exceptionally high. Together, these indicators show that modal importance changes according to whether the researcher measures mass, distance, value, speed, or strategic criticality.

5.2. European Union Modal Split

Eurostat calculates an EU modal split using territorial tonne-kilometres for five modes. In 2024, maritime transport accounted for 67.0% of freight performance, road for 25.7%, rail for 5.4%, inland waterways for 1.7%, and air for 0.2%. Maritime and road transport together represented 92.7% of the measured total (Eurostat, 2026). The result reflects the inclusion of maritime movements within the EU territorial framework; it should not be interpreted as the modal split of purely inland freight.

Table 3. Freight transport modal split in the European Union, 2024

Mode	Share (%)
Maritime	67.0
Road	25.7
Rail	5.4
Inland waterway	1.7
Air	0.2
Total	100.0

Source: Eurostat (2026), online data code tran_hv_ms_frmod.

The EU aggregate also conceals strong geographical variation. Countries with dense rail networks, major bulk corridors, or navigable waterways can achieve modal structures that are impossible elsewhere. Infrastructure alone is not sufficient: service frequency, terminal performance, interoperability, cross-border procedures, and commercial coordination determine whether shippers can actually use a non-road alternative. The European Court of Auditors (2023) concluded that persistent regulatory and infrastructure barriers continue to limit intermodal freight development in the EU.

6. FREIGHT TRANSPORT IN TÜRKİYE

6.1. Domestic Freight Performance by Mode

Türkiye's domestic freight performance is strongly road-oriented. The General Directorate of Highways reports 358.880 billion tonne-kilometres by road in 2025, corresponding to 90.8% of the four-mode total presented in its national comparison. Rail accounted for 23.310 billion tonne-kilometres (5.9%), maritime cabotage for 13.135 billion tonne-kilometres (3.3%), and domestic air cargo for 28 million tonne-kilometres (approximately 0.01%). Compared with 2024, road performance rose by about 3.2%, rail by 17.5%, and maritime cabotage by 6.4%, while air remained very small in tonne-kilometre terms (KGM, 2026).

Table 4. Freight transport performance by mode in Türkiye, 2025

Mode	Million tonne-km	Share (%)	Scope note
Road	358,880	90.8	Movements on the road network under KGM responsibility
Rail	23,310	5.9	National rail freight performance reported in the KGM comparison
Maritime	13,135	3.3	Cabotage freight; tonne-miles converted to kilometres
Air	28	0.0	Domestic loaded/unloaded cargo; baggage and mail excluded in this table
Total	395,353	100.0	Sum of the four reported modes

Source: KGM (2026).

The road share demonstrates a structural pattern rather than a temporary annual fluctuation. Türkiye's industrial and population geography, dispersed production and consumption points, extensive road access, flexible trucking capacity, and limited direct rail access at many facilities reinforce road use. This structure is operationally convenient but increases exposure to congestion, fuel-price volatility, driver constraints, accidents, and road-related emissions. Reducing the share of road does not mean eliminating trucks; it means using them more selectively for collection, delivery, and corridors where no viable alternative exists.

6.2. Mode-Specific Scale and Integration Indicators

Mode-specific indicators provide context but cannot be added to the tonne-kilometre table. Turkish ports handled 553.268 million tonnes of cargo and approximately 14.0 million TEU in 2025, including 414.416 million tonnes of international traffic, 69.157 million tonnes of transit traffic, and 69.679 million tonnes of cabotage (Ministry of Transport and Infrastructure, 2026). These are port-handling volumes, not domestic tonne-kilometres.

TCDD Taşımacılık reported 25.261 million tonnes and 10.240 billion net tonne-kilometres of freight in 2025. Containerized rail freight reached 12.3 million tonnes, while port-connected rail–sea combined transport totalled 8.2 million tonnes, including approximately 4.8 million tonnes of exports and 3.4 million tonnes of imports (TCDD Taşımacılık, 2026).

Türkiye's airports recorded 5.150 million tonnes of "load and cargo" traffic in 2025, comprising 0.929 million domestic and 4.220 million international tonnes (DHMİ, 2026). Because this indicator includes cargo, mail, and baggage, it is broader than pure air freight and is not directly comparable with the domestic air-cargo tonne-kilometres in Table 4.

Table 5. Selected recent freight and logistics indicators for Türkiye

Indicator	2025 value	Interpretation
Total cargo handled at ports	553.268 million tonnes	International, transit, and cabotage; not tonne-km
Containers handled at ports	Approximately 14.0 million TEU	Container throughput; full and empty units
TCDD Taşımacılık rail freight	25.261 million tonnes; 10.240 billion net tonne-km	Operator rail activity
Port-connected rail–sea combined freight	8.2 million tonnes	4.8 million tonnes export; 3.4 million tonnes import
Airport load and cargo traffic	5.150 million tonnes	Cargo, mail, and baggage; domestic and international

Sources: Ministry of Transport and Infrastructure (2026); TCDD Taşımacılık (2026); DHMİ (2026).

6.3. Implications for Türkiye's Modal Structure

The evidence suggests that Türkiye's central policy and design problem is not the absence of non-road freight activity, but the limited integration of that activity into dependable door-to-door services. The country has large ports, growing container activity, substantial rail freight flows, and a strategic position between European and Asian markets. Nevertheless, a shipper chooses an intermodal chain only when the complete service is competitive in cost, frequency, visibility, reliability, and responsibility. Infrastructure investment must also be accompanied by service design and operational coordination.

High-priority interfaces include rail access to ports and organized industrial zones, capacity at logistics centres, terminal operating hours, train-path availability, customs and border procedures, loading-unit supply, and digital data exchange. The Middle Corridor increases the relevance of multimodal coordination because it requires rail, maritime crossings, terminals, and border processes to function as one chain. OECD analysis of the corridor similarly emphasizes that multimodal geography creates both strategic opportunity and coordination bottlenecks (OECD, 2023).

For domestic flows, the largest potential may lie in repeated and consolidatable cargo rather than in attempting to transfer every shipment away from road. Bulk commodities, metals, minerals, automotive products, containers, and high-volume industrial flows are natural candidates. A corridor-based approach can identify origin–destination pairs with sufficient volume and distance, then evaluate terminal location, service frequency, equipment, and road feeder routes. Such analysis is more credible than applying a universal modal-shift target independent of commodity and network conditions.

7. MODAL INTEGRATION AND INDUSTRIAL ENGINEERING IMPLICATIONS

Modal integration is fundamentally an industrial engineering problem because it requires simultaneous decisions about facilities, networks, capacity, schedules, inventories, and information. Strategic decisions include terminal and logistics-centre location, corridor selection, technology and fleet investment, and the architecture of the service network. Tactical decisions include train or sailing frequency, capacity allocation, consolidation policy, timetable coordination, and contractual design. Operational decisions include vehicle routing, loading, terminal sequencing, disruption recovery, and real-time reassignment.

These decision levels are interdependent. Locating a terminal without sufficient consolidated demand creates underutilized capacity; increasing frequency without reliable terminal processing creates queues; minimizing line-haul cost without considering inventory may worsen total logistics performance. Multimodal planning literature accordingly organizes problems across strategic, tactical, and operational horizons and emphasizes network design, service design, and

resource coordination (Macharis & Bontekoning, 2004; SteadieSeifi et al., 2014).

A useful decision-support framework should begin with commodity-specific origin–destination flows and identify feasible chains rather than assuming that all modes are available. Each chain should be evaluated on total cost, end-to-end time, reliability, capacity, safety, emissions, and resilience. Threshold analysis can identify the shipment size and distance at which an intermodal alternative becomes competitive. Scenario analysis can test fuel-price changes, carbon charges, terminal delays, service-frequency changes, and network disruptions. Multi-criteria methods may be used when performance dimensions cannot be reduced credibly to a single monetary value.

Digitalization can reduce, but not remove, interface costs. Electronic documents, interoperable data standards, real-time tracking, terminal appointment systems, estimated-time-of-arrival updates, and shared capacity information improve visibility and coordination. The value of technology depends on institutional adoption and data quality. A sophisticated platform cannot compensate for insufficient service frequency, unclear responsibility, or incompatible operating procedures. The design objective should be a measurable improvement in end-to-end performance, not digitalization as an isolated goal.

Resilience adds a further design dimension. An integrated network may provide alternatives when a road, port, border, or maritime route is disrupted; however, interdependence may also transmit disruption across the chain. Robust plans should reserve critical capacity, specify alternative terminals and routes, maintain visibility of loading units, and define decision rights during recovery. Future research for Türkiye could combine terminal location, service-network design, and vehicle routing

with stochastic demand, disruption scenarios, and environmental objectives.

8. CONCLUSION

Freight transport modes should be compared as end-to-end systems rather than isolated vehicles. Road provides accessibility and flexibility; rail, maritime transport, and inland waterways provide scale; air freight provides speed for high-value and urgent goods; and pipelines provide continuous movement for specialized commodities. Relative performance changes with distance, shipment size, value density, frequency, geography, infrastructure, and reliability. There is therefore no universally best mode. The appropriate choice is the mode or chain that best fits a defined flow and decision context.

Clear terminology is essential. Multimodal transport uses two or more modes; intermodal transport preserves the same loading unit or road vehicle across modal transfers; and combined transport assigns the major leg to rail, inland waterway, or sea while restricting road mainly to the first and last legs. These distinctions support consistent research, statistics, contracts, and policy evaluation.

Recent evidence shows contrasting modal roles. Maritime transport dominates EU territorial freight performance and global trade volume, while air cargo carries little mass but a high share of trade value. Türkiye's domestic freight remains overwhelmingly road-based, despite very large port volumes and material port-connected rail–sea transport. The strategic opportunity is not simply to replace road, but to design dependable services in which road, rail, ports, terminals, and information systems perform complementary functions.

For industrial engineering, the practical agenda is to identify suitable corridors, locate and size terminals, consolidate demand, coordinate schedules, evaluate generalized logistics cost, and design resilient information-supported networks. Modal shift occurs only when the integrated alternative is commercially usable and operationally dependable; infrastructure must be matched by effective service design and coordination.

REFERENCES

DHMİ. (2026). *Havayolunda Cumhuriyet tarihinin rekoru.* General Directorate of State Airports Authority. https://dhmi.gov.tr/Sayfalar/Haber/havayolunda-cumhuriyet-tarihinin-rekoru.aspx

European Court of Auditors. (2023). *Intermodal freight transport: EU still far from getting freight off the road (Special Report 08/2023).* Publications Office of the European Union.

Eurostat. (2026). *Freight transport statistics: modal split.* Statistics Explained. https://ec.europa.eu/eurostat/statistics-explained/index.php?title=Freight_transport_statistics_-_modal_split

Eurostat, International Transport Forum, & United Nations Economic Commission for Europe. (2026). *Glossary for transport statistics (6th ed.).* Publications Office of the European Union.

International Air Transport Association. (2026). *Cargo: Enabling global trade.* https://www.iata.org/cargo/

International Transport Forum. (2022). *Mode choice in freight transport.* OECD Publishing. https://doi.org/10.1787/3e69ebc4-en

KGM. (2026). *Karayolu ulaşım istatistikleri 2025 [Road transport statistics 2025].* General Directorate of Highways. https://www.kgm.gov.tr/SiteCollectionDocuments/KGMdocuments/Yayinlar/YayinPdf/KarayoluUlasimIstatistikleri2025.pdf

Macharis, C., & Bontekoning, Y. M. (2004). Opportunities for OR in intermodal freight transport research: A review.

European Journal of Operational Research, 153(2), 400–416. https://doi.org/10.1016/S0377-2217(03)00161-9

McKinnon, A. (2018). *Decarbonizing logistics: Distributing goods in a low carbon world.* Kogan Page.

Ministry of Transport and Infrastructure. (2026). *Limanlarda Cumhuriyet tarihinin rekoru kırıldı [A record was set at ports]*. https://www.uab.gov.tr/haberler/limanlarda-cumhuriyet-tarihinin-rekoru-kirildi

OECD. (2023). *Realising the potential of the Middle Corridor.* OECD Publishing. https://doi.org/10.1787/635ad854-en

SteadieSeifi, M., Dellaert, N. P., Nuijten, W., Van Woensel, T., & Raoufi, R. (2014). Multimodal freight transportation planning: A literature review. *European Journal of Operational Research, 233*(1), 1–15. https://doi.org/10.1016/j.ejor.2013.06.055

TCDD Taşımacılık A.Ş. (2026). *2025 yılı faaliyet raporu [2025 annual report]*. https://adminapi.tcddtasimacilik.gov.tr/files/pdfs/Faaliyet%20Raporu%202025.pdf

United Nations Conference on Trade and Development. (2025). Review of maritime transport 2025. United Nations. https://unctad.org/publication/review-maritime-transport-2025

Vural, D. (2014). K.K.K.lığı ulaştırma uygulamalarına yönelik çok modlu (multimodal) model önerisi [Multimodal model suggestion for land forces transportation applications] (Doctoral dissertation). Kara Harp Okulu, Savunma Bilimleri Enstitüsü, Ankara.

BUSINESS CONTINUITY MANAGEMENT STANDARDS FROM BS 25999 TO *ISO* 22301: A COMPACT FUZZY STANDARDS-ALIGNMENT MATURITY ASSESSMENT FRAMEWORK FOR THE OPERATIONAL-RESILIENCE ERA

Doğan ŞENGÜL[1]

Cafer Erhan BOZDAĞ[2]

1. INTRODUCTION

Modern organisations deliver their products and services through tightly coupled processes, technologies, suppliers and people and a disruption in any one of these layers can propagate across the system and impair the organisation's ability to operate. Business continuity management (*BCM*) is a management discipline through which organisations identify disruptive threats, evaluate their potential operational consequences and develop coordinated capabilities for maintaining and restoring priority activities, thereby helping to safeguard the interests of key stakeholders, the organisation's reputation and its value-creating activities (*ISO*, 2019). Over five decades, the discipline has moved from a narrow concern with the recovery of computer installations to a board-level component of organisational

[1] PhD in Industrial Engineering. Assistant Professor, Department of Software Engineering, Faculty of Engineering and Natural Sciences, İstanbul Sabahattin Zaim University, İstanbul, Türkiye, ORCID: 0000-0002-2285-3907.

[2] PhD in Industrial Engineering. Assistant Professor, Department of Industrial Engineering, İstanbul Technical University, İstanbul, Türkiye, ORCID: 0000-0003-4522-9071.

resilience and successive standards and guidelines have helped formalise this transition.

This chapter maps the evolution of *BCM* standards and situates that evolution within the wider regulatory turn towards operational resilience. It provides an updated review of the standards landscape[3] and presents a fuzzy diagnostic framework. The chapter pursues three aims. It reconstructs the standardisation pathway from *PAS* 56 through BS 25999 to *ISO* 22301 and its supporting standards. It explains the management-system logic shared by the BS 25999-*ISO* 22301 lineage, namely the plan-do-check-act (*PDCA*) cycle. Finally, it proposes a transparent fuzzy framework for assessing standards-alignment maturity. The framework comprises definitions, propositions, proofs and an assessment procedure intended to support research and, following empirical validation, organisational assessment and longitudinal tracking of standards alignment.

The remainder of the chapter is organised as follows. Section 2 reviews the business continuity literature and its conceptual foundations. Section 3 traces the emergence of *BCM* as a management discipline. Section 4 reconstructs the standardisation pathway. Section 5 sets out the management system and its *PDCA* cycle. Section 6 discusses the operational-resilience era and its regulatory drivers. Section 7 develops the proposed fuzzy maturity assessment framework. Section 8 discusses implications and future research and Section 9 concludes.

[3] This book chapter is derived from and extends the first author's doctoral dissertation, completed at İstanbul Technical University in 2016 under the supervision of the second author (Şengül, 2016).

2. LITERATURE REVIEW

2.1. Business Continuity as a Field of Research and Practice

Business continuity addresses disruptive events that may be infrequent but have severe operational, financial and reputational consequences, including crises, emergencies, disasters, terrorist attacks and epidemics. Interest in the discipline has broadened across public and private, for-profit and not-for-profit organisations, reflecting the demands of shareholders, customers, regulators and wider society. Two structural pressures sustain this interest: the growing diversity of the threats to which organisations are exposed and the increasingly tight coupling of the processes, technologies and suppliers through which they operate, which allows a localised disruption to propagate across the system.

The scholarly literature expanded markedly during the 2000s and became increasingly multidisciplinary, particularly as major disruptive events increased scholarly and managerial attention to continuity; recent bibliometric analysis maps this development and the field's current intellectual structure (Widianti et al., 2024). An early international guidance document was the now-withdrawn *ISO/PAS* 22399:2007 on incident preparedness and operational continuity management (*ISO*, 2007).

2.2. Conceptual Foundations: Continuity, the Management System and Maturity

The field centres on several shared constructs. Business continuity refers to an organisation's ability to continue or resume the delivery of priority products and services at an agreed level and within acceptable time limits during a disruption (*ISO*, 2019). A disruptive incident may reduce an organisation's operational capability below its normal level and continuity planning is

framed around several core parameters: the minimum acceptable level of operation that must be maintained, the recovery time objective within which a disrupted activity, product or service is to be resumed and the maximum tolerable period of disruption beyond which the resulting losses become unacceptable. Business impact analysis supports the determination of these parameters by identifying critical activities, their interdependencies and the resources required for recovery. Where continuity arrangements are absent, or cannot be activated in an integrated way, operational capability may fall below the minimum acceptable level and may not recover within an acceptable time frame, exposing the organisation to losses exceeding its planned tolerances.

These constructs are operationalised through a business continuity management system, a coordinated set of policies, objectives, controls and processes that an organisation establishes, operates, monitors and improves. *ISO* 22301 establishes auditable requirements and a continual-improvement cycle but does not prescribe a maturity scale (*ISO*, 2019). The present chapter therefore adds a maturity-oriented diagnostic layer for internal assessment. Performance evaluation, internal audit, management review and continual improvement provide the management-system basis for repeated assessment over time, while the proposed framework translates that logic into a supplementary maturity measure. This measure is intended to complement, not replace, conformity assessment, internal audit or certification.

Since 2016, the conceptual boundaries of the field have continued to evolve. Business continuity, operational resilience and organisational resilience have converged around the shared goal of sustaining critical functions under stress (Galaitsi et al., 2023); continuity has been linked explicitly to resilience engineering (Steen et al., 2024); and research has expanded to

settings including small and medium-sized enterprises (Awang Ali et al., 2023) and public-sector organisations (Cedergren and Hassel, 2025). In parallel, the regulatory environment examined later in this chapter has increasingly required continuity capability to be supported by documented evidence, testing and structured assessment. Within the literature reviewed for this chapter, few transparent and reproducible instruments were identified for tracking alignment with a reference continuity standard under uncertain maturity judgements. The remainder of this chapter develops such an instrument.

3. FROM DISASTER RECOVERY TO A MANAGEMENT DISCIPLINE

The origins of *BCM* lie in the information technology (*IT*) disaster recovery practices of the 1970s, when organisations that had centralised their operations on mainframe computers recognised that the loss of a single data centre could halt the business. Herbane (2010) reconstructs this history and identifies three distinct phases of management practice together with four phases in the development of the drivers that require organisations to act. In the earliest phase the concern was narrowly technical and reactive, focused on the restoration of computer processing after an interruption. In the second phase the scope widened from technology to the operational processes that technology supports and in the third phase continuity was reframed as a contribution to organisational resilience and, ultimately, as a matter of governance.

Herbane et al. (2004) argued that *BCM* could move beyond a purely functional role, help preserve competitive advantage and assume a strategic rather than merely operational position. The events of the following two decades accelerated that shift. The COVID-19 pandemic reinforced *BCM* as a board-level

concern and exposed the limitations of treating it primarily as a compliance activity. Leading companies had to activate and adapt continuity arrangements on an unprecedented scale (Margherita and Heikkilä, 2021), while interpretations of the discipline shifted across sectors (Sawalha and Anchor, 2024). Galaitsi et al. (2023) document the resulting convergence of business continuity, operational resilience and organisational resilience, three concepts that share a common concern with sustaining critical functions under stress while differing in scope and emphasis.

The central pattern in this development is a steady broadening of scope, from recovery of a technical asset to resilience of the organisation as a whole, accompanied by increasing formalisation through successive standards.

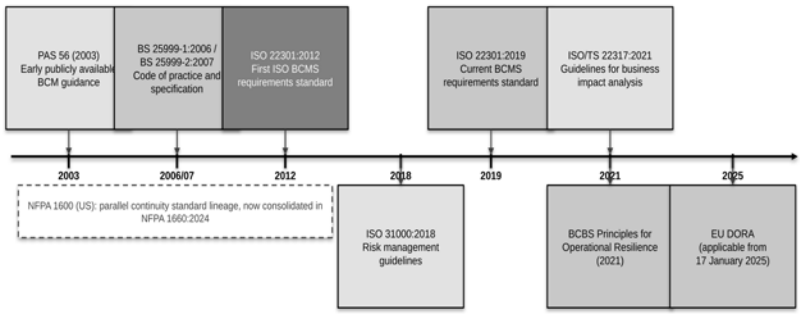

Figure 1. Evolution of the BS-*ISO* business continuity standardisation pathway, shown above the axis, together with selected parallel standards and regulatory developments shown below the axis. The figure presents a selective pathway and does not display every relevant standard.

4. THE STANDARDISATION PATHWAY

The BS-*ISO* standardisation pathway developed through three broad stages: *PAS* 56 as early publicly available *BCM* guidance, BS 25999 as a two-part national standard and *ISO*

22301 as an international *BCMS* requirements standard. Figure 1 summarises the sequence and its regulatory context.

4.1. The Early Guidance: PAS 56

PAS 56, a publicly available specification (*PAS*) issued by the British Standards Institution (*BSI*) in 2003, was among the early widely cited business continuity guidance documents and played an important role in the subsequent BS and *ISO* standardisation pathway (British Standards Institution, 2003). It offered a common vocabulary and a process view of continuity at a time when practice was fragmented across sectors. Alongside it, in the United States, *NFPA* 1600 developed through successive editions as a standard addressing continuity, emergency and crisis management. Its continuity and crisis-management content is now incorporated into the consolidated *NFPA* 1660:2024 standard (National Fire Protection Association, 2019, 2024). Together, these documents helped establish continuity as a repeatable management programme rather than an improvised response.

4.2. The National Standard: BS 25999

PAS 56 was superseded in the United Kingdom by BS 25999, issued in two parts. BS 25999-1:2006 was a code of practice that set out the principles, processes and terminology recommended for *BCM* (British Standards Institution, 2006). BS 25999-2:2007 was a specification; that is, a set of auditable requirements against which an organisation's management system could be certified (British Standards Institution, 2007). The distinction between guidance and specification, which recurs throughout the field, is important, because third-party certification requires an auditable requirements standard, whereas guidance documents do not themselves provide certification criteria. BS 25999-1 formalised a *BCM* lifecycle comprising *BCM* programme management; understanding the organisation;

determining business continuity strategy; developing and implementing a *BCM* response; exercising, maintaining and reviewing *BCM* arrangements; and embedding *BCM* in the organisation's culture.

4.3. The International Standard: ISO 22301 and its Revision

The publication of *ISO* 22301 marked a major transition from national business continuity specifications to an internationally applicable management-system standard, developed by the International Organization for Standardization (*ISO*). *ISO* 22301 was first published in 2012, after which BS 25999-2 was withdrawn. *ISO* 22313 subsequently provided international guidance and BS 25999-1 was also withdrawn. *ISO* 22301 was revised in 2019 as *ISO* 22301:2019, the current requirements standard for a business continuity management system (*BCMS*) (*ISO*, 2019). *ISO* 22301:2019 retained the harmonised high-level structure already used by the 2012 edition, facilitating integration with quality, information security and other *ISO* management systems that share the same clause architecture. *ISO* 22313:2020 provides the accompanying guidance (*ISO*, 2020) and *ISO/TS* 22317:2021 provides guidance on business impact analysis (*BIA*), a process used to determine recovery priorities and continuity requirements (*ISO*, 2021).

ISO 22301 continues to evolve through amendments and periodic revision. *ISO* 22301:2019 was amended by *ISO* 22301:2019/Amd 1:2024. The amendment requires organisations to determine whether climate change is a relevant contextual issue and adds a note recognising that relevant interested parties can have climate-related requirements (*ISO*, 2024). *ISO* 22301:2019 remains the published requirements standard but is marked for revision. *ISO*/CD 22301, the proposed third edition, is currently under development at the committee-draft stage and is intended

to replace the 2019 edition in due course (*ISO*, 2026). Figure 2 sets out this timeline, from the withdrawn 2012 edition, through the published 2019 edition and its 2024 amendment, to the revision now in preparation.

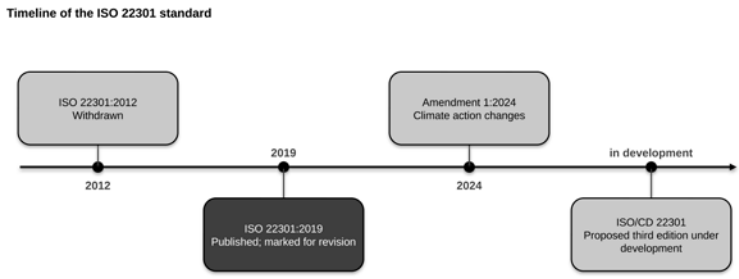

Figure 2. Timeline of the *ISO* 22301 standard, from the withdrawn 2012 edition through the current 2019 edition and its 2024 climate-action amendment to the committee-draft revision *ISO*/CD 22301 under development. Source: developed by the authors from *ISO* (2019, 2024, 2026); status checked in July 2026.

4.4. Selected Supporting Standards

Several supporting standards are particularly relevant to the scope of this chapter. *ISO* 31000:2018 provides the generic risk management framework and vocabulary on which continuity risk assessment draws (*ISO*, 2018) and *ISO/IEC* 31010:2019 catalogues risk-assessment techniques available to analysts, including multi-criteria techniques relevant to the decision-analytic extensions discussed in Section 8 (*ISO* & *IEC*, 2019). These documents are complementary rather than hierarchical: *ISO* 22301 specifies *BCMS* requirements; *ISO* 22313 supports their application; *ISO/TS* 22317 provides additional guidance on business impact analysis; and the *ISO* 31000 family supplies the broader risk-management foundations.

5. THE MANAGEMENT SYSTEM AND THE *PDCA* CYCLE

The BS 25999-*ISO* 22301 management-system lineage is structured around the plan-do-check-act (*PDCA*) cycle, the iterative improvement logic common to *ISO* management-system standards. Figure 3 maps the clauses of *ISO* 22301:2019 onto the four phases of the cycle. In the plan phase the organisation establishes the context of the management system, secures leadership commitment, plans to address risks and opportunities and provides the necessary support, corresponding to clauses 4 to 7. In the do phase, clause 8, the organisation performs the operational work of continuity, namely the *BIA* and risk assessment, the selection of continuity strategy and the development, implementation and exercise of continuity plans. In the check phase, clause 9, it monitors, measures, audits and reviews performance and in the act phase, clause 10, it corrects nonconformities and pursues continual improvement.

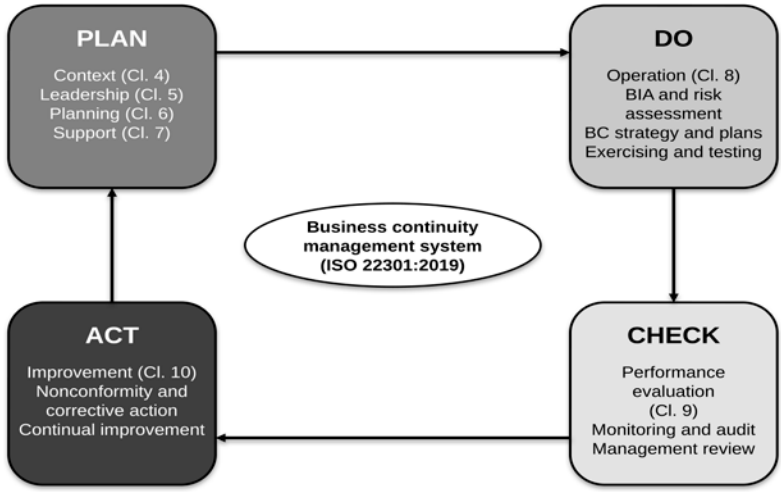

Figure 3. The plan-do-check-act cycle of *ISO* 22301:2019, with the standard's clauses 4 to 10 mapped onto the four phases of the management system.

The *PDCA* structure frames continuity as an ongoing management discipline rather than a one-off project. Each turn of the cycle updates the understanding of the organisation, revises the continuity strategy in the light of monitoring and audit and feeds improvements back into planning. The recent literature reflects this systemic view. Steen et al. (2024) propose a conceptual framework that links continuity to resilience engineering, Awang Ali et al. (2023) integrate organisational resilience and performance into a continuity framework for small and medium enterprises and Widianti et al. (2024) map the intellectual structure of the field and highlight the integration of continuity, the development of continuity frameworks and the comparison of *BIA* frameworks as priority directions.

6. THE OPERATIONAL-RESILIENCE ERA

The regulatory environment surrounding continuity has become more prescriptive in parallel with the standards. The Basel Committee on Banking Supervision (2021) set out supervisory principles for operational resilience, requiring banks to be able to continue delivering critical operations through disruption. In the European Union (*EU*), the Digital Operational Resilience Act (*DORA*), applicable since 17 January 2025, established legally binding information and communication technology (ICT) risk management, continuity, recovery and testing requirements for covered financial entities (European Parliament and Council, 2022). National regulators have introduced parallel sector-specific requirements and in Türkiye the Banking Regulation and Supervision Agency (*BDDK*) requires banks to host their primary and secondary systems domestically and, even in disaster scenarios in which the primary systems are entirely deactivated, to resume activities within a maximum of 24 hours (*BDDK*, 2020).

Together, these instruments mark an operational-resilience era in which continuity, particularly in regulated sectors, has evolved from voluntary good practice into a tested and audited obligation. Public sector bodies have moved in the same direction and Cedergren and Hassel (2025) document both the growth and the remaining gaps in public sector continuity. The practical consequence is an increasing expectation that continuity capability be supported by documented evidence, testing and structured assessment. This expectation motivates the standards-alignment framework developed in the next section.

7. A FUZZY FRAMEWORK FOR STANDARDS-ALIGNMENT MATURITY ASSESSMENT

This section proposes a compact and auditable fuzzy framework for measuring how closely an organisation aligns with a reference continuity standard and for tracking that alignment across successive *PDCA* cycles. Because both maturity classification and assessment-unit salience involve judgement, assessment-unit maturity ratings and salience judgements are represented as triangular fuzzy numbers (TFNs). The fuzzy maturity scores are aggregated into a fuzzy alignment index for reporting, while the defuzzified unit-level weighted gaps are used for priority ranking. The framework is designed for future empirical evaluation and permits its inputs, calculations and outputs to be inspected and reproduced. Figure 4 shows the workflow. The fuzzy-set representation follows Zadeh (1965), while the use of triangular fuzzy numbers draws on the formulation employed by van Laarhoven and Pedrycz (1983).

Definition 1. *Let C denote a finite set of assessment units. In this illustration, C comprises Clauses 4-10 of ISO 22301:2019. A triangular fuzzy number, written with an over-tilde, is a triple whose membership function rises linearly from the lower value to*

the modal value and falls linearly from the modal value to the upper value. For each $c \in C$, the assessor reviews the evidence and assigns one of five ordered levels: L0 (absent), L1 (initial), L2 (defined), L3 (managed) or L4 (optimised). Table 2 maps these levels to the fuzzy maturity score $\tilde{m}_c$.

In empirical applications, C may instead be defined at the subclause or auditable-requirement level. Where top-level clause scores are used, the assessor should specify how subclause evidence is aggregated into each clause-level fuzzy maturity score.

$$\tilde{a} = (a_l, a_m, a_u), \quad a_l \leq a_m \leq a_u \tag{1}$$

For any triangular fuzzy number, the centroid used throughout this section is defined as follows.

$$cen(\tilde{a}) = \frac{a_l + a_m + a_u}{3}$$

Definition 2. *Let each included assessment unit be assigned a strictly positive, analyst-defined triangular fuzzy salience judgement $\tilde{w}_c$ reflecting its relative importance for the stated assessment purpose. These judgements are prioritisation parameters and do not represent an official ISO weighting or hierarchy of requirements. To keep the aggregation well-defined and bounded, the fuzzy salience judgements are defuzzified by the centroid and normalised to strictly positive crisp weights w_c that sum to one, as in Equation (2). Fuzzy quantities are then combined with triangular fuzzy arithmetic, in which addition is componentwise and multiplication by a crisp weight is componentwise, as in Equation (3).*

$$w_c = \frac{cen(\tilde{w}_c)}{\sum_{j \in C} cen(\tilde{w}_j)}, \quad w_c > 0, \quad \sum_{c \in C} w_c = 1 \tag{2}$$

$$\tilde{a} \oplus \tilde{b} = (a_l + b_l, a_m + b_m, a_u + b_u), \quad w_c \otimes (l, m, u) = (w_c l, w_c m, w_c u) \tag{3}$$

Definition 3. *Using the normalised crisp weights obtained from Equation (2), the fuzzy standards-alignment index is computed as the weighted sum of the unit-level fuzzy maturity scores, as shown in Equation (4). Because scalar multiplication and addition preserve triangularity, the resulting index is a triangular fuzzy number. It is defuzzified using the centroid method and Equation (5) rescales the defuzzified value to the unit interval.*

$$\tilde{M} = \bigoplus_{c \in C} (w_c \otimes \tilde{m}_c) \tag{4}$$

$$cen(\tilde{M}) = \frac{M_l + M_m + M_u}{3}, \quad A = \frac{cen(\tilde{M})}{m_{max}}, \quad m_{max} = 4 \tag{5}$$

Definition 4. *For each assessment unit c, the fuzzy unit-level weighted gap $\tilde{g}_c$ is the normalised crisp weight multiplied by the fuzzy shortfall below the maximum maturity value, as defined in Equation (6). The aggregate fuzzy alignment gap $\tilde{G}$ is the sum of the unit-level gaps and equals the complement of $\tilde{M}$ relative to m_{max}. The priority assessment-unit set B contains the unit or units with the largest defuzzified unit-level weighted gap, as defined in Equation (7). All tied units are reported.*

Fuzzy subtraction from a crisp constant k is defined by $k \ominus (l, m, u) = (k - u, k - m, k - l)$.

$$\tilde{g}_c = w_c \otimes (m_{max} \ominus \tilde{m}_c), \quad \tilde{G} = \bigoplus_{c \in C} \tilde{g}_c = m_{max} \ominus \tilde{M} \tag{6}$$

$$B = \{ c \in C : cen(\tilde{g}_c) = max_{j \in C}\ cen(\tilde{g}_j) \} \tag{7}$$

The following propositions establish three basic properties of the defuzzified index. They refer to Equations 2 to 6.

Proposition 1. *Boundedness. Under the normalisation of Equation (2) and the maturity scale specified in Table 2, the defuzzified alignment index cen($\tilde{M}$) lies between zero and the maximum maturity value. The lower bound is attained if and only*

if every assessment unit is at the lowest level and the upper bound is attained if and only if every assessment unit is at the highest level.

Proof. Because the normalised weights are strictly positive and sum to one, each component of the fuzzy index is a convex combination of the corresponding components of the unit-level fuzzy maturity scores. Each such component lies between zero and the maximum maturity value by the maturity scale, so each component of the index lies in that interval and the centroid, being their average, lies between zero and the maximum. Because every weight is strictly positive, the lower bound is attained only when every assessment unit is at the lowest level, whose fuzzy number is zero and the upper bound only when every assessment unit is at the highest level, whose fuzzy number is the maximum. □

Proposition 2. *Monotonicity. The defuzzified alignment index is non-decreasing when any assessment-unit maturity is raised to a higher level and strictly increasing when that assessment unit carries a positive weight. Consequently, moving any positively weighted assessment unit to a higher encoded maturity level cannot decrease the measured alignment.*

Proof. Moving an assessment unit to a higher maturity level weakly increases every component of its fuzzy maturity score and strictly increases at least one component. Multiplication by a positive normalised weight and componentwise addition therefore cannot decrease any component of the fuzzy index and will strictly increase its centroid when the assessment-unit maturity is raised to a higher level. Because the scores enter the aggregate additively, the same conclusion holds for the simultaneous improvement of several assessment units. □

Proposition 3. *Gap identity. The fuzzy alignment gap equals the maximum maturity value minus the fuzzy alignment*

index, so that the defuzzified gap cen($\tilde{G}$) equals the maximum value minus cen($\tilde{M}$). Under a fixed weighting scheme and maturity encoding, maximising the defuzzified alignment index is equivalent to minimising the defuzzified gap and the normalised alignment index satisfies $A = 1 - cen(\tilde{G})/m_{max}$.

Proof. Because the normalised crisp weights sum to one, the lower component of the fuzzy gap is $\sum_c w_c(m_{max} - m_{c,u}) = m_{max} - M_u$. Similarly, its modal component is $m_{max} - M_m$ and its upper component is $m_{max} - M_l$. Therefore $\tilde{G} = m_{max} \ominus \tilde{M}$. Applying the centroid gives $cen(\tilde{G}) = m_{max} - cen(\tilde{M})$. Dividing by m_{max} and using Equation (5) shows that the normalised alignment index equals one minus the normalised defuzzified gap. Under a fixed weighting scheme and maturity encoding, the two quantities therefore move in opposite directions. □

Together, the propositions demonstrate the internal coherence of the defuzzified summary index under the stated encoding and weighting assumptions. Its complement is a diagnostic weighted gap that identifies, through the priority assessment-unit set of Equations (6) and (7), the unit or units making the largest contribution to the weighted alignment gap. The procedure is summarised as Algorithm 1.

Algorithm 1. Fuzzy standards-alignment maturity assessment

Input: assessment-unit set C; evidence base E; fuzzy salience judgements $\tilde{w}_c$; maturity scale L0–L4

Output: fuzzy index $\tilde{M}$; centroid cen($\tilde{M}$); normalised index A; fuzzy gap $\tilde{G}$; defuzzified gap cen($\tilde{G}$); priority assessment-unit set B

1 for each assessment unit c in C do

2 review evidence in E and assign a level, giving the fuzzy maturity $\tilde{m}_c$

3 end for

4 defuzzify the fuzzy salience judgements by the centroid and normalise the resulting values to obtain crisp weights w_c that sum to one

5 $\tilde{M} \leftarrow$ sum over c in C of $w_c \otimes \tilde{m}_c$ (crisp weight times fuzzy maturity)

6 $cen(\tilde{M}) \leftarrow (M_l + M_m + M_u) / 3$; $A \leftarrow cen(\tilde{M}) / m_{max}$; $\tilde{G} \leftarrow m_{max} \ominus \tilde{M}$; $cen(\tilde{G}) \leftarrow m_{max} - cen(\tilde{M})$

7 for each assessment unit c, compute $\tilde{g}_c = w_c \otimes (m_{max} \ominus \tilde{m}_c)$ and its centroid $cen(\tilde{g}_c)$

8 $B \leftarrow$ assessment unit(s) with the largest $cen(\tilde{g}_c)$

9 report $\tilde{M}$, $cen(\tilde{M})$, A, $\tilde{G}$, $cen(\tilde{G})$, the priority assessment-unit set B and the full per-unit maturity and weighted-gap profile

10 schedule the next assessment for the following PDCA review cycle

Illustrative application. In the worked example, C = {4, …, 10}, representing Clauses 4-10 of *ISO* 22301:2019.

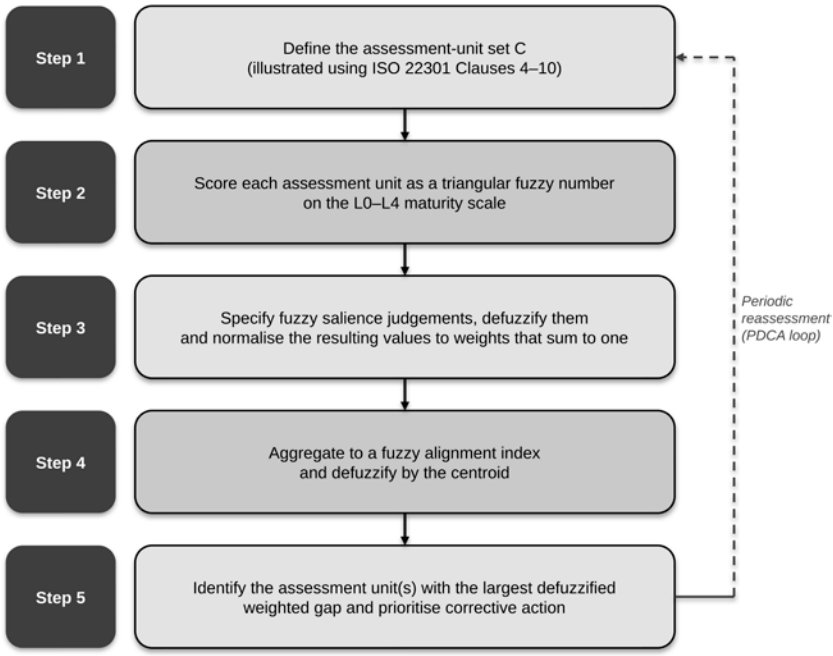

Figure 4. The proposed fuzzy standards-alignment maturity assessment framework, from fuzzy assessment-unit scoring through the defuzzification and normalisation of salience judgements and weighted aggregation to the identification of the priority assessment-unit set, with periodic reassessment closing the loop.

To illustrate the calculation, Table 1 applies the procedure to a hypothetical organisation across Clauses 4-10. Each clause receives a fuzzy maturity score, using the operational descriptors and triangular fuzzy numbers set out in Table 2, together with a fuzzy salience judgement; the fuzzy salience judgements are defuzzified and normalised to crisp weights, which are then used with the fuzzy maturity scores to give the fuzzy alignment index and the defuzzified clause-level gaps that identify the priority clause.

Table 1. A worked example of the fuzzy assessment procedure for a hypothetical organisation across Clauses 4-10.

Clause	Illustrative evidence	Fuzzy maturity	Fuzzy salience judgement → normalised crisp weight	Defuzzified weighted gap
4 Context	Documented context review; interested-party register partially updated	L2 (1, 2, 3)	(0.08, 0.10, 0.12) → 0.10	0.20
5 Leadership	Policy approved; responsibilities documented	L3 (2, 3, 4)	(0.10, 0.12, 0.14) → 0.12	0.12
6 Planning	Objectives defined; incomplete risk and opportunity tracking	L2 (1, 2, 3)	(0.10, 0.12, 0.14) → 0.12	0.24
7 Support	Training and documented information controlled	L3 (2, 3, 4)	(0.10, 0.12, 0.14) → 0.12	0.12
8 Operation	*BIA* and plans exist; exercise coverage incomplete	L2 (1, 2, 3)	(0.23, 0.25, 0.27) → 0.25	0.50
9 Performance evaluation	Internal audit irregular; limited trend analysis	L1 (0, 1, 2)	(0.15, 0.17, 0.19) → 0.17	0.51
10 Improvement	Corrective-action process active	L2 (1, 2, 3)	(0.10, 0.12, 0.14) → 0.12	0.24
Summary		$\tilde{M}$ = (1.07, 2.07, 3.07)	$\Sigma_c w_c = 1.00$	Defuzzified aggregate gap cen($\tilde{G}$) = 1.93

In this illustrative example, the centroids of the fuzzy salience judgements already sum to one. Therefore, the normalised crisp weights equal those centroids: 0.10, 0.12, 0.12, 0.12, 0.25, 0.17 and 0.12. The weighted sum of the fuzzy maturities is the fuzzy alignment index $\tilde{M}$ = (1.07, 2.07, 3.07) on the zero to four scale, with a centroid of 2.07 and a normalised alignment index A of 0.52. The fuzzy alignment gap is $\tilde{G}$ = (0.93,

1.93, 2.93), with a defuzzified value of 1.93. The largest defuzzified clause-level weighted gap is associated with Clause 9 (performance evaluation), at 0.51, slightly exceeding the value for Clause 8, at 0.50. Clause 9 is therefore the initial priority for review and corrective action. Recalculation with equal crisp weights also identifies Clause 9 as the priority, indicating that the priority ranking is unchanged under this alternative weighting scenario. The fuzzy salience judgements and fuzzy maturity ratings in Table 1 are analyst-defined illustrative values rather than ratings or weights assigned by *ISO*. All numerical values in the table are illustrative and do not represent empirical organisational data.

Table 2 provides operational descriptors and corresponding triangular fuzzy numbers intended to support consistent application of the scale across assessors.

Table 2. Operational descriptors and triangular fuzzy numbers for the five maturity levels.

Level	*TFN*	Recommended operational descriptor
L0 (Absent)	(0, 0, 0)	No relevant process, evidence or assigned responsibility can be demonstrated.
L1 (Initial)	(0, 1, 2)	Activities are ad hoc, person-dependent or inconsistently documented.
L2 (Defined)	(1, 2, 3)	The process is documented and implemented and relevant responsibilities are assigned.
L3 (Managed)	(2, 3, 4)	The process is monitored, tested, reviewed and supported by performance evidence.
L4 (Optimised)	(4, 4, 4)	The process is systematically improved using trends, exercises, audit findings and lessons learned.

The descriptors and fuzzy scale are proposed for this framework and require empirical validation before routine organisational application. Degenerate triangular fuzzy numbers are used at the two endpoints so that complete absence and full maturity correspond exactly to the lower and upper bounds of the

index. Alternative endpoint specifications should be examined through sensitivity analysis.

In empirical use, fuzzy maturity scores should be supported by documented evidence and assigned by at least two assessors where practicable. Assessors should record the evidence supporting each level, compare independent ratings and resolve disagreements through documented consensus. Inter-rater agreement should be calculated from the independent ratings before consensus resolution and reported when the instrument is used for research.

The five maturity categories are ordinal. The triangular fuzzy representation accommodates uncertainty in category assignment but does not eliminate the ordinal-to-cardinal assumption introduced when the maturity levels are aggregated numerically. The resulting index should be interpreted as a transparent diagnostic summary under the selected fuzzy encoding and empirical applications should report the sensitivity of the results to alternative admissible fuzzy scales and weighting schemes.

The proposed framework is a diagnostic maturity-assessment instrument. It does not constitute a certification audit, establish formal conformity with *ISO* 22301 or replace requirement-by-requirement professional assessment. A serious weakness in one assessment unit can be partially masked by stronger scores elsewhere, so the per-unit profile and the priority assessment-unit set should always be considered alongside the aggregate index. The purpose of the instrument is to support internal prioritisation, longitudinal monitoring and transparent discussion of implementation maturity.

8. DISCUSSION AND FUTURE RESEARCH DIRECTIONS

The framework is intentionally parsimonious in order to preserve reproducibility and auditability. Because Equation 4 is a weighted aggregate of fuzzy maturity scores, an assessor can inspect the maturity ratings, salience judgements and resulting normalised crisp weights and reproduce the calculation. This reproducibility is consistent with the increasing expectation that continuity capability be supported by documented evidence that regulators, auditors and other assessors can examine.

Three extensions merit study. First, the fuzzy salience judgements could be elicited using a structured fuzzy multi-criteria method rather than assigned directly, thereby connecting the framework to the wider decision-analysis literature and allowing the consistency of expert judgements to be assessed. Second, future work could examine the sensitivity of the index and the priority assessment-unit set to alternative fuzzy scales and defuzzification rules, because these modelling choices may affect aggregate scores. Third, a longitudinal application could track the index across successive *PDCA* cycles to support analysis of continual improvement in relation to Clause 10; however, the index should be interpreted alongside and not as a substitute for, evidence of the suitability, adequacy and effectiveness of the *BCMS*.

9. CONCLUSION

Over five decades, business continuity management evolved from a focus on recovering computer installations into a governed discipline of organisational resilience. Successive standards and guidelines helped formalise this transition. The BS-*ISO* standardisation pathway runs from *PAS* 56 through the two parts of BS 25999 to *ISO* 22301, supported by *ISO* 22313, *ISO/TS*

22317 and the *ISO* 31000 family. The standards landscape is now embedded in a wider environment shaped by the supervisory expectations of the Basel Committee and by legal and regulatory requirements introduced by the European Union and national authorities. The BS 25999-*ISO* 22301 management-system lineage shares the plan-do-check-act logic, while the regulatory instruments discussed above reinforce the expectation that continuity capabilities be evidenced and tested. Building on this logic, the chapter proposes a compact fuzzy standards-alignment maturity assessment framework, proves three algebraic properties of the index; boundedness, monotonicity and the gap identity, and summarises the procedure algorithmically. The framework provides a reproducible basis for the empirical assessment and longitudinal tracking of alignment maturity, subject to further validation.

10. DECLARATIONS

Funding. This research received no external funding.

Conflicts of interest. The authors declare no conflicts of interest.

Note on thesis derivation and related work. This book chapter is derived from and extends the first author's doctoral dissertation, completed at İstanbul Technical University in 2016 under the supervision of the second author. The historical review, early standardisation pathway, business continuity management system concepts and fuzzy decision-making foundations were adapted from the dissertation. The chapter extends this foundation through updated post-2016 literature and standards, the present fuzzy maturity-assessment framework, formal propositions, a worked example and the current regulatory synthesis. A separate companion manuscript (in progress), also derived from the dissertation, will examine the interdependent fuzzy treatment of

continuity-risk criteria within a multi-criteria network decision model and will not include or reproduce the framework, worked example or text presented in this chapter.

REFERENCES

Awang Ali, Q. S, Hanafiah, M. H., & Mogindol, S. H. (2023). Systematic literature review of business continuity management (*BCM*) practices: Integrating organisational resilience and performance in small and medium enterprises (SMEs) *BCM* framework. International Journal of Disaster Risk Reduction, 99, 104135. https://doi.org/10.1016/j.ijdrr.2023.104135

Basel Committee on Banking Supervision. (2021). Principles for operational resilience. Bank for International Settlements.

BDDK. (2020). Regulation on the information systems and electronic banking services of banks (Official Gazette No. 31069). Banking Regulation and Supervision Agency.

British Standards Institution. (2003). *PAS* 56:2003 Guide to business continuity management. *BSI*.

British Standards Institution. (2006). BS 25999-1:2006 Business continuity management. Code of practice. *BSI.*

British Standards Institution. (2007). BS 25999-2:2007 Business continuity management. Specification. *BSI*.

Cedergren, A., & Hassel, H. (2025). Business continuity management in public sector organizations: Development, challenges, and ways forward. Journal of Contingencies and Crisis Management, 33(2), e70055. https://doi.org/10.1111/1468-5973.70055

European Parliament and Council. (2022). Regulation (*EU*) 2022/2554 of 14 December 2022 on digital operational resilience for the financial sector (*DORA*). Official Journal of the European Union, L333, 1–79.

Galaitsi, S. E., Pinigina, E., Keisler, J. M., Pescaroli, G., Keenan, J. M., & Linkov, I. (2023). Business continuity

management, operational resilience and organizational resilience: Commonalities, distinctions and synthesis. International Journal of Disaster Risk Science, 14(5), 713–721. https://doi.org/10.1007/s13753-023-00494-x

Herbane, B. (2010). The evolution of business continuity management: A historical review of practices and drivers. Business History, 52(6), 978–1002. https://doi.org/10.1080/00076791.2010.511185

Herbane, B., Elliott, D., & Swartz, E. M. (2004). Business continuity management: Time for a strategic role? Long Range Planning, 37(5), 435–457. https://doi.org/10.1016/j.lrp.2004.07.011

ISO. (2007). *ISO/PAS* 22399:2007 Societal security: Guideline for incident preparedness and operational continuity management. International Organization for Standardization.

ISO. (2018). *ISO* 31000:2018 Risk management: Guidelines (2nd ed.). International Organization for Standardization.

ISO. (2019). *ISO* 22301:2019 Security and resilience: Business continuity management systems: Requirements (2nd ed.). International Organization for Standardization.

ISO. (2020). *ISO* 22313:2020 Security and resilience: Business continuity management systems: Guidance on the use of *ISO* 22301. International Organization for Standardization.

ISO. (2021). *ISO/TS* 22317:2021 Security and resilience: Business continuity management systems: Guidelines for business impact analysis (2nd ed.). International Organization for Standardization.

ISO. (2024). *ISO* 22301:2019/Amd 1:2024 Security and resilience: Business continuity management systems:

Requirements: Amendment 1: Climate action changes. International Organization for Standardization.

ISO. (2026). *ISO/CD* 22301 Security and resilience: Business continuity management systems: Requirements (Committee Draft, 3rd ed.). International Organization for Standardization. Retrieved 18 July 2026 from https://www.iso.org/standard/93606.html

ISO & *IEC*. (2019). *ISO/IEC* 31010:2019 Risk management: Risk assessment techniques (2nd ed.). International Organization for Standardization and International Electrotechnical Commission.

Margherita, A., & Heikkilä, M. (2021). Business continuity in the COVID-19 emergency: A framework of actions undertaken by world-leading companies. Business Horizons, 64(5), 683–695. https://doi.org/10.1016/j.bushor.2021.02.020

National Fire Protection Association. (2019). *NFPA* 1600 Standard on continuity, emergency and crisis management. *NFPA*.

National Fire Protection Association. (2024). *NFPA* 1660 Standard for emergency, continuity and crisis management: Preparedness, response and recovery. *NFPA*.

Sawalha, I. H., & Anchor, J. R. (2024). Interpretations of business continuity management in the light of COVID-19. Management & Sustainability: An Arab Review, 3(3), 233–248. https://doi.org/10.1108/MSAR-01-2023-0004

Şengül, D. (2016). *Bulanık karar verme ortamında risk değerlendirmesi: İş sürekliliği perspektifi* [Risk assessment in fuzzy decision-making environment:

Business continuity perspective] (Doctoral dissertation, İstanbul Technical University) [in Turkish].

Steen, R., Haug, O. J., & Patriarca, R. (2024). Business continuity and resilience management: A conceptual framework. Journal of Contingencies and Crisis Management, 32(1), e12501. https://doi.org/10.1111/1468-5973.12501

van Laarhoven, P. J. M., & Pedrycz, W. (1983). A fuzzy extension of Saaty's priority theory. Fuzzy Sets and Systems, 11(1–3), 229–241. https://doi.org/10.1016/S0165-0114(83)80082-7

Widianti, T., Dinaseviani, A., Ayundyahrini, M., Sumaedi, S., Rakhmawati, T., Astrini, N. J., Bakti, I. G. M. Y., Damayanti, S., Yarmen, M., Jati, R. K., Yaman, A., Pandin, M., Hidayat, M., Prihanto, I. G., Gunawan, H., & Mahmudi, M. (2024). Business continuity management: Trends, structures and future issues. Business Process Management Journal, 30(7), 2352–2379. https://doi.org/10.1108/BPMJ-01-2024-0046

Zadeh, L. A. (1965). Fuzzy sets. Information and Control, 8(3), 338–353. https://doi.org/10.1016/S0019-9958(65)90241-X

PHYSICAL AND ORGANIZATIONAL ERGONOMIC FACTORS IN THE CLASSIFICATION OF UPPER-EXTREMITY MUSCULOSKELETAL PAIN

Seçil KULAÇ[1]

1. INTRODUCTION

Work-related musculoskeletal disorders are a common occupational health problem associated with discomfort, reduced functional capacity, absenteeism, and impaired work performance. Upper-extremity symptoms involving the hands, wrists, arms, and shoulders can be related to physical demands such as repetitive or forceful movements and sustained physical effort. However, musculoskeletal symptoms may also be associated with organizational characteristics of work, including workload, work pace, job stress, autonomy, supervisor support, and workplace safety conditions. An ergonomic assessment of musculoskeletal health should therefore consider both physical and organizational working conditions (Chan et al., 2022).

The General Social Survey (GSS) Quality of Worklife (QWL) module provides data for examining these factors in a broad working population. It includes measures of physical job demands together with workload, autonomy, supervisory practices, stress, and workplace health and safety conditions. Previous studies using GSS/QWL data have identified repetitive or forceful movements, heavy lifting, and physical effort as relevant factors for musculoskeletal symptoms (Davern et al.,

[1] Öğr. Gör. Dr., Bursa Technical University, Quality Coordination Office, ORCID: 0000-0003-3432-0099.

2024). Organizational and psychosocial conditions, including job stress, time pressure, and supervisor support, have also been associated with musculoskeletal outcomes (Davern et al., 2024; Dick et al., 2020; Waters et al., 2007; Yang et al., 2023).

Most previous GSS/QWL studies have used conventional statistical methods to examine associations between working conditions and musculoskeletal symptoms. Machine-learning methods provide a complementary approach by focusing on classification and allowing multiple predictors to be evaluated simultaneously. Recent reviews indicate that physical exposures, work characteristics, and psychosocial conditions are commonly included in machine-learning studies of work-related musculoskeletal disorders (Chan et al., 2022; Mohd Sallehhudin et al., 2026). However, many applications have focused on specific occupational groups, limiting evidence from broader workforce samples (Hanumegowda & Gnanasekaran, 2022; Sasikumar & Binoosh, 2020; Sohrabi et al., 2024).

The present study uses the 2022 GSS/QWL data to classify self-reported upper-extremity musculoskeletal pain among US workers using Random Forest. Two predictor sets are compared: one containing demographic and working-time variables together with physical ergonomic exposures, and another additionally including organizational ergonomic conditions. The study examines whether organizational variables provide additional classification value beyond physical exposures and uses permutation importance to identify the variables contributing most to classification. Given the cross-sectional design, the findings are interpreted in terms of classification rather than causal relationships.

2. LITERATURE REVIEW

Previous studies using the General Social Survey (GSS) Quality of Worklife (QWL) data have mainly examined associations between working conditions and musculoskeletal symptoms. Waters et al. (2007) and Dick et al. (2020) reported associations of repetitive or forceful hand movements, heavy lifting, and physical effort with musculoskeletal complaints across different QWL waves. More recently, Yang et al. (2023) found that job strain, work–family imbalance, harassment, and discrimination were associated with low back pain after adjustment for physical, occupational, and demographic characteristics. These studies support considering physical and organizational working conditions within the same analysis, although their primary focus was association rather than classification.

Machine-learning studies have examined WMSDs using combinations of ergonomic, individual, occupational, and psychosocial variables. Sasikumar and Binoosh (2020) used postural, physiological, and work-related factors to predict musculoskeletal risk among computer professionals, with Random Forest and Naïve Bayes achieving the highest accuracy in their comparison. Byeon (2024) similarly included ergonomic and psychosocial factors among South Korean male office workers and identified repetitive hand or arm movements, prolonged postures, high job demands, and low job control as relevant predictors.

Studies focusing on other occupational groups have reported similar approaches. Luo et al. (2024) developed models for neck and shoulder WMSDs among healthcare professionals using demographic, occupational, ergonomic, and health-related variables. Fouad et al. (2025) classified musculoskeletal pain across several body regions using demographic, professional,

physical, lifestyle, and occupational information. Their dataset also included working hours and ergonomic practices. Sun and Yuan (2025) applied XGBoost to questionnaire data from coal miners and reported 80.8% accuracy for predicting the degree of musculoskeletal damage. Their analysis included occupational and psychosocial factors as well as symptoms involving the shoulders and hands. Li et al. (2026) also developed WMSD prediction models among coal miners and reported that personal and work-related characteristics contributed to classification, with the best individual model reaching a test AUC of 0.704.

Review studies provide a broader summary of this literature. Chan et al. (2022) reported that machine learning had been used for WMSD risk-factor identification, intervention development, and related prevention research. Mohd Sallehhudin et al. (2026) found that recent ML studies commonly included sociodemographic, workplace, biomechanical, and psychosocial predictors. Frequently examined factors included working hours, job demands, work pace, repetitive or awkward postures, forceful exertion, vibration, and work-related stress. Random Forest was the most frequently used algorithm among the studies included in that review.

Overall, the literature indicates that musculoskeletal classification models can incorporate both physical and organizational working conditions. However, many ML applications have been based on specific occupational groups, while GSS/QWL studies have mainly used regression-based analyses. The present study therefore compares physical ergonomic predictors with a broader predictor set that additionally includes organizational ergonomic conditions using a single Random Forest framework.

3. MATERIAL AND METHODS

3.1. Data Source and Study Sample

Data were obtained from the 2022 General Social Survey (GSS) Quality of Worklife data (Davern et al., 2024). The GSS is a national survey conducted in the United States, and the Quality of Worklife component includes information on working conditions, work organization, occupational exposures, and worker well-being. The 2022 GSS data and accompanying documentation were obtained from NORC at the University of Chicago (Davern et al., 2024).

The outcome was upper-extremity musculoskeletal pain, defined as having experienced pain in the hands, wrists, arms, or shoulders every day for at least one week during the previous 12 months. Respondents with valid outcome information were included in the analysis. The final sample consisted of 2,336 workers, of whom 698 (29.9%) reported upper-extremity pain.

The GSS survey weight was used to estimate descriptive prevalence. Machine-learning model development and evaluation were conducted without survey weighting.

3.2. Study Variables

The predictors were selected to represent demographic and occupational characteristics, physical ergonomic exposures, and organizational working conditions. The variables included in the analysis are presented in Table 1.

Two predictor sets were constructed. Model 1 included the control variables and physical ergonomic exposures. Model 2 included the same variables together with the six organizational ergonomic factors. This structure allowed the additional classification value of organizational working conditions to be evaluated.

Table 1. Variables included in the analysis

Variable group	Variable	Description
Outcome	PAINARMS	Upper-extremity musculoskeletal pain
Control	AGE	Age
Control	SEX	Sex
Control	HRS1	Weekly working hours
Physical ergonomics	HANDMOVE	Repetitive or strenuous hand movements
Physical ergonomics	HVYLIFT	Repeated heavy lifting
Physical ergonomics	PHYEFFRT	Physical effort required by the job
Organizational ergonomics	WORKFAST	Requirement to work at high speed
Organizational ergonomics	OVERWORK	Excessive workload
Organizational ergonomics	STRESS	Work-related stress
Organizational ergonomics	WKFREEDM	Freedom to decide how work is performed
Organizational ergonomics	SUPHELP	Supervisor support
Organizational ergonomics	SAFEHLTH	Workplace health and safety conditions

3.3. Data Preprocessing

Special response codes representing missing or unavailable information were treated as missing values. Missing values for age and weekly working hours were imputed using the median, whereas missing values for the remaining predictors were imputed using the most frequent category. Imputation was performed within the modeling procedure using information from the training data only.

The dataset was divided into training (80%) and test (20%) sets using stratified random sampling according to pain status. The same split was used for both models, and a fixed random seed of 42 was applied to ensure reproducibility.

3.4. Random Forest Modeling

Random Forest was used for classification because it can model nonlinear relationships and interactions among predictors without requiring strong distributional assumptions (Breiman, 2001). Each model consisted of 500 trees. Maximum tree depth was selected from 5, 10, and unrestricted depth using five-fold stratified cross-validation within the training set. ROC-AUC was used as the model-selection criterion.

Because the conventional probability threshold of 0.50 may provide an imbalanced trade-off between sensitivity and specificity, the classification threshold was determined using training data only. Out-of-fold probabilities were generated within the training sample, and the threshold maximizing Youden's J statistic was selected (Youden, 1950):

$$J = Sensitivity + Specificity - 1$$

The selected threshold was subsequently fixed and applied to the independent test set. Thus, the test data were not used for either model tuning or threshold selection.

3.5. Model Evaluation and Variable Importance

Model performance was evaluated on the test set using ROC-AUC, accuracy, sensitivity, specificity, F1 score, and balanced accuracy. The incremental classification value of organizational ergonomic factors was assessed by comparing the performance of Model 2 with that of Model 1.

Permutation importance was calculated for Model 2 using ROC-AUC as the scoring criterion. Each predictor was permuted 30 times, and the resulting decrease in ROC-AUC was used to quantify its contribution to model discrimination. Variable importance was interpreted as predictive contribution rather than as evidence of causal effects.

All analyses were performed in Python using the scikit-learn library.

4. RESULTS AND DISCUSSION

The final analytical sample consisted of 2,336 workers, of whom 698 (29.9%) reported upper-extremity musculoskeletal pain. The weighted prevalence of upper-extremity musculoskeletal pain was 30.9%.

The classification performance of the two Random Forest models is presented in Table 2. The training-derived probability thresholds were 0.286 for Model 1 and 0.296 for Model 2. Both models selected a maximum tree depth of 5 during cross-validation. Model 1, which included control variables and physical ergonomic factors, achieved a ROC-AUC of 0.653 and a balanced accuracy of 0.594. After organizational ergonomic factors were added, Model 2 achieved a ROC-AUC of 0.677 and a balanced accuracy of 0.620. Sensitivity increased from 0.536 to 0.614 and the F1 score from 0.456 to 0.493, whereas specificity decreased from 0.652 to 0.625.

Table 2. Classification performance of the Random Forest models

Performance measure	Model 1	Model 2
ROC-AUC	0.653	0.677
Accuracy	0.618	0.622
Sensitivity	0.536	0.614
Specificity	0.652	0.625
F1 score	0.456	0.493
Balanced accuracy	0.594	0.620

Model 1: control variables + physical ergonomic factors; Model 2: Model 1 + organizational ergonomic factors.

The ROC curves are shown in Figure 1. The addition of organizational ergonomic factors was associated with a 0.024 higher ROC-AUC and a 0.026 higher balanced accuracy on the test set. The increase was therefore modest rather than substantial.

Nevertheless, Model 2 provided better sensitivity and F1 performance, suggesting that organizational working conditions contained some additional information for distinguishing workers with upper-extremity pain. The reduction in specificity indicates a trade-off between identifying a greater proportion of workers with pain and correctly classifying those without pain.

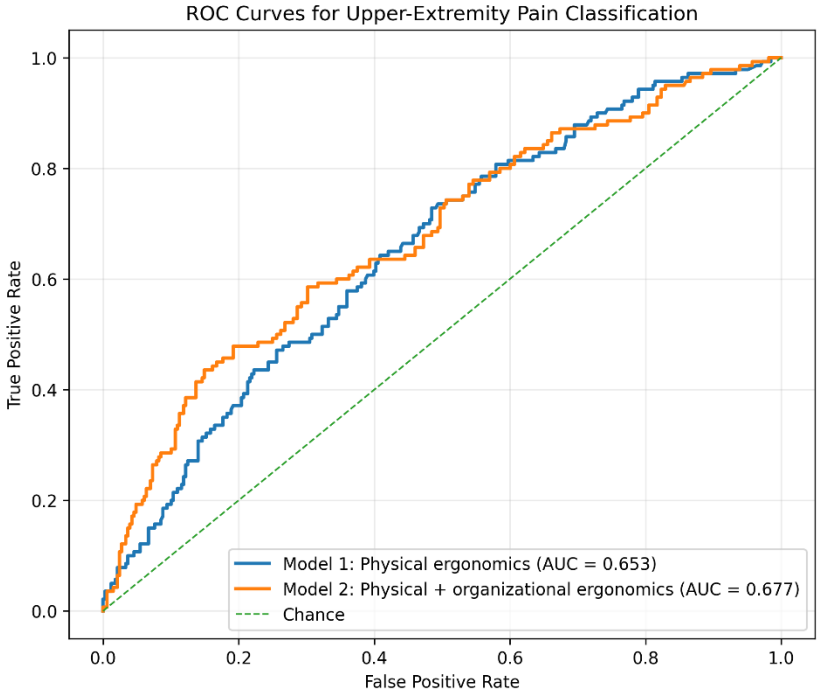

Figure 1. ROC curves for Model 1 and Model 2.

Permutation importance results for Model 2 are presented in Table 3 and Figure 2. Strenuous or repetitive hand movements showed the highest importance, followed by supervisor support. Physical effort, heavy lifting, and work-related stress were also among the more informative predictors.

Table 3. Leading permutation importance results for Model 2

Predictor	Permutation importance
Hand movements	0.0555
Supervisor support	0.0244
Physical effort	0.0116
Heavy lifting	0.0106
Work-related stress	0.0096
Sex	0.0052
Work pace	0.0026
Age	0.0020

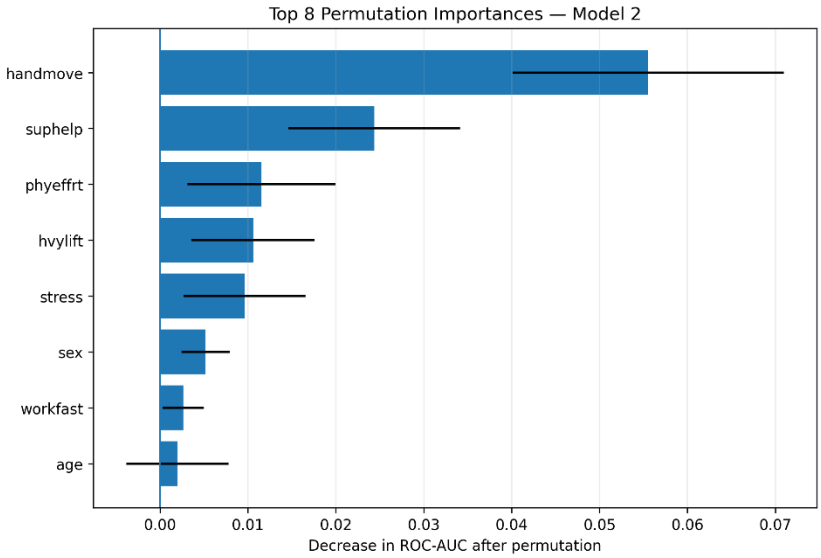

Figure 2. Permutation importance of the eight leading predictors in Model 2.

The prominence of hand movements, physical effort, and heavy lifting is consistent with the role of physical workload in upper-extremity musculoskeletal symptoms. The predictive importance of supervisor support and work-related stress indicates that classification was not based solely on physical exposures. These findings support considering physical and organizational working conditions together when examining work-related musculoskeletal outcomes.

Overall, the models demonstrated moderate rather than high discrimination. The results should therefore be interpreted as evidence of incremental classification value rather than as a highly accurate individual prediction tool. In addition, the cross-sectional and self-reported nature of the GSS data does not permit causal interpretation. Within these limitations, the results suggest that organizational ergonomic factors provide modest additional classification information beyond physical ergonomic exposures.

5. CONCLUSIONS

This study investigated the classification of upper-extremity musculoskeletal pain by considering physical and organizational ergonomic factors using the 2022 GSS Quality of Worklife data. The comparison of the two Random Forest models showed that incorporating organizational working conditions alongside physical ergonomic exposures improved several classification metrics. In particular, the combined model achieved higher ROC-AUC, sensitivity, F1 score, and balanced accuracy, suggesting that organizational factors provide modest additional information for distinguishing workers with and without upper-extremity pain.

The variable importance results further indicated that both physical and organizational working conditions contained information relevant to classification. Strenuous or repetitive hand movements emerged as the most informative predictor, while physical effort and heavy lifting were also prominent. Among the organizational factors, supervisor support and work-related stress also showed predictive importance in the classification model. These findings support an integrated ergonomic perspective in which musculoskeletal outcomes are evaluated not only in relation to physical workload but also in the context of how work is organized and supported.

From a practical perspective, the findings suggest that assessments of upper-extremity musculoskeletal health may benefit from considering both physical exposures and organizational working conditions. Accordingly, physical factors such as demanding hand movements, physical effort, and heavy lifting may be considered alongside organizational factors such as supervisory support and work-related stress.

Future research can extend this framework by comparing multiple machine-learning algorithms and incorporating explainable artificial intelligence methods to examine predictor contributions in greater detail. Survey-weighted machine-learning approaches, occupational or sector-specific analyses, and comparisons across different survey periods could provide further evidence on the generalizability of the observed patterns. Longitudinal data would also be valuable for examining temporal relationships between ergonomic working conditions and musculoskeletal outcomes. In addition, future studies could jointly examine upper-extremity and other musculoskeletal outcomes to provide a broader assessment of work-related musculoskeletal health.

REFERENCES

Breiman, L. (2001). Random forests. *Machine Learning, 45*(1), 5–32. https://doi.org/10.1023/A:1010933404324

Byeon, H. (2024). Predicting occupational musculoskeletal disorders in South Korean male office workers using a robust and sparse twin support vector machine. *Journal of Men's Health, 20*(12), 41–49. https://doi.org/10.22514/jomh.2024.199

Chan, V. C. H., Ross, G. B., Clouthier, A. L., Fischer, S. L., & Graham, R. B. (2022). The role of machine learning in the primary prevention of work-related musculoskeletal disorders: A scoping review. *Applied Ergonomics, 98*, 103574. https://doi.org/10.1016/j.apergo.2021.103574

Davern, M., Bautista, R., Freese, J., Herd, P., & Morgan, S. L. (2024). General Social Survey 1972–2022 [Data file and codebook] (2022 Release 4). NORC at the University of Chicago.

Dick, R. B., Lowe, B. D., Lu, M. L., & Krieg, E. F. (2020). Trends in work-related musculoskeletal disorders from the 2002 to 2014 General Social Survey, Quality of Work Life Supplement. *Journal of Occupational and Environmental Medicine*, *62*(8), 595–610. https://doi.org/10.1097/JOM.0000000000001895

Fouad, D. M., Mahfouz, M. M., Mohamed, M. M., Elzanaty, M. Y., & Abd El-Hafeez, T. (2025). Classification of musculoskeletal pain using machine learning. *Scientific Reports, 15*(1), 27158. https://doi.org/10.1038/s41598-025-12049-9

Hanumegowda, P. K., & Gnanasekaran, S. (2022). Prediction of work-related risk factors among bus drivers using machine learning. *International Journal of Environmental*

Research and Public Health, 19(22), 15179. https://doi.org/10.3390/ijerph192215179

Li, J., Zhang, X., Li, Y., Ding, W., Duan, W., Lim, D., Liang, Y., & Feng, Z. (2026). Determinants of work-related musculoskeletal disorders among coal miners in Jining, China: Development of a predictive risk model. *Frontiers in Public Health, 14*, 1729879. https://doi.org/10.3389/fpubh.2026.1729879

Luo, N., Xu, X., Jiang, B., Zhang, Z., Huang, J., Zhang, X., Tan, Q., Wang, X., Bai, S., Liu, S., Pan, Y., Tang, C., & Zhu, P. (2024). Explainable machine learning framework to predict the risk of work-related neck and shoulder musculoskeletal disorders among healthcare professionals. *Frontiers in Public Health, 12*, 1414209. https://doi.org/10.3389/fpubh.2024.1414209

Mohd Sallehhudin, M. I., Yasin, S. M., Isa, M. R., Razak, T. R., Asraff, M. S. M., Rameli, N. A. C., Shahriman-Teruna, M. M., Salleh, M. M. M., Yusoff, M. Z. M., & Khebir, M. H. A. (2026). Factors associated with work-related musculoskeletal disorders using machine learning approaches: A systematic review. *Annals of Occupational and Environmental Medicine, 38,* e10. https://doi.org/10.35371/AOEM.2026.38.E10

Sasikumar, V., & Binoosh, S. C. A. B. (2020). A model for predicting the risk of musculoskeletal disorders among computer professionals. *International Journal of Occupational Safety and Ergonomics, 26*(2), 384–396. https://doi.org/10.1080/10803548.2018.1480583

Sohrabi, M. S., Khotanlou, H., Heidarimoghadam, R., Mohammadfam, I., Babamiri, M., & Soltanian, A. R. (2024). Modeling the impact of ergonomic interventions and occupational factors on work-related musculoskeletal

disorders in the neck of office workers with machine learning methods. *Journal of Research in Health Sciences, 24*(3), e00620. https://doi.org/10.34172/jrhs.2024.158

Sun, Y., & Yuan, X. (2025). An investigation and prediction of work-related musculoskeletal disorders based on machine learning among coal miners in Western China. In *Proceedings of the 2025 2nd International Conference on Innovation Management and Information Systems (ICIIS 2025)* (pp. 179–186). Association for Computing Machinery. https://doi.org/10.1145/3745676.3745703

Waters, T. R., Dick, R. B., Davis-Barkley, J., & Krieg, E. F. (2007). A cross-sectional study of risk factors for musculoskeletal symptoms in the workplace using data from the General Social Survey (GSS). *Journal of Occupational and Environmental Medicine, 49*(2), 172–184. https://doi.org/10.1097/JOM.0b013e3180322559

Yang, H., Lu, M. L., Haldeman, S., & Swanson, N. (2023). Psychosocial risk factors for low back pain in US workers: Data from the 2002–2018 Quality of Work Life Survey. *American Journal of Industrial Medicine, 66*(1), 41–53. https://doi.org/10.1002/ajim.23444

Youden, W. J. (1950). Index for rating diagnostic tests. *Cancer, 3*(1), 32–35. https://doi.org/10.1002/1097-0142(1950)3:1<32:AID-CNCR2820030106>3.0.CO;2-3

INTEGRATING FINE-KINNEY RISK ASSESSMENT AND LEAN TOOLS TO IMPROVE WORKER SAFETY: A CASE STUDY IN THE FOREST PRODUCTS INDUSTRY[1]

Serap AKCAN YETGİN[2]

Ferhat YURDUNKULU[3]

Cemil ÇEVİK[4]

Mustafa AKIN[5]

1. INTRODUCTION

Companies understand that employee performance is key to their business success. Yet, many companies find it difficult to identify and address safety and ergonomic issues, especially in manufacturing environments where operators are frequently exposed to musculoskeletal stress. Workplace accidents are among the leading causes of productivity loss today. Occupational accidents and occupational diseases occurring in businesses have necessitated the implementation of legal measures. Risk assessment periods are defined according to a business's hazard classification, and in certain circumstances

[1] This research was supported by the TUBITAK 2209-B Projects Fund, under project number 1139B412301931.

[2] Prof. Dr., Tarsus University, Faculty of Engineering, Department of Industrial Engineering, ORCID: 0000-0003-2621-9142.

[3] Undergraduate Student, Tarsus University, Faculty of Engineering, Department of Industrial Engineering, ORCID: 0009-0008-6571-6903.

[4] Master's Student, Tarsus University, Graduate Education Institute, Department of Industrial Engineering, ORCID: 0009-0006-1209-5985.

[5] Undergraduate Student, Tarsus University, Faculty of Engineering, Department of Industrial Engineering, ORCID: 0009-0001-1137-5823.

(technological developments, new regulations, occupational accidents and diseases, near-miss incidents, etc.), reassessments must be conducted before the deadline. Before applying a risk assessment methodology, it is essential for an organization to establish a common understanding of the fundamental occupational health and safety concepts associated with the assessment process (MLSS, 2012). In this context, acceptable risk refers to a level of risk that is consistent with the organization's legal responsibilities and prevention policies and is not expected to adversely affect employees, organizational operations, or work equipment. Prevention encompasses all planned and implemented actions intended to eliminate occupational health and safety risks or reduce them to a minimum throughout the different stages of work activities. A near-miss incident is an event occurring in the workplace that could have resulted in harm to employees, the organization, or equipment, but ultimately does not cause such harm. Risk represents the likelihood that a hazard will result in injury, loss, damage, or another undesirable consequence. Risk assessment is a systematic process involving the identification of hazards present within or originating outside the organization, the evaluation and analysis of the risks associated with these hazards, and the examination of the conditions or factors that may transform hazards into actual risks. Finally, a hazard denotes any existing or potential source, situation, or condition that may cause harm to employees, organizational activities, or work-related assets.

The selection and implementation of occupational risk assessment techniques are influenced by the characteristics of the sector in which they are applied. While certain approaches are sufficiently general to be employed across different industries, some methods have been specifically developed for particular types of activities or working environments (Mullai, 2006). Consequently, the suitability of the selected assessment technique

for the characteristics of the workplace is a critical consideration, since the appropriateness of the methodology may be as important as the results obtained from the assessment itself (Brown, 1993). The choice of an appropriate method should take into account several factors, including the objective of the assessment, applicable legislative requirements, the nature and extent of the information sought, the availability and quality of relevant data, the time allocated to the assessment, the necessity for multidisciplinary or team-based participation, and the scale, complexity, and characteristics of the work being examined (Mullai, 2006).

Risk assessment primarily aims to determine the measures, operating procedures, and control mechanisms required to address potential hazards and reduce the consequences of both intentional and unintended threats within an organization (Özkılıç, 2005). A wide range of methodologies has been developed for this purpose and reported in the occupational health and safety literature. These include Risk Mapping, Preliminary Hazard Analysis, Occupational Safety Analysis, Situation Analysis, Checklist-Based Preliminary Risk Assessment, Preliminary Risk Analysis, Risk Assessment Decision Matrix approaches such as the L-Type and X-Type matrices, Hazard and Operability-related work methodologies, Fault Tree Analysis, the Fine-Kinney method, Failure Mode and Effects Analysis (FMEA), Event Tree Analysis, and Cause-and-Effect Analysis (Özkılıç, 2005). Among these approaches, the Fine-Kinney method has gained considerable acceptance in industrial practice and has been employed in numerous studies addressing occupational risk assessment (Babut, 2011).

Risk assessment is a study conducted to identify existing or potential external hazards in workplaces, analyze and rank the factors that lead to these hazards becoming risks, as well as the risks arising from these hazards, and determine control measures.

The purpose of risk assessments is to identify existing risks in advance, take necessary precautions, and thus prevent workplace accidents and occupational diseases.

Occupational health and safety refer to efforts made to maximize and maintain the physical, mental and social well-being of workers in all occupations and to prevent the deterioration of their health due to working conditions (www.ilo.org). Occupational health and safety have three fundamental objectives: 1- Protection of workers - Creating a healthy and safe working environment, - Protecting workers from health and safety risks arising from the working environment, - Ensuring and improving the health, safety and well-being of workers, 2- Protecting the business - Identifying accidents or undesirable events in advance and taking the necessary measures to prevent possible direct and indirect damage and payments. 3- Protecting production - Ensuring the continuity of production. - Increasing productivity.

In recent years, there has been growing attention on lean production and ergonomics as key approaches to enhancing manufacturing processes. Numerous organizations acknowledge that integrating lean practices with ergonomic principles can simultaneously boost employee productivity and minimize occupational risks. The existing literature includes several studies that explore the combined application of these concepts to improve both operational efficiency and worker health and safety. Botti et al. (2017) focus on developing an assembly line design tool that is both efficient and effective, aligning with lean manufacturing principles while also addressing ergonomic requirements for safe assembly operations. Yunusa-Kaltungo et al. (2017) in their work investigated a continuous improvement-based approach using the root cause method to examine critical errors. Schwerha and Loree (2020) developed a system that incorporates safety and ergonomics with continuous

improvement for better solutions. Brito et al. (2020) investigated lean manufacturing techniques and guidelines in conjunction with safety and ergonomics considerations, aiming to enhance workplace efficiency and employee well-being; their assessment tool was implemented in the plastics packaging industry. Yeshitila et al. (2021) examined the potential of lean thinking to improve safety in offshore oil and gas exploration and production, emphasizing streamlined upstream processes to increase workplace visibility, reduce waste, enhance structural sustainability, mitigate HSE risks, and strengthen operational safety. Afonso et al. (2022) highlighted the significance of combining lean production and ergonomics principles within organizations to simultaneously enhance productivity and improve working conditions. In their study, they employed the Value Stream Mapping (VSM) tool to identify potential areas for improvement and demonstrated its application in a metallurgy factory by integrating Single-Minute Exchange of Die (SMED) techniques with ergonomic assessments. Yousaf et al. (2023) highlight the crucial role of continuous improvement initiatives in the automotive sector and demonstrate how Failure Mode and Effects Analysis (FMEA) serve as an effective tool for achieving and maintaining such advancements. Their study applies the FMEA approach to systematically detect and assess common design and manufacturing failures in automobile rear axle housings. The implementation of the proposed solutions yields multiple advantages, including enhanced customer satisfaction, lower defect rates, improved quality and reliability of products and processes, greater process efficiency, and better utilization of resources. Hock et al. (2024) carried out their study within the semiconductor sector, noting that the industry simultaneously contends with the challenges of risk assessment and process enhancement. To address these issues, they proposed a framework that combines Failure Mode and Effects Analysis (FMEA) with the Plan-Do-Check-Act (PDCA) cycle. This

integrated approach strengthens risk management practices, supports continuous improvement, ensures more efficient use of resources, and facilitates data-driven decision-making, thereby contributing to sustainable organizational development. Ali et al. (2024) reported that their study was directed toward establishing a safer working environment for employees. In their analysis, they applied risk assessment techniques, Failure Mode and Effects Analysis (FMEA), along with the principles of international standards ISO 31000 and ISO 45001 to identify various hazards and assess potential risks. Furthermore, they suggested the use of lean practices such as 6S and Visual Management to improve occupational safety and to minimize both the probability and the impact of possible risks.

The study by Yazdi and Adumene (2025) emphasizes the importance of comprehensive risk assessments to prevent accidents, protect workers, and ensure compliance with AS/NZS 4024.1–2019 standards and Work Health and Safety (WHS) regulations. These assessments identify and evaluate critical hazards, including cutting, tearing and crushing risks, and provide targeted mitigation strategies to address these specific risks.

The purpose of this study is to conduct risk analysis and process improvement practices to improve the adverse working conditions of workers in a chipboard manufacturing facility, protect workers from occupational diseases, and increase productivity and efficiency at the facility. To this end, the risk assessment studies aim to increase productivity and efficiency, increase output, reduce cycle times, reduce errors and scrap in production, reduce the number of malfunctions and downtimes during machine operation, improve ergonomic working conditions for workers, identify hazards, analyze risks, rank risks, and determine control measures.

2. METHODOLOGY

In this section, it is explained that the methods used in risk assessment and process improvement work for employee safety.

2.1. Gemba (Crime Scene) Analysis

In the business world, gemba refers to the place where value is created (Imai, 1997; Reke and Böhlmann, 2021).

Gemba principles: Go and see - Physically go to the scene and see the problem firsthand. Touch, feel, and understand the problem - Go into as much detail as necessary. See cost items and waste firsthand - See waste, fatigue, and unnecessary burdens. Create an environment of unity, love, and respect - Build team spirit and respect. Research, collect data, analyze, and evaluate - Solve the problem together with those who experience it.

The gemba approach should always include the following: The observer must possess a deep-rooted curiosity in action to understand what is actually happening. If they merely make assumptions or develop ideas based on what they hear, then value is lost from the gemba. A strong desire to know what is happening is essential. Directly observe how the work is done. To understand gemba, one must be present. The purpose of gemba is to gain a clearer understanding of gemba behavior and the current reality of the situation through direct observation. Respect others and strengthen the culture. Gemba requires direct interaction with employees while working. If done incorrectly, this can easily create tension between upper management and employees if the employee feels uncomfortable being observed. However, to fully appreciate gemba, one should engage directly with employees, not from a distance. Showing equal respect to everyone is common sense, especially in gemba.

2.2. Muda (Waste) Analysis

It represents the process of identifying any activity that does not create value and can be considered waste, as well as waste in lean production. According to Muda, waste is divided into seven main categories (Bakdaal and Akcan, 2021; Memari et al., 2024): Transportation: The unnecessary transfer of products or materials from one location to another. Inventory: Inventory waste resulting from waiting, repairs, and overproduction. Motion: The excessive or unnecessary movement of an employee or machine to perform a task. Waiting: The idle waiting of operators while machines are operating, equipment malfunctions, or necessary parts are delayed. Overproduction: Production that exceeds the expected and desired level of production. Overprocessing: Unnecessary processing of parts resulting from incorrect or unnecessary process progress. Defects: The rework of defective materials that do not meet quality standards or the remanufacturing of faulty products.

2.3. Finne Kinney Risk Analysis

Finne Kinney Risk Analysis originated in the United States in calculating the explosion risks of ammunition depots in military areas. It uses mathematical values to calculate risks, followed by a graphical interpretation by ranking high-risk groups. Today, this method has become an important method for determining hazard risk levels in businesses. The Finne Kinney method was first proposed by Fine in 1971 (Fine, 1971). It is a method developed by Kinney (Kinney and Wiruth, 1976). This method emphasizes the probability dimension of risk. The Kinney method has become widespread in the United States and Western European countries. The numerical values used in the Finne Kinney method are generally divided into three parameters (probability (P), frequency (F), and severity (S)). A risk priority number (RPN) is obtained by multiplying these three parameters

(RPN = P*F*S), and risks are ranked. Corrective and preventive actions are recommended based on risk levels.

Knowing the probability, frequency, and severity values facilitates accurate scoring in the risk analysis plans that businesses need to prepare (Kinney and Wiruth, 1976). Probability: The probability of visible and invisible hazards occurring in businesses (Table 1). Frequency: The frequency with which employees are exposed to foreseeable and unforeseen hazards in the workplace over time (Table 1). Severity: The extent of damage caused to the environment by the possibility of hazardous sources occurring in the business, the magnitude of the negative health consequences on employees, or in short, the magnitude of the harm is called severity. Depending on the severity, the degree of harm is reduced by replacing the hazardous with the non-hazardous (Table 2). The risk priority number (RPN) and risk assessment results obtained from the risk analysis are shown in Table 2.

Table 1. The Values for Likelihood of Hazardous Event and the Exposure Factor

Likelihood of hazardous event		The exposure factor	
Probability	Value	Frequency	Value
Virtually impossible	0,1	Very rare (yearly)	0,5
Practically impossible	0,2	Rare (a few per year)	1
Conceivable but very unlikely	0,5	Unusual (monthly)	2
Only remotely possible	1	Occasional (weekly)	3
Unusual but possible	3	Frequent (daily)	6
Quite possible	6	Continuous	10
Might well be expected	10		

Table 2. The Values for Possible Consequences and the RPN Definitions

The possible consequences		The RPN definitions	
Severity	Value	Risk score	Risk situation
Noticeable (minor first aid accident)	1	R>400	Very high risk; consider discontinuing operation
Important (disability)	3	200<R<400	High risk; immediate correction required
Serious (serious injury)	7	70<R<200	Substantial risk; correction needed
Very serious (fatality)	15	20<R<70	Possible risk; attention indicated
Disaster (few fatalities)	40	R<20	Risk; perhaps acceptable
Catastrophe (many fatalities)	100		

3. CASE STUDY AND FINDINGS

The integrated enterprise in question produces raw and melamine coated MFC and Chipboards, laminated flooring, fire-resistant MFC and Chipboards, moisture-resistant MFC and Chipboards, painted panels, honeycomb-filled decorative panels, glossy panels, countertops and door panels, which are needed by the furniture, decoration and construction industries.

3.1. Chipboards

Chipboard is a panel produced by combining wood or lignified sawdust with synthetic resin adhesives and pressing them under high temperature and pressure. The primary characteristics of chipboard are its ergonomic structure and affordability. It is less expensive than conventional wood and plywood. It is produced in thicknesses ranging from 6 mm to 40 mm. Its density ranges from 500 to 700 kg/m3. Chipboards, used in various applications, have varying dimensions depending on their intended use. Chipboards began as an alternative to lumber. They are a wood material that is easier to cut and assemble when

cut into different sizes. Chipboards can be used as flooring, ceilings, and walls within homes. They are also used in place of materials that form the support points of a three-dimensional design. They are also used in furniture production.

3.2. Problem Definition

The process flow during the production of chipboards produced at the plant is as follows: raw material storage, chipping, wet chip storage, drying, dry chip storage, gluing, laying, cold pressing of chipboards, hot pressing of chipboards, sizing, sanding, and storage (Figure 1). Analysis of data obtained from the plant revealed that during product production in the hot-pressing unit of chipboards, the press shut down during the change of mold and the press weight switch position adjustment caused unergonomic conditions and potential risks. This leads to both a high risk of workplace accidents and inefficiency in the plant.

This study aims to eliminate the risks arising from malfunctions in the chipboards hot pressing unit during the production of Chipboards in the plant and to improve ergonomic conditions.

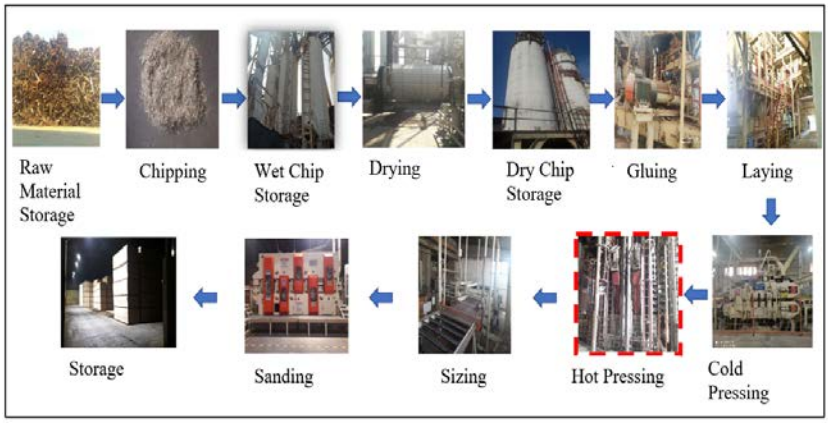

Figure 1. Process Flow Chart for Chipboards Production

3.3. Gemba Analysis

To analyze the crime scene of the problem under investigation, the following concepts are explained first: Press Slowdown Switch: This allows the press to close slowly.

Press Closed Switch: This allows the press to switch to high pressure. Switch Position Adjustment: This allows the press to switch to high pressure according to the paste thickness during production changes.

When the problem was examined on-site, it was determined that if the switch position adjustment was not made or forgotten when switching from 18mm to 30mm, the press would not switch to high pressure and the desired thickness would not be achieved. This would result in losses before the sanding process. Furthermore, if the switch position adjustment was not made or forgotten when switching from 30mm to 18mm, the press would switch to high pressure too early, which would damage the simultaneous arms and cause the sheet to burst.

As a result of the crime scene analysis, it was determined that electrical maintenance personnel must adjust the switch during thickness changes during production. However, this adjustment poses ergonomic and OHS risks. To adjust the position of the switches, the electrical maintenance technician first climbs the ladder and then crosses the fence to the other side of the ladder. Ergonomics risks related to heights were identified here (Figure 2). Another result of the crime scene analysis is that an electrical maintenance technician was exposed to a temperature of 122 degrees Celsius for 84 seconds while adjusting the switch positions, with the press in the open position. The distance between the technician and the heat source was 10 centimeters. Movements at these high temperatures and close to them pose a significant risk (Figure 3).

Figure 2. Actions Performed by Personnel During Switch Replacement

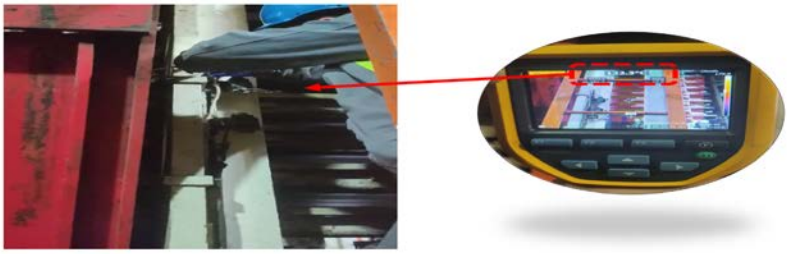

Figure 3. Temperature Factor During Switch Replacement

Finally, during the scene analysis, it was observed that electrical maintenance personnel were positioning switches at a height of 150 cm, using a challenging position, with one foot on the step and the other on the switch support. This height hazard during switch replacement poses a risk of injury to the maintenance personnel from falling (Figure 4).

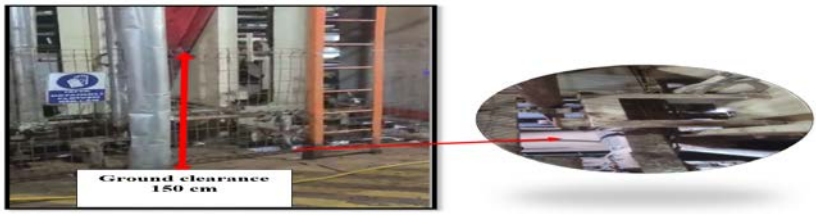

Figure 4. Height Hazard During Switch Replacement

3.4. Muda (Waste) Analysis

With the Muda (waste analysis) analysis, the delays, unnecessary movements, unnecessary operations and risks that may occur during the switch replacement (Figure 5) were determined.

Problem-related waste type	Pareto analysis	Trend analysis	Photograph	Video	Spaghetti diagram	FMEA	OHS risk analysis	Ergonomics risk analysis	Other
Waiting									
Defects									
Overproduction									
Transportation									
Motion									
Overprocessing									
Unnecessary stock									
Insecurity									
Inefficiency									
Resource consumption (water, electricity, natural gas, etc.)									

Figure 5. Muda (Waste) Analysis Table

Waiting: When adjusting the switch position for a production change, electrical maintenance technician spends 148 seconds adjusting the switch position. Since the switch position is adjusted 30 times per year, the total time spent is 68.4 minutes per year. The average number of position adjustments is shown in Figure 6. Waste incurred during switch position adjustment is defined as waiting and unnecessary motion (Figure 7).

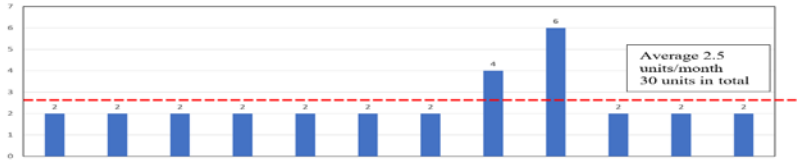

Figure 6. Trend Analysis for 30mm/25mm Production Change by Month

Figure 7. A Moment While the Switch Position is being Adjusted

Motion: Electrical maintenance technician travel from the workshop to the press area during production thickness changes, stopping at two stations, a total of 40 steps. Each time, they make 32 meters of unnecessary movement. Because switches are repositioned for thickness changes 30 times a year, the electrical maintenance personnel travel 1,920 meters per year. Overprocessing: During production thickness changes, electrical maintenance technician loosens the bolts holding the press closing and weighting switches, using an allen wrench, and fix them in the appropriate position (Figure 8). Insecurity: Electrical maintenance technician climbs the ladder to adjust the switch position and make non-ergonomic and risky movements to the other side (Figure 9). The electrical maintenance technician adjusts the switch position in an unsafe and risky manner by placing one foot on the ladder and the other foot on the switch support (Figure 10).

Figure 8. Switch Position Adjustment

Figure 9. Using a Ladder When Changing a Switch

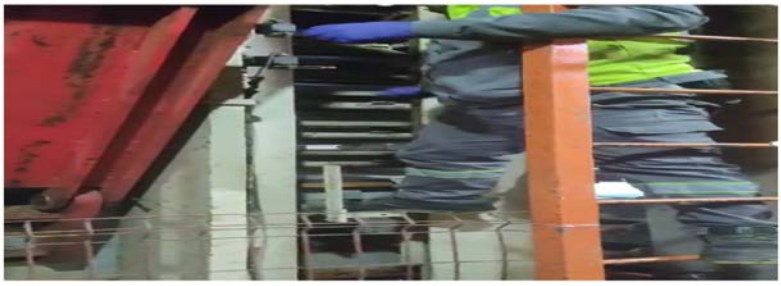

Figure 10. Risky Movements When Using a Ladder During Switch Replacement

3.5. Finne Kinney Risk Analysis

In the risk analysis we conducted for the press closing and weighting switch position adjustment during the chipboard press thickness change, 4 essential, 2 important, 7 possible and 1 insignificant risk were identified. Some of these risks are shown in Figure 11.

ACTIVITY AND SUB-STEPS	Routine		HAZARD	RISK DEFINITION	Source of Hazard	Risk Assessment				Risk Category
	Y	N				P	F	S	RPN	
Walking to the risk zone		X	T-6-b irregularity of the working area	Tripping out/over	GROUND	3	2	7	42	Possible risk
Switch position adjustment		X	T-6-d irregularity of the working area	Difficulty of access in emergency situations	PRESS	3	2	40	240	Substantial Risk
Switch position adjustment		X	T-24 hot oil splash	Burn	HOT OIL PIPE	1	2	15	30	Possible risk

Figure 11. Table of Possible Risks in Switch Replacement

4. CONCLUSIONS

This study investigated the potential risks and unergonomic conditions resulting from the press die change during product production in the chipboard hot pressing unit. As a result of the risk analysis conducted in this study, four major and two significant risks were reduced to potential risk levels after the actions taken. The analysis reduced the risk level of four 240-point major risks to 75% after the proposed improvement recommendations, reducing the risk level to below 60 points. Thus, the wasteful waiting, unnecessary movements, and unnecessary processes identified in the analysis were completely eliminated.

In the study encountered several challenges in implementing the proposed measures. These included: the cost of production shutdowns for the business, the adaptation of maintenance personnel to the new electronic control system, and technical incompatibilities in integrating existing equipment with the new system. To overcome these challenges, the implementations were carried out during planned maintenance shutdowns, targeted training was provided to personnel, and pilot trials were conducted before the system was commissioned to identify potential failures in advance. Furthermore, collaboration between maintenance and production teams reduced resistance to the changes.

In addition, this study can be similarly applied in sectors such as wood products, automotive, metalworking and food industries, where maintenance, mold changes, adjustment operations and manual interventions are intensive.

REFERENCES

Afonso, M., Gabriel, A.T., Godina, R. (2022). Proposal of an innovative ergonomic SMED model in an automotive steel springs industrial unit. Advances in Industrial and Manufacturing Engineering, 4, 100075.

Ali, M., Kassem, S.S., Elatriby, S.A. (2024). Enhancing Safety Measures in a Steel Manufacturing Facility; Factory X Case Study. 2024 International Conference on Decision Aid Sciences and Applications (DASA). DOI: 10.1109/DASA63652.2024.10836454.

Babu,t G., Moraru, R., Cioca L. (2011). Kinney-Type Methods: Useful or Harmful Tools in the risk assessment and management process. International Conference on Manufacturing Science and Education-SIBIU-Romania.

Bakdaal, B., Akcan, S. (2021). Analysis of Waste in A Small-Scaled Manufacturing Facility and The Process Improvement Studies. Research & Reviews in Engineering-1, Gece Publishing, 107-120.

Botti, L., Mora, C., Regattieri, A. (2017). Integrating ergonomics and lean manufacturing principles in a hybrid assembly line. Computers & Industrial Engineering 111, 481–491.

Brito, M., Vale, M.V., Leão, J., Ferreira, L.P., Silva, F.J.G., and Gonçalves, M.A. (2020). Lean and ergonomics decision support tool assessment in a plastic-packaging company. Procedia Manufacturing, 51,613-619.

Brown, J.D. (1993). Preventing Accidental Releases of Hazardous Substances. Professional Safety. 38(8): 23-23.

Fine, W.T. (1971). Mathematical evaluations for controlling hazards (No. NOLTR-71-31). Naval Ordnance Lab., White Oak. Md.

Hock, H.D., Amalina, N., Muhammad, N. (2024). Synergizing FMEA and PDCA for superior risk management and process improvement in the semiconductor industry: a case study. International Journal of Production Management and Engineering, 12(2), 180-194.

ILO. www.ilo.org

Imai, M. (1997). Gemba kaizen: a commonsense low-cost approach to management. New York: McGraw-Hill Professional. s. 13. ISBN 978-0-07-031446-7.

Kinney, G.F., Wiruth, A.D., (1976). Practical Risk Analysis for Safety Management. China Lake, CA: NWC Technical Publication 5865, Naval Weapons Centre, pp 1–20.

Memari, A., Panjehfouladgaran, H.R., Rahim, A.R.A., Ahmad, R. (2024). The impact of lean production on operational performance: a case study. Asia-Pacific Journal of Business Administration Vol. 16 No. 3, 2024 pp. 530-552.

Ministry of Labor and Social Security, (2012). Occupational Health and Safety Risk Assessment Regulation. Number: 28512. Ankara: Official Gazette of the Republic of Turkey.

Mullai, A. (2006). Risk Management System-Risk Assessment Frameworks and Techniques. DaGoB (Safe and Reliable Transport Chains of Dangerous Goods in the Baltic Sea Region) Project Office, Turku School of Economics, 5st ed. Turku: Finland, p: 172-28.

Özkılıç, Ö. (2005). Occupational Health and Safety Methodologies, Management Systems and Risk Assessment Methodologies. Ankara.

Reke, E., Böhlmann, N. (2021). Developing Middle Managers with Gemba Training. IFIP Advances in Information and Communication Technology, 610: 271-277.

Schwerha, D., Casey, A., Loree, N. (2020). Development of a system to integrate safety, productivity, and quality metrics for improved communication and solutions. Safety Science, 129- 104765.

Yazdi, A. (2025). Innovative risk management for machine safety: insights from AS/NZS 4024 standards. The International Journal of Advanced Manufacturing Technology (2025) 137:659–682.

Yeshitila, D., Kitaw, D., and Jilcha, K. (2021). Applying lean thinking to improve operational safety in oil and gas industry. Open Journal of Safety Science and Technology, 11, 120-141.

Yousaf, M.U., Aized, T., Shabbir, A., Ahmad, M., Nabi, H.Z. (2023). Automobile rear axle housing design and production process improvement using Failure Mode and Effects Analysis (FMEA) Engineering Failure Analysis 154, 107649.

Yunusa-Kaltungo, A., Kermani, M.M., Labib, A. (2017). Investigation of critical failures using root cause analysis methods: Case study of ASH cement PLC. Engineering Failure Analysis, 73, 25-42.

YALIN HİZMET YAKLAŞIMI İLE ACİL SERVİS SÜREÇLERİNİN İYİLEŞTİRİLMESİ: DEĞER AKIŞ HARİTALAMA UYGULAMASI

Betül TURANOĞLU ŞİRİN[1]

1. GİRİŞ

Günümüzde firmalar arasında rekabet maksimum seviyeye ulaşmıştır. Bunun için de yenilik ve değişikliklere uyum sağlamak, ayak uydurmak gerekmektedir. Yeni sistemlere, teknolojilere uyum sağlamak zorundadırlar. Aksi takdirde bu rekabet ortamında yarışta geride kalmaya mahkûm olurlar. Yalın üretim sisteminin temel amacı israfı önlemektir. İsrafı önlemek amacıyla mevcut sistemlerde sürekli iyileştirme ve geliştirme yapılmaktadır.

Bu çalışmada, bir araştırma hastanesinin acil servisinde yalın hizmet anlayışını sağlamak amacıyla yalın üretim tekniklerinden biri olan Değer Akış Haritalama (DAH) temel metot olarak kullanılmıştır. DAH adımları tek tek uygulanmış olup önce değer akışı belirlenmiş, sonrasında mevcut durum haritası çıkarılarak gelecek durum için bir plan tasarlanmıştır. Gelecek durum haritasının çıkarılması işleminden sonra acil servis için tasarlanan değer akışı değerlendirilmiştir.

DAH çalışması sonucunda mevcut durumdaki işlem, bekleme ve temin süreleri belirlenmiş, tespit edilen israf ve israf kaynakları için önerilerde bulunulmuştur. Öneriler sonucunda tasarlanan gelecek durum haritasına göre bekleme sürelerinde

[1] Doç. Dr., Atatürk Üniversitesi, Mühendislik Fakültesi, Endüstri Mühendisliği Bölümü, ORCID: 0000-0002-7910-6312.

%52,05; işlem sürelerinde %12,5 ve temin sürelerinde %40 oranında iyileştirmeler sağlanmıştır.

2. YALIN DÜŞÜNCE KAVRAMI

Yalın düşünce yaklaşımı, öncelikle değer kavramının ortaya konulmasını, değer yaratmayan faaliyetlerin ayıklanmasını ve değer oluşturan süreçlerin etkin bir akış içerisinde düzenlenmesini esas almaktadır. Bu yaklaşımda, müşteri talebi doğrultusunda süreçlerin kesintisiz olarak yürütülmesi ve süreç performansının sürekli iyileştirilmesi hedeflenmektedir. (Yılmaz, 2012).

Yalın üretimin temel ilkeleri, mühendis Eiji Toyota ve beraber çalıştığı mühendis Taiichi Ohno'nun öncülüğünde 1950'lerde Toyota fabrikasında atılmıştır. İkilinin Amerika gezisinde edindiği bilgiler öncülüğünde kitle üretim sisteminin Japonya için uygun olmadığına karar vermişlerdir. Bu kararla birlikte yalın düşüncenin ilk adımları atılmıştır (Balcı, 2006).

Yalın düşüncenin temel amacı; değerin ilk hammaddeden başlayarak son kısım olan müşterinin eline hiçbir kesinti olmadan hızlı bir şekilde ulaştırılmasıdır. Diğer adı Toyota Üretim Sistemi (Tam Zamanında Üretim) olarak ifade edilmektedir (Yurdagül, 2010).

Yalın düşünce uygulamaları sayesinde süreçlerde ortaya çıkan israfların sistematik biçimde azaltılması ve mevcut kaynakların daha fazla değer üretmeye yönelik kullanılması, işletmeler açısından maliyetlerin düşürülmesine, kârlılığın ve rekabet gücünün artırılmasına katkı sağlamaktadır. Bunun yanı sıra, elde edilen kazanımlar müşterilere daha kaliteli, ihtiyaçlarına daha uygun ve daha düşük maliyetli ürün ve hizmetler sunulmasına olanak tanımaktadır. Yalın yaklaşımın farklı sektör ve faaliyet alanlarında yaygınlaştırılması ise işletme düzeyindeki

bu kazanımların toplumsal refah ve ekonomik zenginlik üzerinde de olumlu etkiler oluşturmasını sağlayabilmektedir.

Yalın üretim, geleneksel seri üretim sistemlerine kıyasla daha az kaynak kullanımı ve daha sade süreç yapısı üzerine kuruludur. Bu yaklaşımda üretim faaliyetlerinin gereksiz karmaşıklıktan arındırılması, stok seviyelerinin ihtiyaç duyulan düzeyde tutulması ve hatalı ürünlerin en aza indirilmesi amaçlanmaktadır. Bununla birlikte yalın üretim, müşteri ihtiyaçlarındaki farklılıklara cevap verebilmek amacıyla daha geniş bir ürün çeşitliliğinin etkin ve esnek bir biçimde üretilmesine olanak sağlayan bir üretim anlayışını ifade etmektedir.

Yalın işletme yaklaşımının temelini oluşturan ve işletmelerin bu anlayış doğrultusunda faaliyet göstermelerini sağlayan başlıca ilkeler aşağıda sunulmuştur (Womack ve Jones, 1998):

- **Değer:** Yalın üretimin ilk ilkesi aynı zamanda yalın olma yolunda atılan ilk adımdır. Müşteri tarafından üretici, değer katan olarak görülmektedir. Bu yüzden müşteriler tarafından yapılan değerlendirmeler ve tanımlara göre üretim yapmak daha doğru olmaktadır. Üreticilerin yapması gereken müşterilerle arasındaki iletişimi geliştirmesidir. İsrafın ortadan kaldırılıp, maliyetin belirlenmesi için üreticiler ile müşterilerin değeri birlikte analiz etmesi gerekmektedir.

- **Değer akışı:** Buradaki fikir, bir sayfada, süreç boyunca malzeme / ürün akışının bir "haritasını" çizmektir. Amaç, değer yaratmayan her adımı belirlemek ve sonra bu savurgan adımları ortadan kaldırmanın yollarını bulmaktır.

- **Akış:** Akış ilkesi; süreçlerin, çalışanların ve kurum kültürünün birbiriyle uyumlu şekilde ele alınmasını ifade etmektedir.

- **Çekme:** Çekme sisteminde dengesiz durumu ortadan kaldırarak, müşteri talep ettikçe diğer üretime uyarı gitmekte ve çalışmaktadır. Böylece maliyetlerin azalmasına, gereksiz stok ve kalitesiz ürün meydana getirmenin önüne geçmiş bulunmaktadır.
- **Mükemmellik:** Adımları gerçekleştirmek harika bir başlangıçtır, ancak beşinci adım olan mükemmellik belki de en önemlisidir: Yalın düşünme ve süreç iyileştirmeyi kurumsal kültürünüzün bir parçası haline getirmektir. Kazançlar birikmeye devam ettikçe, yalının statik bir sistem olmadığını ve mükemmelleşmek için sürekli çaba ve dikkat gerektirdiğini hatırlamak önemlidir. Nihayetinde amaç mükemmellik (ulaşılamaz) değil, aksine sürekli iyileştirme olarak bilinen bir kavram olan bunun peşinde koşmaktır.

3. MATERYAL VE METOT

3.1. Değer Akışı Haritalama (DAH)

DAH, bir değer akışındaki mevcut durumun görselleştirilmesi tekniğidir. Tüm sistemin optimizasyonu için süreçteki malzeme ve bilgi akışının resmedilmesidir. Akıştaki israfı ve kaynaklarını görmeye yarayan DAH, mevcut durumu analiz ederek süreç içerisindeki faaliyetleri haritalandırır ve bütün akışın nasıl işlemesi gerektiğinin planlamasını yapmaya yardım eder (Kılıç, 2016).

Yalın üretim/hizmette amaç sistemdeki israfların önlenmesidir. DAH, bu amaç doğrultusunda mevcut sistem üzerinde israfları, akışın olmadığı noktaları görmeyi ve önlenmesi için gelecek durum haritası çıkarmayı hedeflemektedir.

Değer bakış açısı, süreci parça parça incelemeyi değil, bütün süreci ele almayı amaçlamaktadır. Hedefi parçaları değil

bütünü iyileştirmektir. Yani DAH, tüm sistemin optimizasyonu için kullanılan bit yalın üretim yöntemidir.

Değer katmayan işlemler süreçteki israfları oluşturmaktadır. Oluşan israfların önlenmesi işletmeye maliyet ve zaman açısından katkı sağlamaktadır. DAH, bu israfları ve kaynaklarını tespit etmekte ve israflar çıkarıldıktan sonra akışın sürekli hale gelmesine yardım etmekte kullanılan bir tekniktir. Akış için gerekli tüm faaliyetleri bir bütün olarak görmeye yaramaktadır. (Güleryüz, 2012).

DAH tekniği genel olarak 4 adımdan oluşmaktadır. Bu adımlar:

- ✓ Ürün grubunun seçilmesi: Değer akımının, liderinin ve sınırlarının belirlenmesi, ürün grubu ve harita sınırlarının belirlenmesi.
- ✓ Mevcut durum haritasının çıkarılması: Mevcut durumun analiz edilmesi.
- ✓ Gelecek durum haritasının çıkarılması: Gelecek durumun analiz edilmesi ve belirlenen hedefleri karşılayıp karşılamadığının tespit edilmesi.
- ✓ İş planının hazırlanması ve uygulanması: Uygulama planı hazırlanması, kazanımların belirlenmesi ve sonuçların ölçülmesi.

4. ARAŞTIRMA BULGULARI

4.1. Ürün Aile Seçimi

DAH'a başlamak için öncelikle ürün yada hizmet ailesi belirlenmiştir. Çalışmanın yapıldığı hastanenin acil servisinde (AS) hastaların geçirmiş olduğu prosesler, sağlık kuruluşu olması nedeniyle çok çeşitlidir. Bu çalışmada acil servisteki tüm işlem faaliyetlerini içeren bir ürün ailesi seçilmiş ve bu ürün ailesi

üzerinden haritalandırma gerçekleştirilmiştir. Ürün/hizmet ailesi olarak Danışma-Kayıt-Triaj-Muayene-Laboratuvar-Röntgen-Tomografi-Ultrason seçilmiştir.

4.2. Mevcut Durum Haritası

4.2.1. Hasta Beklenti ve İhtiyaçlarının Belirlenmesi

Değer akış haritalama, müşterilerin memnuniyetinin üst seviyede olacağı şekilde belirlenip hazırlanmalıdır. Burada müşteri, hastalardır. Hastaların memnuniyeti için hasta bilgi ve ihtiyaçlarının belirlenmesi gerekmektedir. Aşağıda hastaların memnuniyetini sağlamak için gerekli maddeler yer almaktadır.

- Hastaların bilgilendirilmesi
- Doğru muayene
- İlk teşhisin doğru konulması
- Beklemelerin olmaması
- Hastanenin temizliği
- Gürültünün olmaması
- Ziyaret saatlerinin uygun olması
- Hastane sıcaklığının insan bedenine uygun olması
- Havalandırma belli aralıklarla yapılması
- Hastanedeki personellerin anlayışlı ve güler yüzlü olması

Acil servise gelen bireyler hastalıklarına şifa bulmak için gelmektedir. Bu süreçte ilk teşhisin doğru olması hastayı memnun edecektir. Çünkü tedavi de doğru uygulanmış olacaktır. Hastaların yakınmasının en büyük nedenleri yanlış tedavi, bilgilendirmenin açıklayıcı olmaması ve bekleme süresinin uzun olmasıdır.

4.2.2. Sistem Ölçütleri

Acil serviste elde edilen veriler 3 ölçüte göre değerlendirilmektedir. Bunlar;

- İşlem Zamanı (C\T): Hastaların işlemden geçtikleri zamandır. Değer katan zaman dilimidir.
- Bekleme Zamanı (W\T): Hastaların geçtikleri süreçlerin dışında kalan verimsiz zamandır. Değer katmayan zaman dilimidir.
- Temin Zamanı (L\T): Hastaların sistemde geçirdikleri toplam zamandır.

Acil serviste gözlem ve ölçümler sonucu elde edilen veriler bu 3 ölçüte göre sınıflandırılacak ve harita üzerinde gösterilecektir.

4.2.3. Acil Servis İçin Takt Zamanının Hesaplanması

Bu bölümde, ele alınan acil servis için takt zamanı hesaplanmaktadır. Takt zamanı müşteri talebini karşılamak için gerekli olan süreyi ifade etmektedir. Acil serviste müşteri, hastalardır. Hastaların talebini karşılamada gerekli olan süre için; 2020 yılında söz konusu acil servise gelen hasta sayısı (147.154), hastanenin istatistik biriminden elde edilmiş olup takt zamanının hesaplanmasında bu sayı kullanılmaktadır.

Acil serviste net çalışma süresi tam gündür. 365 günde 24 saat kesintisiz hizmet verilmektedir. Bir gün 2 vardiyadan oluşmaktadır. Acil sağlık personeli 08:00'da gece ekibinden nöbeti teslim alır; 16:00'da gece ekibine nöbeti devrederler.

- 08:00-16:00 gündüz vardiyası
- 16:00-08:00 gece vardiyası

Toplam Çalışma Süresi= 24saat/gün × 60 dakika/saat =1440 dakika= 86400 saniye/gün

Günlük Net Çalışma Süresi= 24 saat/gün= 1440 dakika/gün = 86400 saniye/gün

Günlük Talep= 147754/365= 404,8≈405 hasta/gün

Takt Zamanı= Günlük Net Çalışma Süresi/ Günlük Talep

Takt Zamanı= 86400 saniye/gün / 405 hasta/gün = 213,33≈214 saniye/hasta

214 saniye/hasta≈3,6 dakika/hasta

Takt zamanının hesabı sonucunda acil servise ortalama 3,6 dakikada bir hasta geldiği belirlenmiştir.

4.2.4. Acil Servis İçin Ana Proseslerin Belirlenmesi

Gözlemler sonucunda hastaların geçtiği 7 ana proses elde edilmiştir:

- ***Kayıt*:** Acil kayıt bölümü diğer kayıt birimlerinden ayrıdır. Acil servisin girişinde yer alan bu bölümde hasta bilgileri kendisi veya yakınları tarafından HBYS olarak isimlendirilen sisteme kaydedilmektedir. Hastalar muayene odasına gönderilmeden önce hasta kabul biriminden acil muayene kaydı yaptırarak başvururlar. Bu bölümde, 3 adet bilgisayar başında 3 adet personel bulunmaktadır. Hastanın kimlik bilgileriyle HBYS'ye girilerek acil servise kaydı yapılmaktadır. Kaydı yapılan hastaya barkod verilmektedir. İşlem süresi (C/T) ortalama 1 dakikadır.
- ***Triaj*:** Kayıt bölümünün çaprazında yer alan triaj bölümünde çalışanlar hastanın dosyasını açarak, şikayetine göre gerekli bölüme yönlendirme işlemi yapmaktadırlar. Triajda renk kodlamasına göre hasta sınıflandırması gerçekleştirilmektedir. Yeşil, sarı, kırmızı ve siyah renk kodlarının bulunduğu uygulamada yeşil renkli alana (acil olmayan) basit sağlık sorunları bulunan hastalar yönlendirilmektedir. Sarı alanda (acil) yaralanmış bir şekilde tıbbi bakıma ihtiyacı var olan

hastalar yer almaktadır. Bu durumdaki hastalar sarı renkli muayene odasına yönlendirilmektedir. Kırmızı renk kodu (çok acil), hayati risk taşıyan veya durumu kritik düzeyde olan hastaları ifade etmektedir. Siyah renk kodu (ölü veya yaşam beklentisi olmayan), hayatta kalma olasılığı bulunmayan ya da ölümcül düzeyde ağır yaralanmaları olan hastaların sınıflandırıldığı grubu ifade etmektedir. Transport işlemini de triajda yer alan personeller yapmaktadır. Triaj uygulaması için işlem süresi (C/T) ortalama 5 dakikadır.

- ***Muayene*:** Triajda yönlendirilen hasta yeşil, sarı veya kırmızı renkli muayene odalarına yönlendirilmektedir. Muayene odalarında görev yapan hekimler tarafından hastaların şikâyetleri, mevcut alerjileri, kullandıkları ilaçlar ve vital bulguları değerlendirilerek ön tanı süreci gerçekleştirilmektedir. Muayene işleminin ortalama tamamlanma süresi (C/T) yaklaşık 10 dakika olarak belirlenmiştir.
- ***Laboratuvar*:** Doktorun hasta epikriz formuna doldurduğu laboratuvar istemine göre görevli hemşire hasta başında kan alır. Alınan kan örnekleri spor adı verilen tüplere koyularak laboratuvara gönderilmektedir. Kan alma için ortalama işlem süresi (C/T) ortalama 2 dakikadır.
- ***Tomografi*:** Tomografi istemi için hasta, hastanın yakınları varsa onlarla yoksa personel ile tetkikleri yapılması için tomografi bölümüne yönlendirilir. Doktorun verdiği epikriz formu ile gelen hastanın, epikriz formunda istenen bölgesinin görüntüsü çekilmektedir. Ortalama işlem süresi (C/T) 3 dakikadır. Görüntülerin sisteme yüklenmesi 5 dakika sürmekte, 5 dakika sonra sistem üzerinden doktorun bilgisayarına düşmektedir. Hastanın sonucu elde etme süresi 15 dakikadır.

- ***Röntgen*:** Röntgen istemi için, doktorun verdiği epikriz formu ile gelen hastanın, epikriz formunda istenen bölgesinin röntgeni çekilmektedir. Ortalama işlem süresi (C/T) 2 dakikadır. Görüntüler sisteme yüklendikten sonra anında sistem üzerinden doktorun bilgisayarına düşmektedir. Hastanın sonucu elde etme süresi 15 dakikadır.
- ***Ultrason*:** USG istemi için, doktorun verdiği epikriz formuyla gelen hastanın ultrasonu çekilmektedir. Ultrason için ortalama işlem süresi (C/T) 4 dakikadır. Hastanın görüntüleme yapıldıktan sonra sonucunu elde etme süresi 15 dakikadır.

4.2.5. Takt Zamanı ve Prosesteki İşlem Sürelerinin Analizi

Kayıt, tomografi, röntgen ve laboratuvar işlemlerinin işlem sürelerinin takt zamanına uygun olduğu belirlenmiştir. Buna karşılık, diğer işlem adımlarının sürelerinin takt zamanını aştığı görülmüştür. Takt zamanının üzerinde gerçekleşen işlemler, hasta talebine zamanında yanıt verilmesini engelleyebileceğinden, bu süreçlerde oluşan gecikme ve israfların belirlenerek ortadan kaldırılması önem taşımaktadır.

Şekil 1'deki grafikte takt zamanı ve prosesteki işlemlerin süreleri belirtilmektedir. Şekil 2 ise, mevcut durum haritasını göstermektedir.

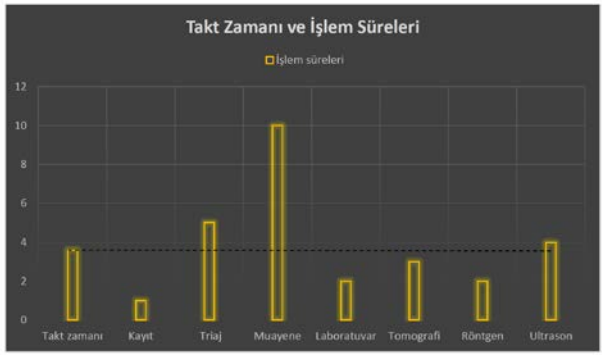

Şekil 1. Takt zamanı ve işlem süreleri

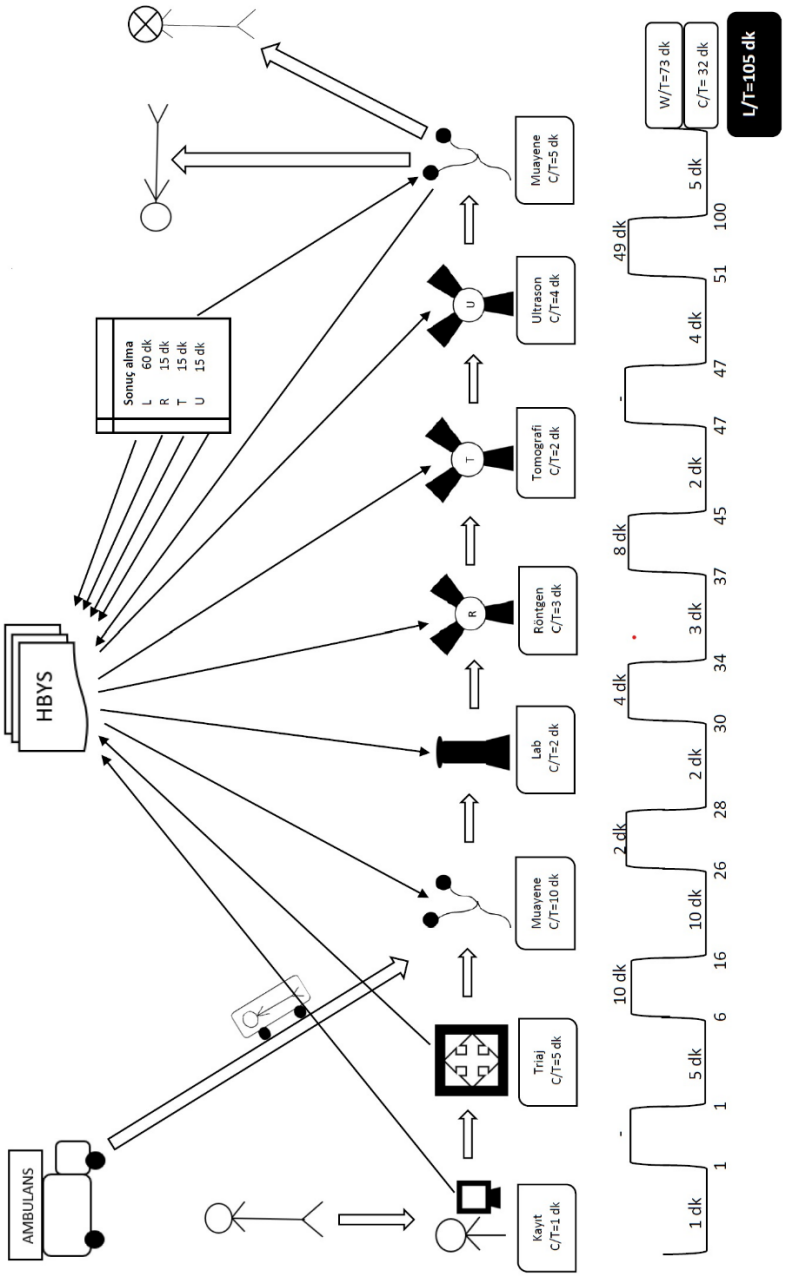

Şekil 2. Mevcut durum haritası

4.3. Mevcut Durumun Değerlendirilmesi

Bu bölümde acil serviste yalın ilkeler oluşturulmakta, sonrasında oluşturulan yalın ilkeler doğrultusunda değer akışındaki 7 temel israf belirlenmektedir.

Tablo 1'de acil servis için oluşturulan yalın ilkeler bulunmaktadır.

Tablo 1. Acil servis için yalın ilkeler

Müşteri değeri	Olabildiğince kısa sürede tedavi
Değer akışı	Hastanın acil serviste geçirdiği süreçteki israfların belirlenip kaldırılması
Akış	HBYS'nin doğru ve hızlı kullanımı ile hastanın süreçte aksatılmadan işlemlerini yapabilmesi
Çekme sistemi	Hastanın tedavisi için acil servisin yeterli malzeme ve iş gücü sağlaması
Mükemmellik	Hastanın olabildiğince kısa sürede doğru tedaviyi almasının sağlanması

Yalın ilkelerin doğru şekilde değerlendirilebilmesi için değer akışında belirtilen israfların belirlenmesi gerekmektedir. Yalın üretimde 7 Muda bulunmaktadır. Bunlar; hatalı üretim, fazla üretim, fazla stok, bekleme, gereksiz işler, gereksiz taşıma, gereksiz hareketlerdir.

Tablo 2'de mevcut durum haritasının değerlendirilmesi sonucunda ortaya çıkan temel 7 israf yer almaktadır.

Tablo 2. Acil serviste 7 temel israf

Hatalı üretim	HBYS'ye yanlış bilgi girişi Hatalı triaj Hatalı muayene Hatalı tetkik sonuçları
Gereksiz hareketler	Hastanın gereksiz dolaşımı Kan tetkiki için örneklerin laboratuvara götürülmesi
Fazla üretim	Aşırı talep durumunda gereğinden fazla sayıda hastanın muayene edilmesi
Gereksiz işler	Gereksiz radyolojik tetkik Gereksiz kan tetkiki
Fazla stok	Triajda hasta kuyruğu Muayene öncesi hasta kuyruğu

	Kan alınacak hasta kuyruğu Röntgen öncesi hasta kuyruğu Tomografi öncesi hasta kuyruğu Tekrar muayenede hasta kuyruğu
Gereksiz taşıma	Tetkikler için epikriz formunun taşınması Kan tetkiki için örneklerin laboratuvara taşınması
Bekleme	Triaj için bekleme Muayene için bekleme Kan alınması için hemşire bekleme Röntgen öncesinde ekleme Tomografi öncesinde bekleme Radyolojik sonuçlar için bekleme Laboratuvar sonuçları için bekleme Tetkik sonucu göstermek için bekleme

AS'de danışma işini kayıt görevlileri ve triaj görevlileri yapmakta ayrıca bir danışma bölümü bulunmamaktadır. Yoğunluk olduğu zamanlarda kayıt ve triaj dışında bilgi alacak hastalar bu bölümlerde kalabalık oluşturmakta bu durum da kayıt ve triaj bölümünde karmaşıklığa sebep olmaktadır. AS'nin girişinde bir danışma bölümünün bulunması kayıt ve triajda çalışan personelin iş yükünü azaltacak, bu bölümler önünde oluşacak karmaşıklığın da önüne geçecektir.

Oluşturulacak danışma birimi sistemin sürekli akışını sağlayabilmek için farklı çalışmalar yapabilmelidir. AS'nin en büyük problemlerinden olan yoğunluğa rağmen 112'nin hasta getirmesi olayında danışma birimi etkin kullanılabilir. AS'nin kapasitesini, anlık durumu hakkındaki bilgiyi güncel tutarak sistemin sürekli akışında etkin rol oynayabilir.

AS'de yapılabilecek en önemli iyileştirmeler triaj bölümündedir. Triaj bölümünde gelen hastaların dosyaları açılarak yönlendirilmesi yapılmakta, hastalar sınıflandırılarak muayene odalarına alınmaktadır. Transport işlemini de triaj görevlileri yapmaktadır. Triaj görevlilerinin iş yükünü azaltmak için 5S (ayıklama, düzenleme, temizleme, standardizasyon, disiplin) çalışmasının yapılması önerilmektedir.

AS'de triaj biriminin konumundan dolayı bazı hastalar bu bölüme uğramadan içeri geçebilmekte, bu durum da muayene odalarında karmaşıklığa ve hastanın gereksiz dolaşımına sebep olmaktadır. Triaj biriminin konumunda yapılacak değişiklik ve alanın düzenlenmesi sonucunda bu durumun önüne geçilecektir.

Triaj bölümünde hastanın şikayetleri doğru değerlendirilirse doğru sınıflandırma yapılabilir. Hastaların muayene odalarına alınmasının sıralaması doğru yapılırsa gerçek acil hastalar gerekli tetkik ve tedaviye zamanında erişebilir. Bu bölüm etkin kullanıldığı takdirde verilen hizmetin kalitesi artacak, zaman verimli kullanılacaktır.

Triaj bölümü için diğer bir öneri, bölümde bir uzman hekimin bulunması gerektiğidir. AS'ye başvuran her hastaya bakılma zorunluluğu bulunmaktadır. Gelen hastaların, uzman hekim tarafından şikayetleri, öyküleri dinlenirse gerçekten acil olan hastalar belirlenebilir, tetkik ve tedavi gerektirmeyen hastalar öneri ve reçeteyle süreçte fazla dolaşmadan taburcu edilebilir. Bu durumda doktorlar acil olmayan hastalarla zaman kaybetmeyecek, daha az hasta görecek ve AS'de iş yükü azalacaktır.

Triaj uygulamasından sonra içeri alınan hastalar muayene odalarına polikliniklerdeki gibi ekranlar vasıtasıyla alınırsa triaj görevlilerinin ve doktorların iş yükü hafifleyecektir.

Muayeneden sonra kan tetkiki için hemşireler hasta başına gelerek numune almaktadır. Alınan kan örnekleri laboratuvara elde taşınmaktadır. Bu, AS için yalın hizmette israftır. Bu israfın önüne AS'ye pnömatik sistemin kurulmasıyla geçilebilecektir. Pnömatik sistemle laboratuvara kan örnekleri anında gönderilecek, hataların önüne geçilecek ve hemşirelerin iş yükü azaltılabilecektir.

Röntgen, tomografi, ultrason gibi tetkikler için hasta doktorun verdiği epikriz formuyla ilgili bölümlere

başvurmaktadır. Bu form yerine HBYS'nin etkin kullanılması gereksiz taşımanın önüne geçecektir.

Süreçteki en uzun işlem süresi laboratuvar sonuçlarının çıkmasıdır. Otoanaliz makinesinden sonuçların çıkma süreleri Hemogram için 20 dakika, Biyokimya için 30 dakika, Sedimantasyon için 40 dakika, TİT için ise 10 dakikadır. Ancak hasta bu sonuçların çıkmasını Hemogram için 20 dakika, Biyokimya için 60 dakika, Sedimantasyon için 60 dakika, TİT için ise 20 dakika beklemekte hatta aşırı talep durumunda bu süreler daha da artmaktadır. Bunun önüne geçebilmek için sonuçların çıkma sürecindeki israflar çıkarılmalı, sonuçlar makineden çıkınca anında doktorun ekranına düşmelidir. Bu durumda bekleme süreleri azaltılacak, AS'de boş beklemenin önüne geçilecektir.

Röntgen, tomografi, ultrason tetkiklerinin sonuçları da röntgen anında, tomografi 5 dakika içerisinde, ultrason sonuçları da sisteme yüklenir yüklenmez doktorların ekranına düşmekte ancak hastalar bu tetkiklerin sonucunu almak için (her biri için) 15 dakika bekletilmektedir. Bu bekleme de israf olarak görülmektedir. Sonuçlar doktorun ekranına düşer düşmez hasta bilgilendirilirse süreçteki boş beklemenin önüne geçilebilecektir.

Tetkik ve tahlil sonuçlarında hasta ve yakınlarını bilgilendirmek için muayene odaları önüne kurulacak olan ekranlar kullanılırsa muayene odalarındaki karmaşanın önüne geçilecek, hasta sonucu çıkar çıkmaz doktorla görüşecek fazladan bekleme süresi engellenmiş olacaktır.

AS'de diğer sorun personelin sık değişmesidir. Yalın anlayışta varyasyon istenmeyen durumdur. Bu duruma engel olunursa oluşabilecek hatalar da azaltılacaktır.

AS'de bu önerilerle yoğunluk ve iş yükü azaltılacak; eksik anamnez sonucu gereksiz tetkik, laboratuvar ve radyolojide yoğunlaşma, gereksiz takip, sonuçlarda gecikme, bekleyen hasta

sayısında artış, AS'de artmış yoğunluk, artan yoğunluk sebebiyle azalan zaman, azalan zamanın sebep olacağı eksik anamnez döngüsü kırılacaktır.

Muayene süresinde, röntgen ve tomografi tetkikleri öncesindeki bekleme sürelerinde azalmalar olacak, hasta laboratuvar ve tetkik sonucunun çıkmasını gereğinden fazla beklemeyecektir. Verilen hizmetin kalitesi artacak, AS'de zaman verimli kullanılacaktır.

Tüm bu önerilerinden sonra gelecek durum haritası Şekil 3'teki gibi oluşturulmuştur.

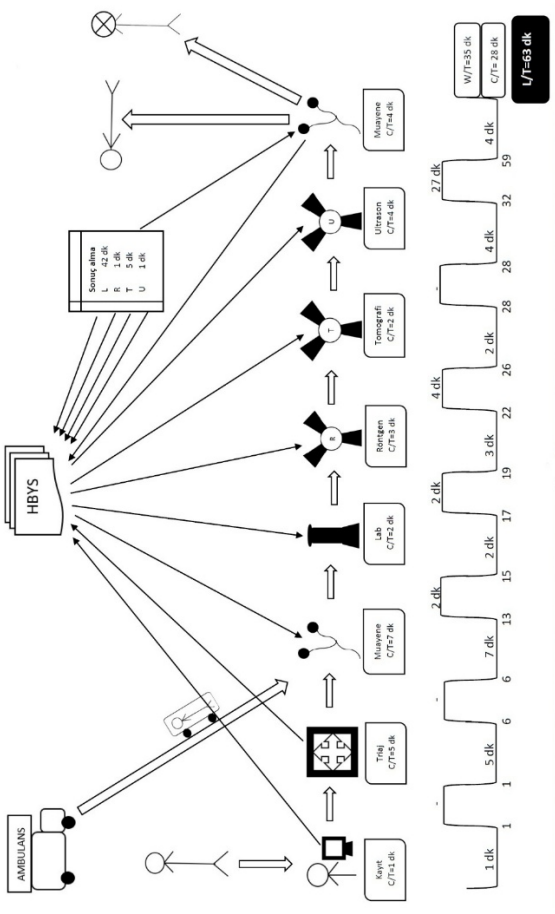

Şekil 3. Gelecek durum haritası

5. SONUÇ VE ÖNERİLER

Bir araştırma hastanesinin acil servisinde gerçekleştirilen bu çalışmada, DAH tekniği kullanılarak hizmet işletmelerinde yalın düşüncenin uygulanabilirliği araştırılmıştır. Hastanın AS'de geçtiği tüm sürecin gösterildiği harita ile mevcut durum analiz edilerek değer akışı üzerinde değerin nasıl aktığı gözlemlenmiş, sistemin sürekli akışına engel olan israf ve israf kaynakları belirlenmeye çalışılmıştır. Belirlenen israf ve kaynaklarının önüne geçebilmek için sistemin sürekli akışını sağlayabilecek önerilerde bulunulmuştur. Öneriler doğrultusunda gelecek durum haritalandırılmış süreçte olabilecek iyileşme oranları hesaplanmıştır. Bu hesaplamalara göre uygulanan DAH çalışması sonucunda gelecek durum haritası ve mevcut durum haritası karşılaştırıldığında; mevcut durum haritasında bekleme süresi (W/T) 73 dakika, işlem süresi (C/T) 32 dakika toplamda temin süresi (L/T) 105 dakika olarak belirlenmiştir. Öneriler sonucunda çizilen gelecek durum haritasında bekleme süresi (W/T) 35 dakikaya, işlem süresi (C/T) 28 dakikaya, dolayısıyla temin süresi de (L/T) 63 dakikaya düşürülmüştür. Mevcut durum haritasında israf olarak görülen ve toplam akış süresine değer katmayan işlemlerin süresi 73 dakika (4380 saniye) iken gelecek durum haritasında bu süre 35 dakikaya düşürülmüştür. Bu değer katmayan işlem sürelerinin toplam akış sürelerine oranlarına bakıldığında mevcut durum haritasında %69,5 iken gelecek durum haritasında %55,5 olarak belirlenmiştir. Toplam akış süresi mevcut durum haritasında 105 dakika iken gelecek durum haritasında 63 dakika olarak hesaplanmıştır. Bu da önerilen iyileştirmelerle akış süresinin %40 oranda azaldığını göstermektedir. Bekleme süresinde 38 dakikalık azalma gerçekleştirilmiş, %50'den fazla iyileştirme sağlanmıştır. İşlem süreleri oranlandığında %12,5 oranında iyileştirme olduğu belirlenmiştir.

KAYNAKÇA

Balcı, D. (2006). Tam zamanında üretim felsefesinin hizmet sistemlerine uygulanabilirliği: Gazi Üniversitesi Tıp Fakültesi Hastanesi Erişkin Acil Servisi'nde bir uygulama (Yüksek lisans tezi). Gazi Üniversitesi, Fen Bilimleri Enstitüsü, Ankara.

Güleryüz, D. (2012). Yalın yönetim sistemlerinin hastanelere uyarlanabilirliği ve bir hastane uygulaması (Yüksek lisans tezi). Sakarya Üniversitesi, Fen Bilimleri Enstitüsü, Sakarya.

Kılıç, A. (2016). Otomotiv yan sanayinde yalın üretim uygulaması (Yüksek lisans tezi). İstanbul Ticaret Üniversitesi, Fen Bilimleri Enstitüsü, İstanbul.

Womack, J. P., & Jones, D. T. (1998). Yalın düşünce (N. Acar, Çev.). İstanbul: Sistem Yayıncılık.

Yılmaz, E. (2012). Siparişe göre üretim yapan sistemlerde yalın üretim uygulamaları (Yüksek lisans tezi). İstanbul Teknik Üniversitesi, Fen Bilimleri Enstitüsü, İstanbul

Yurdugül, U. (2010). Değer akışı haritalandırma yöntemi ve bir uygulama (Yüksek lisans tezi). İstanbul Teknik Üniversitesi, Fen Bilimleri Enstitüsü, İstanbul

ENDÜSTRİ MÜHENDİSLİĞİ ALANINDA

GÜNCEL KONULAR VE

AKADEMİK DEĞERLENDİRMELER

yaz
yayınları

YAZ Yayınları
M.İhtisas OSB Mah. 4A Cad. No:3/3
İscehisar / AFYONKARAHİSAR
Tel : (0 531) 880 92 99
yazyayinlari@gmail.com • www.yazyayinlari.com